Astrid Svee

Development and testing of an Acoustical Plankton Recorder

Thesis for the degree doktor ingeniør

Trondheim, March 2006

Norwegian University of Science and Technology
Faculty of Information Technology,
Mathematics and Electrical Engineering
Department of Electronics and Telecommunication

NTNU
Innovation and Creativity

NTNU
Norwegian University of Science and Technology

Thesis for the degree doktor ingeniør

Faculty of Information Technology,
Mathematics and Electrical Engineering
Department of Electronics and
Telecommunication

ISBN 978-82-471-1013-3 (printed version)
ISBN 978-82-471-1027-0 (electronic version)
ISSN 1503-8181

Doctoral theses at NTNU, 2007:46

Printed by NTNU-trykk

Abstract

Recent years have brought cross-disciplinary focus on possibilities, constraints and consequences of large scale zooplankton harvesting. Development of acoustic measurement technology is an important part of that work. Because of the small size of the plankton, the measurement frequencies have to be high compared to fishery acoustics. Based on a model of the size and shape of the plankton and its physical properties, the use of multiple frequency measurements will allow inverse modeling of the size and concentration of plankton. This thesis presents the development and test results of an Acoustical Plankton Recorder (APR). The system uses three frequencies, 200 kHz, 710 kHz, and 1 MHz. The system parameters are designed with a focus on measuring the zooplankton *Calanus finmarchicus*, which plays an important role in the Norwegian Sea ecosystem. The APR is a prototype instrument built to gain experience for future generations of instruments for plankton measurements. Different aspects of multi-frequency acoustical measurements are discussed with a focus on uncertainties and critical factors. The results from various experiments and measurements are presented. The estimated concentration of scatterers from data recovered by the Acoustical Plankton Recorder shows good agreement with biological samples.

Preface

This dissertation is submitted to the Norwegian University of Science and Technology, NTNU, in partial fulfillment of the requirements for the degree of Doktor ingeniør. The work has been performed at the Acoustic group at the Department of Electronics and Telecommunications, NTNU, in the years from 2002 to 2007. My work has been a part of a Strategic University Program granted to a consortium of NTNU faculties by the Norwegian Research Council for the years 2001 to 2006. In addition to the research activity, the work included compulsory courses corresponding to one year full-time studies, as well as one year teaching assistant duties.

Acknowledgements

I wish to thank my supervisor, Jens Hovem, for all his help throughout my work at the Department of Electronics and Telecommunications. Without him this dissertation would not have been completed. I also would like to thank my coworkers at the Acoustics group for an interesting time. Special thanks to Øyvind Lervik, who has done a great job on the instrument and has been accommodating me during my measurements. I am grateful to my fellow colleague on the Calanus project both for letting me participate on measurement cruises and for answering all my biological questions. I would also particularly like to thank my father, Erik Dahl, for his patient and competent comments to the writing of this thesis and Bojana Garjic for her useful comments to this thesis. At last but not least I would like to thank my husband, Even Svee, for all his support throughout these years.

Contents

List of Figures

List of Tables

Chapter 1

Introduction

About 70% of the surface of the Earth is covered by water and the ocean has at all times offered important resources for humans. During the 20th century new technologies increased the efficiency of large scale exploitation of sea resources. Acoustical echo sounders made it possible to observe fish through the water and this has resulted in the fish harvesting techniques and fishing stock management regimes seen today.

But fish contributes only a small portion to the resources in the sea. The major part of the biomass consists of plankton. The possible exploitation of zooplankton as a resource has thus become an area of increasing interest during the last years.

1.1 The Calanus project

This thesis is part of the Strategic University Program "Calanus" carried out by a consortium of NTNU faculties and departments and supported by Norwegian Research Council for the years 2001-6. The program addresses large-scale harvesting of zooplankton from a value chain perspective, including biological, technological, and social aspects. The main objective of the Calanus project is to clarify possibilities, constraints, and consequences of large-scale application of marine zooplankton as fish feed and as industrial raw material.

One of the objectives of the project is development of method and equipment for acoustical plankton detection. The equipment is an essential tool for estimation of the quantity of plankton present in the sea. The Acoustical

Plankton Recorder (APR) is the subject of this thesis. It has been developed and tested in compliance with of the objectives for the project.

The instrument has been, and will be, used to perform acoustic measurements to gain information about the biomass distribution of plankton in time and space. The biomass measurements by means of an acoustical plankton recorder could be used to collect the biomass data needed as input data for an ecosystem model, which plays a key part in the Calanus project.

1.2 Acoustical methods for detection of plankton

There are many different applications of acoustic waves under water. Electromagnetic waves are strongly attenuated in salt water and can only propagate short ranges. Acoustic waves, however, can travel over long distances. The application of acoustical systems includes the detection, classification and mapping of bodies and properties of the sea and the sea bottom. In addition acoustics is used for underwater positioning and communication.

The use of acoustic methods to study zooplankton is relatively new compared with acoustics in the fishery science. In order to detect an object acoustically under water, it is desirable that the wavelength of the sound is on the order of, or shorter than, the size of the object. Plankton is much smaller than fish, and it is therefore necessary to use much higher frequencies for plankton detection than for fish detection. However, the use of high frequencies limits the range of the system due to absorption in the sea water.

Some commercially available acoustical systems for plankton detection exist, and a few prototype acoustical systems have been developed by other institutions.

A Multifrequency Acoustic Profiling System (MAPS) is one of the more complex acoustic instruments built for studying zooplankton [Holliday et al., 1989]. It was developed to make rapid high-density spatial coverage. The 21 frequencies span from 100 kHz to 10 MHz, which limits the range of the system to a few meters. Several generations of this system have been developed over the last decades under the joint sponsorship of ONR (Office of Naval Research, USA) and NSF (National Science Foundation, USA). The system has two modes of operation, towing with dynamic depth control and casts at discrete locations and times.

One of the commercially available acoustical systems that can be used for plankton research is the DT-X/DE-X^{TM} system from BioSonics Inc. The sys-

tem can operate multiple transducers with frequencies 38, 70, 120, 200, 420, or 1000 kHz. This system can be controlled remotely, wired or wireless. Another system that can be used for plankton measurements is the EK60 Scientific Sounder system^{TM} from Simrad AS. It can operate at several frequencies simultaneously, in the range from 18 to 200 kHz.

Multiple-frequency echo-ranging sensors (TAPS) [Holliday et al., 2003] have been deployed in both up-looking mode from the bottom and for moorings looking up, down and horizontally. These systems have been used to measure thin layers of plankton.

1.3 Other methods and instrumentation for plankton detection

Biological sampling methods are and have been used to measure concentration of plankton. These methods are based on sampling of plankton in nets. Sophisticated plankton samplers with different towing mechanisms, sensors, and gauze have been developed and are commercially available.

1.4 Motivation for the instrumentation

The objective of this work was to build a multi-frequency system that could measure zooplankton in different size groups. The system was designed to have high resolution both in time and range and to measure as low concentration of plankton as possible. The system parameters of the instrument were to be adaptable to the task and measure plankton concentrations typically seen in the sea in the range 15 to 20 meters.

The instrumentation hardware runs on batteries and therefore the electronics was designed to be energy efficient. One of the possible future applications of the system is mounting in a buoy.

In such a configuration one can measure biomass as a function of space and time without an operator at the measurement site. Other sensors in the same buoy could give additional information that could be used to improve the accuracy of biomass estimates.

There are considerable advantages of designing and building a new instrument. The main advantage is the flexibility of such a system. The number of

transducers and the frequency of these transducers can be chosen according to the intended application of the instrument. The size of the plankton of interest influences the frequencies that are advantageous. Designing, building and testing the system gives the designer control over the different parts of the system. The instrument can be modified as new needs are identified and serve as a prototype for future generations of plankton recorders. The instrument is intended for research and a diversity of measurement situations and experiments could be of interest.

The parameters of the acoustical system are set to measure plankton in general and the zooplankton species *Calanus finmarchicus* in particular. The *Calanus finmarchicus* has a special focus in the Calanus project and has therefore also named the project. This species plays a key role in the Norwegian Sea ecosystem and is the dominant herbivore plankton. With a body size of between 1 and 3 mm, the optimal frequencies for detection of such plankton is approximately 1 MHz. This requires high frequency transducers. More detail about plankton size versus optimal frequency is given in Chapter 2 and 3.

1.5 Overview of the thesis

The thesis consists of three parts. The first part presents the theory of plankton acoustics. The second part describes the configuration, construction, verification, and calibration of the Acoustical Plankton Recorder. The third part shows experimental results and some measurement results from cruises on the fjord, and summarizes the conclusion that can be drawn from this work.

Chapter 2

Acoustic Theory

The propagation of sound in water depends on various physical parameters in the sea and the frequency of the sound. The performance of the system is also dependent on characteristics of the transducers. The system described in the following is designed for a specific purpose. This chapter contains a short explanation of parameters that are important for an acoustical system and a background for the choice of parameters for the Acoustical Plankton Recorder (APR). The APR itself is described in detail in Chapters 4 and 5.

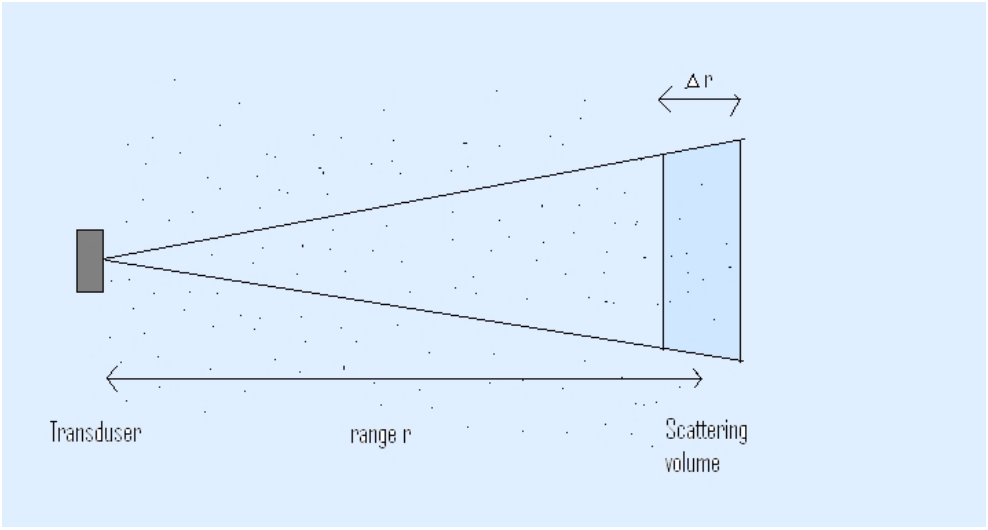

Figure 2.1: A sketch of the measurement situation.

Figure 2.1 gives an overview of the measurement situation. Sound pulses are

transmitted from the transducer with a given beamwidth. The sound waves that propagate through the water are scattered by the objects in the water. The received signal at the transducer at a time t consists of the backscattered signal from the objects inside a volume V_0 at a range r from the transducer in addition to noise from the sea. The time elapsed from a ping is transmitted until the backscattered signal from range r is received, is $t = \frac{2r}{c}$, where c is the sound speed in water.

The first section of this chapter describes different acoustical parameters. The influence of the parameters on the design and properties of the APR is covered in particular. In the last section the sonar equations for such a system are stated and accounted for. Some of the parameters and equations are given in decibel units. This is common in acoustics because the parameters cover many orders of magnitude.

2.1 The acoustical parameters

2.1.1 Absorption

Sound propagation in water is limited by absorption. The absorption in seawater is caused by viscosity, thermal conductivity, and relaxation processes due to the salt in the water. There exist many empirical formulas for absorption calculations. One of the most used is from Francois and Garrison [1982a,b]. According to this formula the total acoustic absorption is

$$\alpha = \frac{A_1 P_1 f_1 f^2}{f^2 + f_1^2} + \frac{A_2 P_2 f_2 f^2}{f^2 + f_2^2} + A_3 P_3 f^2 \tag{2.1}$$

The coefficients A_1, A_2, A_3, P_1, P_2, and P_3 are functions of the temperature, salinity, pressure, and the pH value of the water, and f_1 and f_2 are the relaxation frequencies of boric acid and magnesium sulfate.

Figure 2.2 shows the absorption as a function of frequency for typical environmental parameters. Notice the logarithmic units on the axis. It is clear from this figure that the absorption increases rapidly at high frequencies.

The influence of absorption on the APR

Keeping in mind the physical parameters of the sea, the best way to reduce the absorption seems to be application of as low frequencies as possible. But the choice of operational frequency of a system is influenced by additional factors.

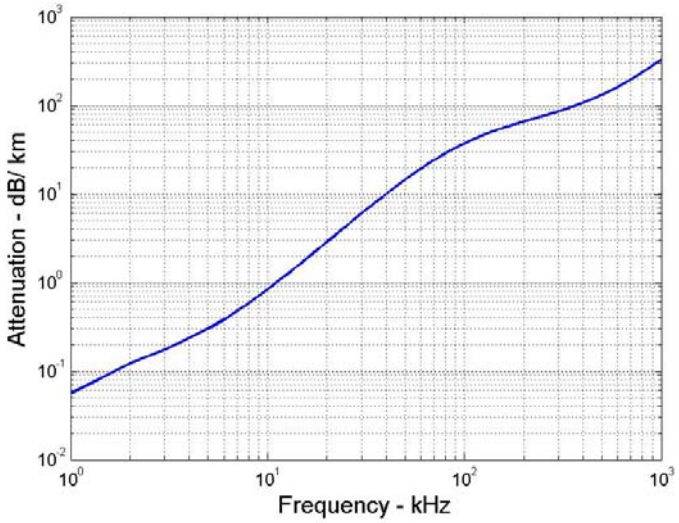

Figure 2.2: Absorption of sound as a function of frequency for sea water at the surface for water temperature 15°C, salinity 35 ppt, and pH 8.

The APR uses the measurement frequencies 200 kHz, 710 kHz, and 1 MHz for reasons explained in the next section. The absorption at these three frequencies for typical ocean conditions are given in Table 2.1. The salinity, pH, and depth are kept constant in this table while the absorption for different water temperatures is given.

Table 2.1: The absorption for different water temperature, T, for the three frequencies of the APR. The salinity, S, is 35 ppt, the depth is zero and the pH is 8 in these calculations.

Temperature	**200 kHz**	**710 kHz**	**1 MHz**
T=5°C	0.046 dB/m	0.227 dB/m	0.418 dB/m
T=10°C	0.054 dB/m	0.204 dB/m	0.359 dB/m
T=15°C	0.066 dB/m	0.199 dB/m	0.328 dB/m

The absorption in water at high frequencies depends strongly on the temperature. As absorption is the limiting factor for the range of a measurement system, the maximum range of the system will change with changing water conditions. Variation in the other parameters would influence the absorption to a less degree than variation in the temperature.

2.1.2 Selection of frequency

There are many considerations to take into account in the choice of operational frequency and the number of frequencies for an acoustic system. As seen above, the rapid increase in absorption with increased frequency argues for low frequencies. The wish to detect small object on the other hand argues for high frequencies, as will be explained later in this section and more detailed in Chapter 3. A compromise has to be made between these requirements. In addition to the physical requirements there are technical and practical aspects. The size of the transducer is related to the frequency. As the useful frequencies for plankton measurement are so high, the transducers will be relatively small. But there are few commercially available transducers in the frequency range of interest. The arguments for the use of multiple frequencies are explained in Chapter 3. The choice of the number of frequencies for a system will thus be a compromise between several considerations. An increase in the number of frequencies could improve the accuracy of the resulting data, but would also complicate the instrument.

The choice of the frequency for the APR

The system is designed to cover plankton with sizes from about 1 to 3 mm. The optimal frequency is close to the resonance frequency of the specific body length. The resonance frequency is defined as the maximum frequency of the first peak in target strength versus frequency. Based on the scattering models for plankton described in Chapter 3, and the physical properties of the *Calanus finmarkicus*, which is the species of interest in this project, the target strengths of modeled plankton with length 1, 2, and 3 mm are presented in Figure 2.3.

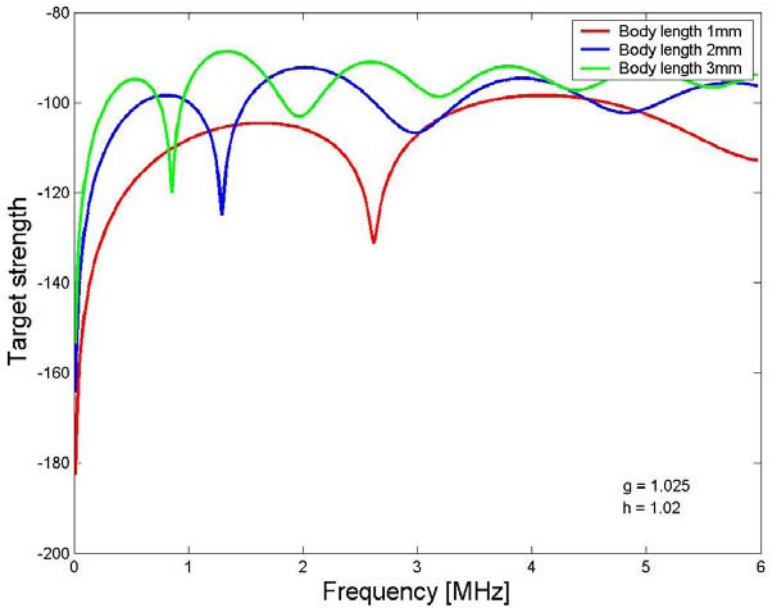

Figure 2.3: Target strengths versus frequency for modeled plankton of 1, 2, and 3 mm length. The plankton model and properties used in this model are described in Chapter 3.

The resonance frequencies for *Calanus finmarchicus* ranges from about 500 kHz to 1.5 MHz, see Figure 2.3. This frequency corresponds to a wavelength of twice the diameter of the equivalent sphere, which has been used to model the plankton, giving a constructive interference between the incoming sound wave and the wave reflected from the back side of the sphere. In the development of the instrument it was decided to use three channels with the frequencies 200, 710, and 1000 kHz both because these frequencies were in the desired

frequency span and these transducers were available at the Institute. From Figure 2.3 it is clear that the target strength of plankton is very low at 200 kHz, especially for the small plankton. This frequency was chosen to be used to distinguish between objects with a greater size than plankton, usually fish, and plankton. The 710 kHz and 1 MHz frequencies are suitable for detection of plankton in the size range of interest.

2.1.3 Target strength

One measure of the backscattering properties of an object is the target strength. The target strength, TS, is a logarithmic measure of backscatter of sound in dB referred to 1 m^2

$$TS(f) = 10\log(\sigma_{bs}(f)) = 20\log(|L_{bs}(f)|) \tag{2.2}$$

where $\sigma_{bs}(f)$ is the backscattering cross section and $L_{bs}(f)$ is the backscattering length.

The backscattering cross section is a measure of the proportion of the incident energy that is backscattered by a target and it is defined by

$$\sigma_{bs} = r^2 I_{bs}/I_{in} \tag{2.3}$$

where r is the distance between the point where the intensity of the incoming wave, I_{in}, and intensity of the backscattered wave, I_{bs}, is measured. The intensity is defined as the power passing perpendicularly through a unit area, equal to 1 m^2. This definition of the backscattering cross section requires that the intensity of the waves is measured in the far field of the target. If the measurements of the intensity are done far from the target, the definition of the backscattering cross section should contain a factor compensating for the absorption. For an incoming sound wave with a specific direction and frequency, the backscattering cross section for a specific target is a constant. The backscattering length is the square root of the backscattering cross section.

The target strength depends on factors like the frequency used, the size and shape of the scatterer, and the physical parameters of the scatterer. Chapter 3 describes the properties of plankton and presents a model for estimating the target strength of one individual plankton.

In a measurement situation clouds of plankton rather than individual ones are measured. The total target strength of the measurement volume depends on the concentration of plankton, plankton size, the beamwidth, pulse length, and frequency.

2.1.4 Beamwidth

The beamwidth of a transducer depends on the frequency and size of the transducer. The half intensity beamwidth is defined as the angle between the directions where the acoustic intensity is half of the axial values (through the axis).

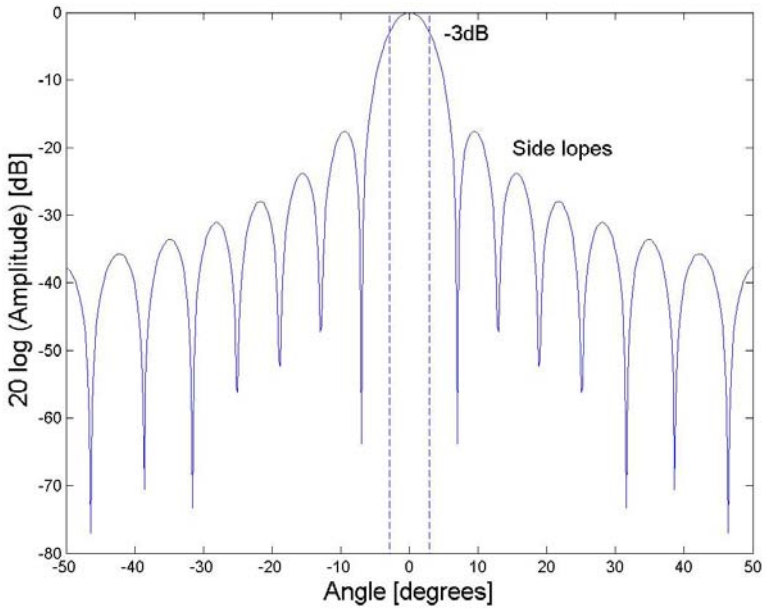

Figure 2.4: The directivity function of a circular plane disk with a radius $a = 5\lambda$.

Figure 2.4 show the directivity pattern of a circular symmetric transducer with a radius $a = 5\lambda$. The beamwidth of this transducer defined as the angle between where the amplitude has dropped to -3 dB, is about 5.9 degrees in this example. The intensity in the first side lobes is almost -17.5 dB lower than the axial intensity.

Equivalent beam angle

Another measure for the beam pattern is the equivalent beam angle, ψ. The equivalent beam is the solid angle of the ideal conical beam that produces the same echo-integral as the real transducer when the targets are randomly

distributed in space angle, see Simmonds and MacLennan [2005]. It is also called the reverberation angle of the transducer.

The beam pattern and sampled volume of the APR

Measurements of the beam pattern of the transducers used in the APR are presented in Chapter 4. The beam pattern of the transducers and the pulse length define a volume sample. An illustration of the sample volume is shown in Figure 2.1. The volume that has been illuminated by the beam is

$$V_0 = \frac{c\Delta T}{2} r^2 \Omega \tag{2.4}$$

where c is the sound speed, ΔT is the pulse length, r is the distance to the scatterers, and Ω is the solid angle. The pulse length and the beamwidth or equivalent beamwidth set the limits for the spatial resolution. In the argument that a backscattered signals received after a time t comes from an object in a distance $r = t\frac{c}{2}$, it is assumed that multiple scattering is negligible. Optimally one should measure the scattering from the same volume of water for all frequencies. But since the transducers have to be separated in space and the beamwidths are not the same for the transducers, this will only be approximately true. Since the ocean is variable, the scattering measurements at different frequencies should be made with as small time intervals as possible.

2.1.5 Noise level

The noise is the unwanted part of the received signal. The acoustic noise in the sea is caused by many sources, including physical ones, biological ones, as well as artificial noise from vessels. At high frequencies thermal noise is important.

In Figure 2.5 the important noise sources in the sea are shown as a function of frequency. The noise level is given as the noise spectral level which is the intensity in dB measured in a 1 Hz frequency band with reference to the intensity in dB of a plane sound wave with 1 μPa sound pressure [Hovem, 2006]. The natural background noise level follows a group of curves, called Knutsen curves, which depend on the wind speed. For frequencies above a couple of hundreds kHz the thermal noise is the dominating source of noise. The thermal noise level increases with frequency. Table values of the noise spectral level in the sea for the chosen frequencies are from 49 to 55 dB re 1 μ Pa, Hz.

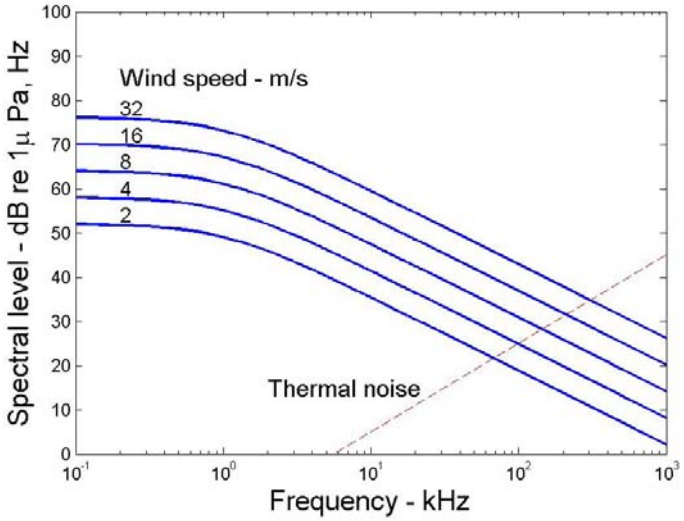

Figure 2.5: The noise level in the sea as a function of frequency.

The electrical noise in the receiver is added to the measured signal and is likely to be the dominating noise source in fishery acoustics, see Simmonds and MacLennan [2005]. The electrical noise is temperature dependent and does also depend on the electrical noise in the environment where the system is placed, which makes measurements of electrical noise troublesome in the laboratory. Chapter 6 discuss the noise level in more detail.

2.2 The sonar equations

A set of equations results by combining the properties of the transmitting and receiving system and a model for propagation loss in the water. The equations are given both for scattering from single targets and for clusters of targets, in logarithmic units. The notation in the equations follows the definitions by Hovem [2006].

The echo level

The echo level, EL, is a function of the source level, SL, transmission loss, TL, and the target strength of the scatterer given as

$$EL = SL - 2TL + TS \tag{2.5}$$

The source level SL is defined as the sound pressure level on the beam axis in dB relative to 1μPa at a reference distance of 1 meter.

A simple transmission model based on spherical sound propagation and absorption gives a formula for transmission loss

$$TL = 20\log(r/r_0) + (r - r_0)\alpha \tag{2.6}$$

where r_0 is the reference distance of 1 meter.

A more realistic model for the transmission loss could be implemented with additional knowledge of the sound speed. The sound speed and the absorption depend on the temperature, salinity, and depth in the water.

If there is one object in the beam with an unknown target strength, TS, and the source level is known, this target strength can be found by measuring the echo level and using Equation 2.5. In the case of clusters of objects, such as in the situation for plankton, the target strength in this equation is the combined target strengths of all plankton in the volume resolution cell. Pulses with pulse

length ΔT are transmitted into the water. Objects have to be separated in range by at least $\Delta r = \frac{c\Delta T}{2}$ for the individual echoes to be resolved. The receiver records the backscattered echo as a function of time. The echoes from the individual targets combine to form a received signal that is continuous with varying amplitude. The received signals from the multiple targets are superimposed and the differences in phase cause the signal amplitude to fluctuate. The targets with random position imply random phase in the backscattered echo from the targets and the instantaneous amplitudes can be described by a Rayleigh distribution provided there is a sufficient number of scatterers. The probability function of the Rayleigh distribution is independent of the number of (in this case) scatterers and the measured mean intensity is proportional to the number of targets. The mean intensity is found by integrating over the return from several pings. If the density of scatterers were to be very high, acoustical extinction and multiple scattering effects would influence the intensity of the backscattered sound. The next chapter contains more on the scattering from multiple targets.

Assuming that there is a linear relation between the number of scatterers with individual backscattering cross section, σ_{bs}, and the received intensity, a volume backscattering coefficient, s_V, can be defined as

$$s_V = \frac{\Sigma\sigma_{bs}}{V_0} \tag{2.7}$$

where V_0 is the sampling volume and $\Sigma\sigma_{bs}$ is the sum of the backscattering cross sections of all the objects in the volume. In logarithmic units the volume backscattering strength is given as

$$SV = 10\log\frac{s_v}{s_{v,ref}} \tag{2.8}$$

where the reference is $s_{v,ref} = 1m^{-1}$.

The echo level for the cluster of objects can be expressed as

$$EL = SL - 2TL + SV + 10\log\frac{V_0}{V_{ref}} \tag{2.9}$$

where V_{ref} is 1 cubic meter.

Receiver sensitivity

The properties of the receiving system converting the received pressure on the transducer to the measured voltage on the electrical side is given in the

receiver sensitivity, RS, measured in dB re $V/\mu Pa$

$$RS = 20 \log \frac{U_{res}}{U_{ref}} - EL \tag{2.10}$$

where U_{res} is the measured voltage of the system and U_{ref} is 1 Volt. A more detailed explanation on how the receiver sensitivity is defined and measured for the APR is given in Chapter 5.

2.2.1 Target strength and volume scattering strength

Combining Equations 2.5 and 2.10, the target strength and volume scattering strength can be calculated

$$TS = 20 \log \frac{U_{res}}{U_{ref}} - RS - SL + 2TL \tag{2.11}$$

$$SV = 20 \log \frac{U_{res}}{U_{ref}} - RS - SL + 2TL - 10 \log \frac{V_0}{V_{ref}} \tag{2.12}$$

where the first equation can be used for single objects and the second equation is used for measurement on clusters of objects.

Chapter 3

Plankton Acoustics

The difference between acoustic instrumentation used to study zooplankton and fish is caused by the small size and physical properties of the plankton. In plankton acoustics individual plankton is not considered, but rather a concentration of them. The scattering signals from individual plankton overlap and the composite signal contains the overall backscattering from a cloud of plankton. Because of the small size of the plankton, the measurement frequency has to be high compared to fishery acoustics, and therefore the maximum range of any plankton detection system will be limited by the high absorption at high frequencies in seawater.

In fishery acoustics estimates based on single frequencies can be used for fish assessment and stock management. One of the reasons for this is that the wavelength used in fishery acoustics is typically large compared to the fish size. For the fish with swimbladder the frequency is usually far above the resonance frequency since the wavelength of the sound is usually larger than the dimension of swimbladder. Still the prediction of the target strength of fish is complex, [Holliday and Pieper, 1995], and small changes in the angle of the swimbladder causes large variations of the target strength. The target strength of fish is much greater than for plankton mostly because of the size difference but also due to different material properties.

There are two different problems connected to acoustic scattering. The forward problem can be stated as follows: Given the geometrical and acoustical features of the target, what will be backscattered? The inverse problem is this: Given some echoes, what kind of target produced them? The last question is the most difficult to answer and it is the problem that has to be dealt with when measuring plankton in the sea.

The echoes returned from a multi-species aggregation combine to form a single acoustical signal. The acoustical signal is determined by the backscattering strength in the sampled volume of water at a particular frequency. The total echo-integral is measured as a function of range from the transducer. One echo does not give the information needed to identify the targets that produce the detected echoes. The non-monotropic character of the target strength of the plankton makes it impossible to distinguish uniquely a change in size or a change in abundance with the use of only one frequency. A single larger scatterer may produce the same signal as many small scatterers and one object with strong scattering properties produces the same signal as many weak ones. With multiple frequencies more than one volume backscattering signal of (ideally) the same water volume can be measured. Information on the size of the scatterers can be found by comparing the signals. With the use of a model for the different plankton present, one can convert the acoustical volume backscattering data to measures of concentration and size of plankton.

A two-frequency system [Greenlaw, 1979] can be used in cases where the water volume is dominated by a single plankton size that is not known beforehand. The result is an estimate of both the size and the number of plankton. The assumptions are: One single size of organisms has to dominate, an acoustical model can be used for these organisms, multiple scattering effects are negligible, shadowing effects are also negligible, dependence of the reflectivity on any other parameter (depth, temperature) is known. Furthermore, stationarity of the system is assumed. Plankton of several size groups can be estimated by measuring at many different frequencies.

3.1 Scattering models for plankton

The backscattering of sound from one zooplankton has been modeled in different ways depending on the type of plankton. Plankton is often divided into groups according to anatomical properties. Typical acoustical categories of plankton are as fluid-like, elastic shelled, and gas bearing. The models used for the various groups differ, and the target strengths are very different because of the different properties of the plankton. For instance, the signal from gas bearing plankton can be very strong compared with fluid-like organisms of the same size.

The newest generations of models are numerical. Photos or computerized tomography (CT-scans) are taken of the plankton and serve as bases for the modeling. Numerical integration yields estimates of scattering for realistic

animal shapes at different sizes and selected orientations. These techniques are mostly used for large zooplankton.

Fluid-like plankton are usually modeled as spheres or cylinders. Models based on finite-length straight and bent cylinders are used by Stanton et al. [1998], and Stanton and Chu [1998]. These models are developed for the plankton group euphausiids, which are generally much larger and have a more oblong shape than *Calanus finmarchicus*. For small zooplankton like *Calanus finmarchicus*, the relevant model is the fluid-sphere. Anderson [1950] solved the wave equation for scattering from a fluid sphere embedded in the fluid.

This simple model was chosen in this work both because of the shape and small size of *Calanus* and since there is limited information on its physical properties. In addition there is considerable variation in these parameters during the year.

3.1.1 The truncated sphere model

The truncated sphere model described by Holliday [1992] is a simplification of the Anderson model. The target strength in this model includes only the two first terms of the modal solution of Anderson's model, which corresponds to the monopole and dipole vibration modes of the sphere. The argument for doing this is that the zooplankton are not perfect spheres and do not have the symmetry properties of a sphere. The model states,

$$L_{bs} = \frac{ia}{ka}\left(\frac{1}{1+iC_0} - \frac{3}{1+iC_1}\right) \tag{3.1}$$

where L_{bs} is the backscattering length. The relationship between the backscattering length, backscattering cross section, and the target strength is defined in Equation 2.2.

The different factors of Equation 3.1 are described in the following. The two parts in this equation correspond to the two modes of the scattering from a sphere included in the truncated sphere model. Equation 3.1 uses the notation of Medvin and Clay [1998] where a is the radius of the model sphere and k is the wave number of the incoming sound in water. The factors C_0 and C_1 are,

$$\begin{aligned} C_0 &= \frac{j_0^{'}(k_1a)n_0(ka) - ghj_0(k_1a)n_0^{'}(ka)}{j_0^{'}(k_1a)j_0(k_1a) - ghj_0(k_1a)j_0^{'}(ka)} \\ C_1 &= \frac{j_1^{'}(k_1a)n_1(ka) - ghj_1(k_1a)n_1^{'}(ka)}{j_1^{'}(k_1a)j_1(k_1a) - ghj_1(k_1a)j_1^{'}(ka)} \end{aligned} \tag{3.2}$$

The derivative of the Bessel, $j_m^{'}(x)$, and Neumann, $n_m^{'}(x)$, functions are expressed in Bessel, $j_m(x)$, and Neumann functions, $n_m(x)$, where m is the order of the function and x is the argument.

$$\begin{aligned} j_0^{'}(x) &= -j_1(x) & n_0^{'} &= -n_1(x) \\ j_1^{'}(x) &= \frac{1}{3}j_0(x) - \frac{2}{3}j_2(x) & n_1^{'} &= \frac{1}{3}n_0(x) - \frac{2}{3}n_2(x) \end{aligned} \tag{3.3}$$

The density and sound speed of the plankton are given in the model as ratios between the properties of the plankton and the water surrounding the plankton.

$$g = \frac{\rho_{plankton}}{\rho_{water}} \qquad h = \frac{c_{plankton}}{c_{water}} \qquad k_1 = \frac{k}{h} \tag{3.4}$$

The ratio between the density of the plankton modeled as a sphere and that of water is g and the ratio of the sound speeds is h. Here, k_1 is the wave number inside the sphere.

Figure 3.1 shows the target strength of a truncated sphere. The parameters of the model are taken for typical values of *Calanus finmarchicus*.

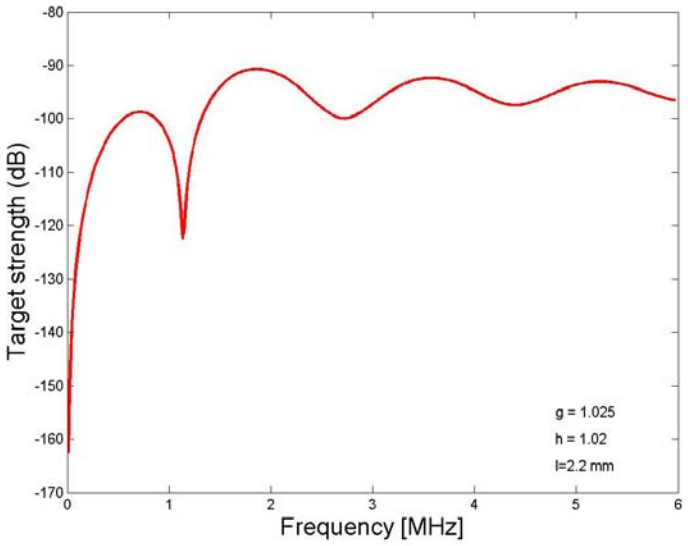

Figure 3.1: Predicted target strength with typical physical properties of 2.2 mm *Calanus finmarchicus*.

To the first approximation the model acts as a high-pass filter with the cut-off frequency at the point where the product between the wave number and the

radius of the sphere, ka, is equal to unity. The resonance frequency is defined as the frequency of the first maximum in the target strength. Below the resonance frequency the target strength decreases rapidly. For a given radius of the sphere, a, the target strength is very low for low frequencies. This property can be used to distinguish the size of a scatterer by comparing the target strength measured with the different frequencies. Above the resonance frequency there is a sharp drop in the target strength before it increases and oscillates around a constant value. The truncated fluid sphere model has proved in experimental studies to give a better representation of the scattering from small zooplankton than the full fluid sphere model, [Holliday and Pieper, 1995] and [Pieper and Holliday, 1984]. This can be explained by plankton lacking the geometric symmetry properties of the sphere.

The target strength of $-97dB$ at the resonance frequency of a plankton, modeled as truncated sphere as shown in Figure 3.1, can be compared with a typical target strength of -30 dB for a 40 cm cod for a typical frequency used in fishery acoustics. This means that about $5 \cdot 10^6$ plankton of this size are required to produce the same echo level as one fish.

3.2 *Calanus finmarchicus*

Figure 3.2: An adult *Calanus finmarchicus*. (Photo by Nils Tokle)

The Acoustical Plankton Recorder is designed with a special focus on measuring the plankton species *Calanus finmarchicus* (Figure 3.2). The reason is that this species is very abundant in the Norwegian Sea ecosystem, which is the territory of particular interest.

The word "plankton" is derived from Greek and means drifting. Many zooplankton species can swim up and down, migrate in the water column, but are horizontally drifting with the water current. Zooplankton act as a link in the food chain between phytoplankton on one hand and fish and whales on the other. The role of zooplankton in the ecosystem is complex and there are many different zooplankton present in the Norwegian Sea [Skjoldal, 2004].

Copepods is the numerically dominant group of zooplankton and *Calanus finmarchicus* is the dominant species of copepods in the Norwegian Sea. The word "copepod" literally means "oar-footed". Copepods have legs that they use for swimming and the adult individuals have bodies with a distinct front and abdominal part. They are single sexed. Copepods grow in steps by mounting their exoskeleton and Figure 3.3 shows the stages of the lifecycle. The lifecycle of *Calanus finmarchicus* consists of 12 stages. The eggs hatch

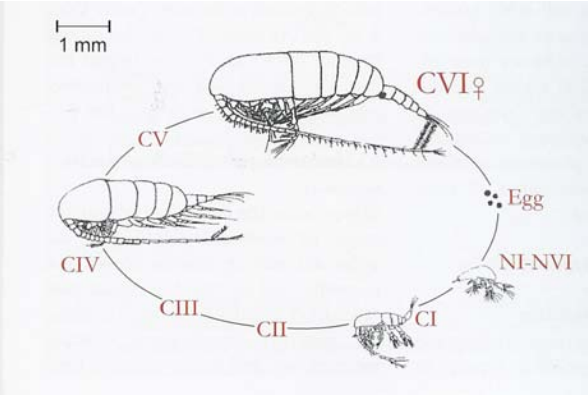

Figure 3.3: The life stages of copepods. (The figure is taken from Skjoldal [2004].)

into nauplius larvae. The nauplii develop through six stages (NI to NVI) and then change into a shape that resembles the adult individual and go through six copepodite stages (CI-CVI). The rate of development depends on the environmental conditions and particularly the food supply. Before the animals migrate down to deeper depth, as stage CIV to CVI individuals, they have accumulated a high fat content. This fat is used during the winter. The high concentration of the plankton is strongly linked to the current. It is expected

that high concentrations of them occurs trapped in deep parts of fjords during winter. The average abundance of the grown stages of *Calanus finmarchicus* in the Atlantic water outside the Norwegian coast has been reported to vary between 5000 to 40000 individuals per m^2 (0 to 200 meters depth), [Skjoldal, 2004].

Calanus finmarchicus has a relative *Calanus hyperboreus*, which is a larger copepode species with a length of 6-9 mm. Although this is also a common species, in this text *Calanus* refers to *Calnus finmarchicus*.

The morphological properties of the zooplankton vary for the different species, and so do the acoustical properties. There are a large number of species of zooplankton present and a continuum of sizes present within each species.

3.2.1 Physical properties of *Calanus finmarchicus*

Prediction of the scattering strength from a plankton modeled as a fluid sphere requires knowledge of the radius, density, and sound speed of the individual animal.

The value of the radius of a non-spherical zooplankton can be defined in several ways. One is to use the radius of a sphere having the same displacement volume as the plankton. Using this method there is a need for a relationship between the length of the plankton and the radius of the model sphere for every species of interest. A general relationship between the radius, a, and length, L, of the plankton is given by

$$a = \gamma L^{\delta} \tag{3.5}$$

According to Greenlaw and Johnson [1982] the measured values for *Calanus finmarchicus* were $\gamma = 0.21$ and $\delta = 1.02$. As an example this means that a *Calanus* of the length 2.2 mm has an equivalent sphere radius of about 0.47 mm.

The length of the plankton means the body length without the tail. A fellow PhD-student on the Calanus project, Tokle [2006a], has carried out measurements of the length of *Calanus finmarchicus* in the Trondheim fjord. The measurements were conducted during 14 days from the autumn 2002 to the summer 2003. Net samples were taken from different layers of water from the bottom up to the surface.

The measured length of the adult stages individual are shown in Figure 3.4 where the number of *Calanus* is plotted as a function of the length. The discrete division of the data in length classes is caused by the measurement

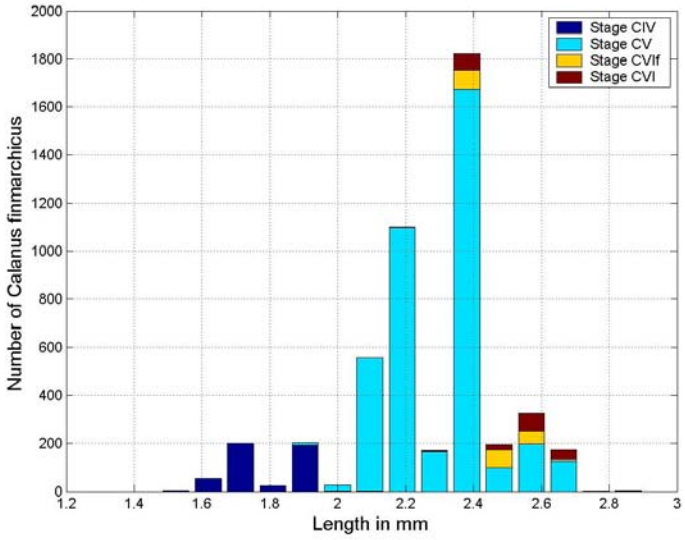

Figure 3.4: The body length of *Calanus finmarchicus*. (Data from Tokle [2006b])

method. The absolute value of the plankton concentration of each stage is highly influenced by the season the plankton was sampled. The results also show the variation in the length of the zooplankton. Even with plankton of one stage the data indicate that the body length varies with depth and season.

The density and sound speed of the plankton are given in the model as ratios between the properties of the plankton and the water surrounding the plankton defined in Equation 3.4. At a given frequency, the scattering strength increases with increasing g and h, and in addition to that it increases with size.

Different methods can be used to measure the sound speed and density of the plankton. The properties for *Calanus finmarchicus* have previously been measured and reported by Gross and Raymont [1942], Køgeler et al. [1987], Foote et al. [1996], and Knutsen et al. [2001]. They have all concluded that such measurements are very difficult to perform since the plankton is difficult to handle. An overview on the methods used to measure these properties can be found in Knutsen et al. [2001]. The ratio between the material density of *Calanus* and the density of water, g, varies strongly according to the stage of the *Calanus*. The values for the density ratio between *Calanus finmarchicus* and water from Knutsen et al. [2001] are given in Table 3.1. Køgeler et al. [1987] have measured the mass density of *Calanus* to vary from 1.022 to 1.036

Table 3.1: The measured density ratio g between *Calanus finmarchicus* and seawater.

Life stage	CIV	CV	CVIf
Knutsen et al.	1.0116 ∓ 0.0020	1.0081 ∓ 0.0021	1.0142 ∓ 0.0034

gcm^{-3}, which corresponds to a density ratio, g, from 0.996 to 1.010. In his paper there is less information on the stages of the copepods, but it is interesting to notice that the plankton is less dense than water for part of the year. This is also found from measurements done by Foote et al. [1996]. The value of the density ratio varies between 0.983 and 1.036.

There is very little reported data available in the literature on the sound speed of *Calanus finmarchicus*. Køgeler et al. [1987] have conducted sound speed measurements on mixtures of *Calanus finmarchicus* and *Calanus hyperboreus*. The overall sound speed ratios over one year were measured to 1.027 ± 0.007. Measurements on only *Calanus finmarchicus* conducted by Foote et al. [1996] resulted in a speed ratio of 1.015 ± 0.009.

It is evident that the variation in and the uncertainties of the acoustical properties set the terms for the accuracy in the concentration estimates of the plankton. According to Køgeler et al. [1987] the magnitude of the variation of the density of *Calanus* is so great that mathematical models should be tuned to the season. According to Greenlaw [1977] 1% change in the density contrast will result in 2 dB change in the target strength. In Figure 2.3 in Chapter 2 the target strength of a modeled *Calanus* was plotted as a function of frequency for body length 1, 2, and 3 mm. The figure shows that the general target strength increases with increasing size of the model sphere. It also shows that the resonance frequency is dependent on the plankton length and that the frequency with the dip in target strength is proportional to $\frac{1}{L}$ of the plankton.

Figure 3.5 shows the target strength according to the fluid sphere model for two of the extreme values of the density ratio reported in the literature. The target strength is very much dependent on the density of the plankton. This is especially the case for the frequency range of interest for such measurement between 0.5 and 1 MHz.

Figure 3.6 shows the target strength with the two measured values for the sound speed of the *Calanus*. The figure shows that the variation in the reported measurements of sound speed ratio has a much smaller impact on the target strength of the model sphere than what is the case for the density ratio.

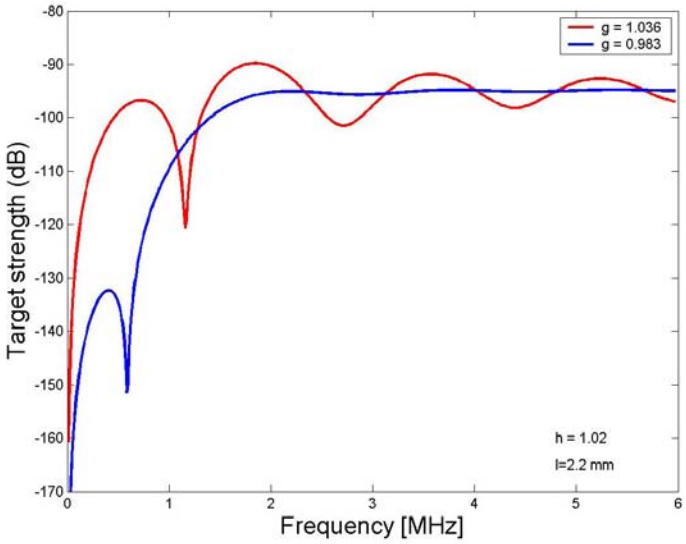

Figure 3.5: Modeled target strength for *Calanus finmarchicus* with body length 2.2 mm and sound speed ratio, h, equal to 1.02. The figure show the target strength for the density ratio, g, equal to 1.036 and 0.983.

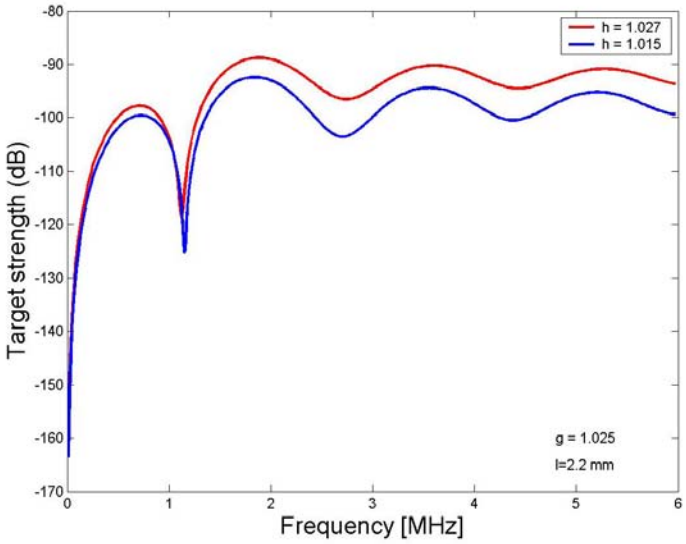

Figure 3.6: Modeled target strength for *Calanus finmarchicus* with body length 2.2 mm and density ratio, g, equal to 1.025. The figure show the target strength for the sound speed ratio, h, of 1.015 and 1.027.

3.3 Estimation of zooplankton population

The strength of the volume scattering from the zooplankton is a function of the concentration and size distribution of the plankton and the measurement frequency of the transducer. The scattering model gives the relation between these parameters. The overall accuracy of these estimations of the plankton size distribution and concentration depends on the accuracy of the measurements of volume scattering from the organisms, the accuracy of the individual scattering behavior of the organisms, and the accuracy of the estimation method itself.

It is assumed that the total scattering intensity is equal to the sum of the intensities of the contributions from each individual plankton in the beam. If the scatterers are uniformly and homogeneously distributed inside the beam, the effects of range and transducer directivity can be corrected for. The transducer properties and the transmission of the sound in water are described in more detail in Chapter 2.

According to the assumption of linearity between the total intensity of the scattering and the sum of the intensity contributions from the individual plankton, shadow effects and multiple scattering effects are assumed to be negligible. For the populations of small zooplankton typical seen in the sea, this assumption is thought to be valid. A theoretical study of the shadowing effect in densely aggregated zooplankton layers has been conducted by Gorska [2000] and Gorska and Chu [2001] where it was found that the extinction can be neglected for small krill species which size are much larger than *Calanus finmarchicus*.

Since the measurement of the volume reverberation is a stochastic quantity, the data has to be averaged over several backscattered echoes. The measurements are subject to random errors due to the finite number of measured echoes. The accuracy of the measurements is limited by noise both originating from the sea and the receiver electronics. Further elaboration on the statistical description and sources of errors in measuring the backscatter signals from clouds of scatterers can be found in Greenlaw and Johnson [1983]. The validity of the linearity assumption is questionable if the concentration of plankton is low.

The method of multi-frequency estimation of zooplankton concentrations, which is based on the linearity assumption, is described in the following. The notation in the equations follows the notation of Medvin and Clay [1998].

The volume scattering coefficient, s_V, was defined in Equation 2.7. Given a linear relationship between the sum of the backscattering cross sections and

the number of scatterers inside a 1 m^3 volume, the volume backscattering coefficient can be stated

$$s_V(f) = n < \sigma_{bs} > \tag{3.6}$$

where n is the number of the scatterers per cubic meter and $< \sigma_{bs} >$ is the mean backscattering cross section. The volume scattering coefficient is a function of the frequency.

The multi-frequency estimation method states that with a number of M frequencies, M volume scattering coefficients can be defined, one for every frequency

$$s = \begin{bmatrix} s_V(f_1) \\ s_V(f_2) \\ \vdots \\ s_V(f_M) \end{bmatrix} \tag{3.7}$$

The size distribution of the scatterers is represented by N size classes. The density within the size classes is represented with a vector n.

$$n = \begin{bmatrix} n_1 \\ n_2 \\ \vdots \\ n_N \end{bmatrix} \tag{3.8}$$

The scattering matrix, S, is defined by the mean volume backscattering coefficient, s, for every frequency and size group. The scattering matrix is given by

$$S = \begin{bmatrix} s_{f_1,1} & s_{f_1,2} & \cdots & s_{f_1,N} \\ s_{f_2,1} & s_{f_2,2} & \cdots & s_{f_2,N} \\ \vdots & & & \\ s_{f_M,1} & s_{f_M,2} & \cdots & s_{f_M,N} \end{bmatrix} \tag{3.9}$$

The mean volume scattering coefficient, s, for every frequency and size group is calculated from the model of the scatterers.

The problem to be solved can be expressed on a matrix form

$$s = Sn \tag{3.10}$$

Equation 3.10 are solved with respect to n. The mathematical estimation problem of solving this equation is not a simple one. There are several ways to estimate the density of every size group. Small errors in the measured

volume backscattering intensity can produce large variation in the estimates. The solution method has to minimize the inherent instability of the problem. Both least square and regularization estimation methods have been used in plankton research, [Greenlaw and Johnson, 1983]. The least square method has been used in this work.

The least squares solution according to Smith and Franklin [1969] is given by

$$\begin{aligned} n^{est} &= \frac{S^T s}{S^T S} \qquad for \quad M \geq N \\ n^{est} &= \frac{S^T s}{(S S^T)} \qquad for \quad M < N \end{aligned} \tag{3.11}$$

For more measurements than unknowns, $(M \geq N)$, the least-squares solution minimizes

$$\epsilon^2 = \epsilon^T \epsilon = (Sn^{est} - s)^T (Sn^{est} - s) \tag{3.12}$$

For $M < N$ the euclidean length of $\left\| n^{est} \right\|$ is minimized.

Calibration errors within the system and the plankton models inaccuracy to represent the spectrum of plankton present will produce inaccurate estimates.

To eliminate the possibility of getting negative concentrations of plankton, an additional constraint to the least square problem is added. This is solved by the NNLS (Nonnegative Least Squares) algorithm by Lawson and Hanson [1974].

$$Minimizes \quad ||Sn - s|| \quad when \quad n_i \geq 0 \qquad \text{for all i} \tag{3.13}$$

The NNLS algorithm has been used in plankton acoustics to solve the inverse problem. According to Holliday and Pieper [1995] experimental work has shown that the NNLS method can allow solutions for cases that are under-determined by factors between 1.5 and 2, meaning the number of size classes N can be up to almost twice the number of measurement frequencies M.

3.3.1 Estimation of plankton concentrations from the APR

One measurement for the APR is defined as the average over several pings. The number of pings, or the duration of one measurement series, can be chosen in the control software of the system, but the default value is 16 pings.

The number of size groups and their properties can be set in the processing software. The default value for the system is three size groups. For the three

frequencies of the APR, the volume backscattering coefficients are

$$s = \begin{bmatrix} s_V(200) \\ s_V(710) \\ s_V(1000) \end{bmatrix} \tag{3.14}$$

In calculations with three size groups, 1, 2, and 3 the scattering matrix is

$$S = \begin{bmatrix} s_{200,1} & s_{200,2} & s_{200,3} \\ s_{710,1} & s_{710,2} & s_{710,3} \\ s_{1000,1} & s_{1000,2} & s_{1000,3} \end{bmatrix} \tag{3.15}$$

The solution of the least square problem reduces to

$$n^{est} = \frac{s}{S} \tag{3.16}$$

which is solved with the use of the NNLS method.

3.3.2 The selection of size groups

The multi-frequency estimation method described earlier in this section will work poorly for situations where there is a linear relationship in the target strength between the frequencies and sizes of the objects. This is approximately the case in the region where the product between the wave number and radius of the model sphere, ka, is much greater than unity for all measurement frequencies, which means that the objects are large compared to the wavelength of the sound wave. The groups should therefore be located in the nonlinear region of the size/ frequency - dependent scattering strength.

There is a nonlinear relationship in target strength between the chosen frequencies of the APR and object sizes corresponding to small zooplankton. It is desirable to set the size groups in such a way that one gets an estimate of the objects with the typical size of the key species. Biological data as shown in Figure 3.4 can be used as input for this selection. In doing this, the backscattered signals from the larger objects have to be separated from the part of the measured signal caused by plankton. This can be achieved by choosing a size group for objects that are larger than plankton. The scattering cross-section is small for all applied frequencies for objects smaller than the adult stages of *Calanus finmarchicus*. This makes the system unsuitable for objects with radius less than 0.25 mm. Most of the backscattered signals without the contribution from larger objects than plankton are caused by scatterers in the size

range of plankton. For selection of size groups in this range, prior knowledge of the relevant plankton can be used. There it is crucial to be aware of the limitations of the method, as small differences in the object size cause large differences in the estimated concentration.

Chapter 4

The Acoustical Plankton Recorder

This chapter describes the configuration and manner of operation of the Acoustical Plankton Recorder. The design of the equipment started in 2001. The circuit boards were built on prototype circuit boards designed in 1995 by the company Oceanor AS in Trondheim, Norway. The rest of the instrument has been developed and built at NTNU as a part of this work. The measurements on and calibration of the instrument are described in Chapter 5 and the post-processing software for APR in Chapter 6.

4.1 Overview of the APR

A sketch of the instrument is shown in Figure 4.1. The system consists of a computer and a coupling unit above water, connected to a steel cylinder which is lowered into the sea. The electronics inside the cylinder is connected to the transducers with cables, and the transducers are mounted on a plate attached to the end-plate of the cylinder. The system has three transducers with the frequencies 200, 710, and 1000 kHz. Background information on the choice of frequencies for the system is given in Chapter 2 and 3. The hardware of the instrument is described in two separate parts in this text, under the headings the probe and the acquisition system. The probe includes all parts of the instrument that are lowered into the water. The acquisition system includes the system above water. The instrument could in principle be pointing in any direction.

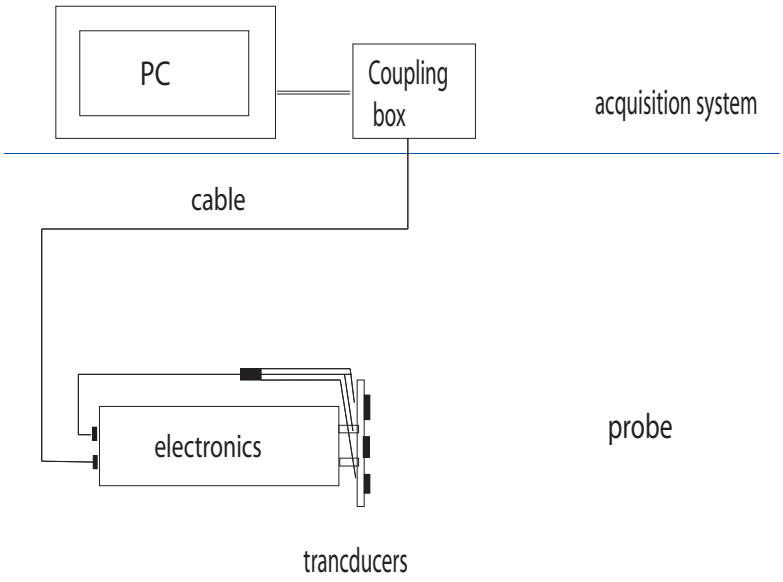

Figure 4.1: A sketch of the Acoustical Plankton Recorder.

4.2 The probe and its contents

The probe includes all underwater parts of the instrument including the transducers, electronics, steel cylinder and cables. A photography of the open cylinder and the end-plate with the transducers is shown in Figure 4.2.

4.2.1 The transducers

The same piezoelectric transducers are used both for transmission and reception. The transmission and reception properties of the transducers are presented in Chapter 5.

The transducers are placed on a steel end-plate which is mounted to the steel cylinder. The transducers are positioned in a triangle to maximize the overlap of the beam, see Figure 4.2.

The transducers with resonance frequencies 200 kHz and 710 kHz have been purchased from Simrad AS (Transducer type 200_7^{TM} and 710-30-EP^{TM}). The third transducer at 1000 kHz was produced at the Department of Electronics and Telecommunications, NTNU. The two Simrad transducers were calibrated

Figure 4.2: A photography of the open cylinder containing the electronics. The transducers are shown to the right. The 1 MHz transducer is the smallest one to the left, the 710 kHz is to the right and the 200 kHz is at the bottom.

by the manufacturer at the time they were purchased, but new calibration was conducted of all three transducers during the work at the laboratory.

4.2.2 The electronics

The electronic circuits of the system are contained inside a steel cylinder, see Figure 4.2. The electronics consists of a control unit, three circuit boards for transmission and three boards for reception, one for each frequency. The electronics and transducers for one frequency are referred to as one channel in this text. The control unit inside the cylinder is coupled to the control and timing of the system from the computer.

The transmitter boards are composed of an oscillator circuit, switches to control the oscillator signal, and an amplifier circuit. Sinusoidal signals are generated by crystal oscillators at the frequencies 200 kHz, 710 kHz, and 1 MHz. The oscillators run as long as the power for the channel is turned on. A pulse signal controlled by the acquisition system switches the oscillator circuit on and off. The amplifier circuit is designed for minimum energy consumption and the gain is regulated by a switch to be low between the transmitted pulses. A capacitor has to be charged before a pulse can be transmitted to the transducers. A detailed description is given in Appendix A. The output signal can be measured at the output of the electronics before the cable to the transducers.

The received signals at the transducers pass through several electronic circuits. The receiver circuit boards consist of a protection circuit, band-pass filter, envelope detector, low-pass filter, and a three amplifiers. A schematic presentation of the order of operations of the receiver electronics for all channels is shown in Figure 4.3.

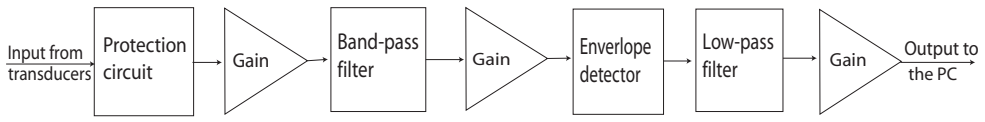

Figure 4.3: A sketch of the principle stages of the receiver electronics.

The circuit description of the electronics is given in Appendix A. The electronics has been furnished with ten test points to ensure easy access to the analog signals during testing in the laboratory. Chapter 5 addresses measurements

of the analog signal at different positions through the receiver electronics and the total gain of the electronics at each channel.

When the power of one channel is turned on by the acquisition system, the receiver and transmitter circuit are connected to the batteries. This is done in the control unit inside the cylinder. The control unit also controls that the received signal from the active channel is sent to the acquisition system. It manages the signal from the acquisition system that connects the oscillator to the rest of the transmission circuit to make pulses with a specified pulse length. The signals to and from the acquisition system are described in more detail in Section 4.3.

4.2.3 The cylinder and the cables

The cylinder also contains the batteries. Rechargeable NiMH-batteries are mounted inside the cylinder. The positively charged battery, SK1218L, has a capacity of 18 Ampere-hours (+12V) and drives both the receiver and transmission electronics. The negatively charged battery, SK129L, has a capacity of 9 Ampere-hours (-12V) and is used by the receiver electronics. Newly charged, the voltage of the batteries is about $\pm$13.5 V, but it decreases towards about $\pm$12 V after some use.

A 100 meter cable runs from the acquisition system to the probe. The 12-core screened cable is isolated with waterproof PVC and has an outer diameter of 16 mm. The cable between the cylinder and the transducers is 1.5 meter. The cable is PVC-covered and splits up into six cables at the transducer end of the cable. At the time the cable was purchased it was intended to use six frequency channels; this was later reduced to three channels and therefore three of the cable ends are not used and sealed.

The stainless steel cylinder is 84 cm long and the total length is about 1 meter with the transducers attached. The diameter of the cylinder is 21 cm. The size of the cylinder and the mounting of the electronics ensure easy access to the electronics when the cylinder is opened. This is important for this prototype instrument which has requested comprehensive testing and adjusting of the different components of the system. The cylinder is sealed with a rubber gasket to prevent water from entering into it. Furthermore, it is equipped with a moisture sensor which switches on a red light in case of a water leakage.

4.3 The acquisition system

The term acquisition system refers in this text to the part of the APR that is above the water. The PC contains the control system for the APR and the system for logging measured data. The PC is connected to a coupling box, which is connected to the probe through a 100 meter cable.

The development of the control and data logging system began in 2003. The system has been made flexible and modifications are possible as different needs for the system are identified. The data control system has several tasks. Firstly it activates the different channels. Pulses can then be sent and received on this channel. Secondly, it transmits pulses with desired properties such as pulse length and repetition frequency. The acquisition system records the measured signals from each of the three channels. A flowchart of the data acquisition system is presented in Figure 4.4. The system is described in detail later in this section.

4.3.1 Specification of the acquisition software and hardware

The data control and acquisition system is built up of a computer (currently a Dell optiplex GX270^{TM}) with a built in PCI card (DT303^{TM}) and accompanying software. The hardware (DT303^{TM}) and software (DT Measure Foundry^{TM}) are bought from the company Data Translation Inc. The PCI card provides a multifunctional data acquisition unit, which contains analog input lines, digital I/O lines, and counter/timer channels. The analog inputs have a 12 bits resolution and a sampling rate of 400 kS/s. The DT Measure Foundry^{TM} test and measurement application builder software is used for software design. A photography of the interface of the developed program produced with DT Measure Foundry^{TM} is shown in Figure 4.5.

The PCI bus interface chip on the card allows for high speed, bus-mastering data to the host computer. A block of memory is set aside in the computer and the board performs bus master data transfer without CPU intervention, allowing the CPU to perform data analysis and graphics.

The total system performance of the DT303^{TM} card is specified with the ENOB (Effective Number of Bits) measurement. Derived from a board's signal-to-noise ration, ENOB specifies the overall accuracy of the A/D transfer function. The ENOB of the board is specified to be 11.5 bits.

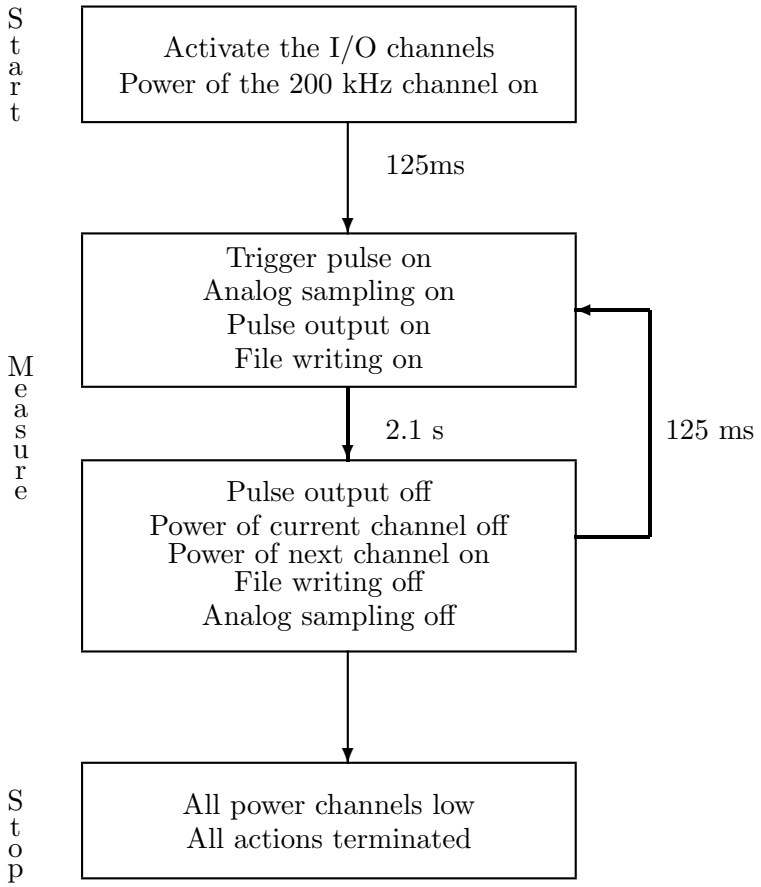

Figure 4.4: A flowchart of the data acquisition system.

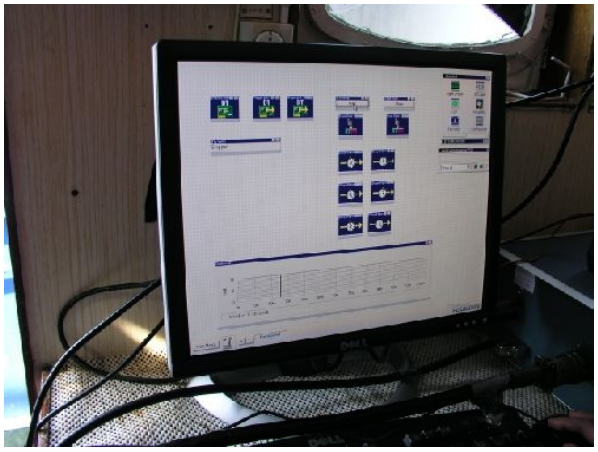

Figure 4.5: A photography of the acquisition software interface.

4.3.2 Coupling to the electronics

Three types of signals are sent between the computer and the electronics. The power control signals and pulse output signals run from the computer to the probe, and the received analog signals pass through the electronics in the probe to the computer.

Power control

The electronics are constructed so that only the active channel (the one which sends acoustic pulses into the water) is powered because the system is constructed to run on batteries. The power channel on the PCI card switches the electronics of this channel on so that it will be connected to the batteries in the cylinder.

Pulse output

The pulse output from the PCI card in the computer controls the properties of the pulse transmitted into the water. The length of the output pulse is equal to the length of the transmitted pulse with number of periods corresponding to the different frequencies.

Analog signal in

The active receiver channel sends the input signal to the computer. For this reason only one analog channel is used to record the received signals. The gain of the electronics is adjusted to exploit the whole range of the computer.

4.3.3 Realization of the acquisition system

The flow chart in Figure 4.4 represents the different steps of the acquisition system. Each step is described in the following. Figure 4.6 shows the different signals as a function of time. There are two timers that control the different actions. The hardware timer on the PCI card is very accurate, while the accuracy of the software timer is more limited.

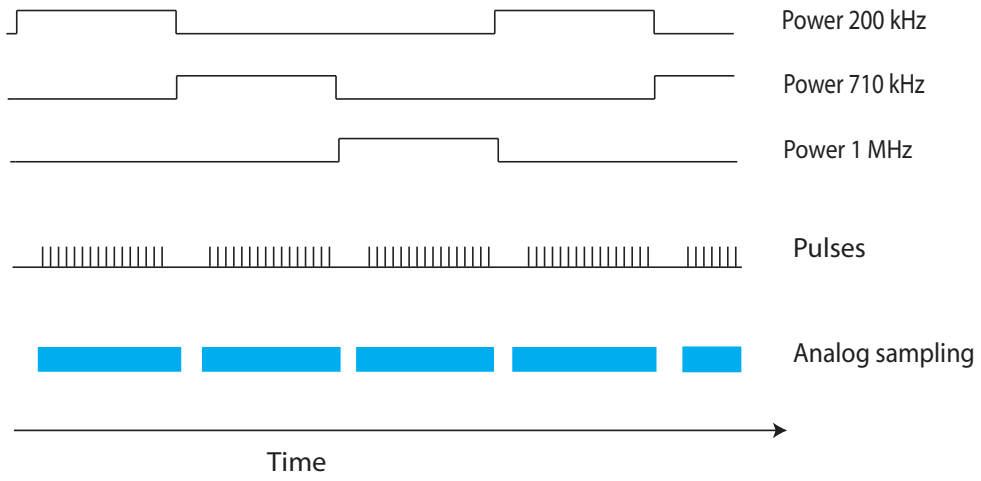

Figure 4.6: The three power signals, the pulse output signal and the analog sampling as a function of time.

Power control of the three channels

Digital I/O lines are used for the power control channels. In the beginning all the three power channels are turned on. The 200 kHz channel is set high and the 710 kHz and 1 MHz channels are set low. This means that power is supplied only to the electronics of the 200 kHz electronics (the power signal from the PCI card connects the electronics of this channel to the batteries).

When the power to the first channel is turned on, a delay operation is activated. This means that no actions are taken from the software until the delay time has elapsed. The reference value for the delay time is 125 ms allowing a capacitor to be charged so that pulses with the desired power can be transmitted.

After the delay time has elapsed, a sequence of actions takes place. The trigger pulse (see Rate generation) is turned on. Then the output pulse channel is turned on. The analog sampling input channel is turned on. The first output pulse and analog sampling will now start when the first trigger pulse

is detected. The file writer function is turned on when the analog sampling starts. Data buffers are written to file (see The acquisition of the signals). Then another delay operation is activated. The default value of this operation is 2.1 seconds. During this time the system will continuously emit pulses with specified repetition rate and pulse length for this first channel. When the delay time has elapsed another sequence of actions will start. The trigger pulse is turned off. This also occurs to the analog data channel and the I/O channel for the pulse output. Then writing to file is stopped and the power channel for the 200 kHz channel is set low. The power to the 710 kHz channel will now be set high and a delay operation (with default value 125 ms) will be activated during which time the capacitor of the 710 kHz electronics will be charged. The sequence of actions will be the same for this channel as for the previous one. The same happens for the 1 MHz channel. After the 1 MHz channel has been run, the 200 kHz channel will run again and the system will switch between the three channels until the stop button is pressed and all actions are terminated.

The timer/counter functions on the PCI card are not specified to be used to trigger the digital I/O lines that are used for the power signals. A software timer has to be used to control these operations. The accuracy of this Windows timer makes it impossible to time events with higher accuracy than 10 ms. But this has no effect on the accuracy of the system, since the timing of the transition of the power signals from low to high is not critical. The actions of the acquisition system are sequenced so that one power signal will be turned off before the next one is switched on.

Rate generation

To create the desired pulse repetition three counter/timer channels on the PCI-card are used. Two of the channels, counter 0 and 1, are cascaded to make a timer signal that triggers the third counter, counter 2. Figure 4.7 shows the timer signal from the cascaded counters and the pulse output signal that is emitted to the electronics.

Each of the counter/timer channels are 16 bits. The two first counters cascaded produce a 32-bit channel. The internal counter/timer clock uses a 20 MHz time base. For the 32-bit cascaded counter, the frequency that can be specified for the clock output signal is between 0.00465 Hz and 10 MHz. This corresponds to a rate of the output signal of between 1μs to 215 s. (In the case of a single counter the minimum output frequency would give an output rate of about 3 ms, which is too fast for the purpose of the data logger.)

A reference value of 8 Hz is used for the output rate of the cascade counter.

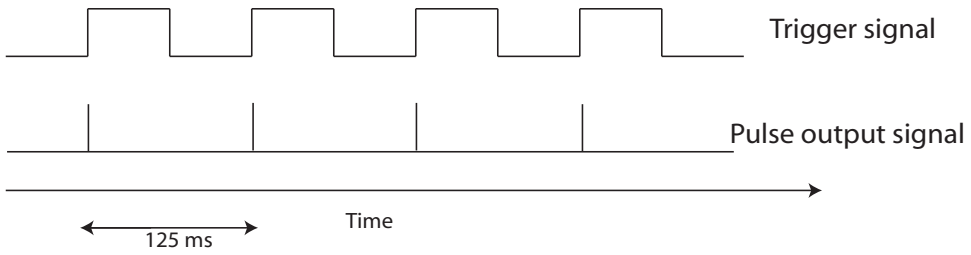

Figure 4.7: The upper signal is the 8Hz (default) signal produced by the DT303^{TM} card that works as a hardware trigger for the second signal. The second signal is the output pulse signal sent to the electronics of the instrument.

This corresponds to a pulse repetition rate of 125 ms. The counter is controlled by the software. When the counter is turned on it generates a continuous pulse output signal. This output signal is used as a trigger signal, an external clock, for the third counter. The third counter is used in the repetitive one-shot mode. This means that a pulse is transmitted every time the counter is triggered. The length of the transmitted pulses is regulated by the software, but as a reference value a 0.1 ms pulse is used. This transmitted pulse controls the pings emitted by the transducers.

The acquisition of the signals

The analog signal from the electronics is connected to an AD-converter on the PCI card. The analog low-pass filter has a cut-off frequency of about 17 kHz so that the analog signal has to be sampled at a rate above 35 kHz which corresponds to the Nyquist frequency. The sampling frequency is set to the default value of 50 kHz. This corresponds to the analog signal being sampled every 20 ms. The clock source of the sampling is that of the PCI card.

The voltage varies between 0 and 10 V. The analog input signal from the electronics is unipolar and the analog amplification is adjusted for each channel to exploit the entire voltage range. Consequently, the amplification in the software is set to 1. The analog input resolution of the PCI card is 12 bits, and the specified ENOB (Effective Number Of Bits) is 11.5 bits. Tests show that the measured data is digitalized into 2.5 mV steps, which corresponds to a resolution of almost 12 bits.

The start of the analog input is triggered by the same trigger as the pulse

transmission of the rate generator. The first rising edge of the upper signal in Figure 4.7 starts the sampling of the data. The data is continuously sampled into data buffers. The default buffer size is set to 6250. This corresponds to 0.125 seconds of sampling. The stop in the analog sampling is controlled by the software trigger. Only full data buffers are saved so that additional sampled data caused by the slow reaction of the software trigger will not be recorded. Every data file will have exactly the same size.

The data can be saved in two formats. The default save setting saves the data as ASCII files. The writing of this data is more time consuming than the alternative format, but the advantage is that the files can be imported directly into MATLAB^{TM} for further signal processing. The other format is software defined and can only be accessed through the Data Translation Inc software. Data saved in this format can be converted later, but while writing these files is fast the conversion of the data is very time consuming. Since 16 pings are emitted in the default setting, 16 buffers with 6250 values, totally 100000 values, will be saved in each file. The extra time consumed on the file writing as ASCII files is in the order of 0.2 seconds for every file.

Since the trigger pulse, which is very accurate, controls both the pulse transmission and the start time of the analog sampling, the return time of the first ping will occur at the same position in every data file, and there will be exactly 125 ms between every ping.

The coupling box

An electronic safety switch is used to secure that all power channels cannot be turned on simultaneously. If this happened (could be the case during the setup of the computer before the software is turned on) no signal would be sent to the instrument.

The moisture sensor is connected to a lamp in the coupling box, which will light up in case water is leaking inside the steel cylinder.

Chapter 5

Verification and calibration

The performance of all parts of the APR has been verified through comprehensive testing. Properties of the system are reported in this chapter. The variations, uncertainties and critical parts and parameters of the system are addressed.

The calibration of the system is the determination of the transfer function between the voltage in the transmitting and receiving electronics and the pressure of the sound pulse in the water. Calibration of the system is necessary to be able to calculate the system parameters both in sending and receiving signals and in turn to analyze the received data.

The calibration was conducted with a calibrated hydrophone and standard targets whose acoustic scattering properties were known. The verification and calibration measurements described in this chapter are a resume of a number of measurements on the APR conducted at different times during the project.

5.1 The facility and measurement procedure

The main items used in these measurements were a hydrophone, the water tank, and the oscilloscope. All measurements were conducted at the Department of Electronics and Telecommunications at NTNU.

The water tank used for all calibration measurements has the size 2x3x2 meters. The tank was cleaned and filled with water and left overnight to avoid particles and bubbles in the water. The transducers, hydrophone, and measurement spheres were washed with a wetting agent to avoid air bubbles on

the surface of the equipment.

The hydrophone used in this calibration is Model ITC-6128^{TM} from International Transducer Corporation, see Figure 5.1. It is designed as a calibration hydrophone for high frequency measurements. The hydrophone was calibrated from the manufacturer in the frequency range from 100 kHz to 1 MHz. The beam pattern of the hydrophone in the XY plane showed very little variation to changes in angles referred to the reference point of the hydrophone. For the 200 kHz and 1 MHz frequencies, the variation within ten degrees around the reference point was below 0.25 dB. For the 710 kHz frequency the variation was somewhat larger, but well below 1 dB. The attached 12 ft PVC cable was wired with the shield and low terminal to ground as was the case for the calibration of the hydrophone.

Figure 5.1: The Model ITC-6128^{TM} hydrophone from International Transducer Corporation used in the calibration measurements.

The hydrophone was mounted directly to the oscilloscope. A Dual-Channel Digital Oscilloscope by LeCroy Corporation was used for measurements of the electrical characteristics. The input impedance of the oscilloscope was $1 Mohm$. The errors introduced by the wiring of the hydrophone to the oscilloscope should be less than 0.05% for the 200 kHz signals and even less than that for the higher frequencies.

The calibration was conducted in fresh water. This was done because the tank used for this measurement did not have access to seawater. It was considered to make seawater from sea salt and fresh water, but this idea was abandoned because there were concerns about salinity gradient within the tank. The difference in absorption from fresh to sea water was compensated for in the analysis.

The three transducers were mounted to the steel plate, see Figure 5.2. The

Figure 5.2: A photography of the transducers mounted on the wall of the water tank. The upper left transducer is the 1 MHz transducer produced at the Department of Electronics and Telecommunications at NTNU. The upper right is the 710 kHz and the lower is the 200 kHz transducer produced by Simrad AS.

steel plate was connected to a steel bar, which then was firmly attached to the side wall of the tank. The transducers were pointing in the horizontal direction. The position of the hydrophone and standard spheres were recorded in the vertical and horizontal directions. The hydrophone was mounted on a metal rod and the cable connected to the hydrophone was attached directly to the oscilloscope. The standard spheres were suspended in a small net of 0.2 mm fish line.

The use of a known hydrophone for calibration is a secondary method of calibration [Bobber, 1988]. The accuracy of secondary calibrations can never be better than the accuracy of the primary calibration of the reference hydrophone.

The calibration of the transmitting response of the system was made by placing a hydrophone with known free-field voltage sensitivity at the distance d from the transducer and on its acoustical axis.

In order to have free-field condition it was important to avoid interference from the boundaries (sidewalls, bottom, and surface). Because the system uses

pulsed sound the effects of interference originating from boundaries, standing waves, and electrical crosstalk are eliminated or at least reduced by time gating. In addition it was important to have a low ambient noise level and to use a water medium free from anything that can cause refraction and scattering. In the far field of the transducer the linear field decreases exponentially with range. The standard criteria according to Bobber [1988] for the far field of a circular piston are

$$d \geq \frac{\pi a^2}{\lambda} \tag{5.1}$$

For the transducers used on the Acoustical Plankton Recorder, this requires the distance between source and receiver to be more than 0.6 meters.

The calibration was conducted at one channel/frequency at a time. The pulse length was 0.09 ms if not specified otherwise. The electronics and control and acquisition system were connected and ran in the same way as the system used at sea. The position of the hydrophone was then moved horizontally through the beam with 1 cm intervals. When the exact position of the maximal signal was found in the horizontal direction, this coordinate was used and the beam pattern was measured with 1 cm intervals in the vertical direction. This was done for all frequencies with a transducer - hydrophone distance of 1 meter and repeated for a distance of 2 meters.

5.2 The transmitter

5.2.1 Pulses

Pulses of desired length are generated in the electronics. Figure 5.3 through 5.8 show the transmitted pulses from the electronics to the transducers. The pulse length in these figures is 0.09 ms for all three frequencies. The upper left panel of each figure shows the entire pulse in the time domain. The lower left panel of the figures contains a segment of the pulse. The right panel contains the frequency spectrum of the transmitted pulse.

Both the time and frequency representation of the pulses show that the signals are not clean sinusoidal signals, but contain higher harmonics. The frequency representations demonstrate that the fundamental frequencies are 200 kHz, 710 kHz, and 1 MHz, respectively.

When the oscillator is turned on, the pulse goes through a transition period before it reaches steady state. When the pulse control is turned off, the system continues to oscillate at its resonance frequency and the pulse goes through

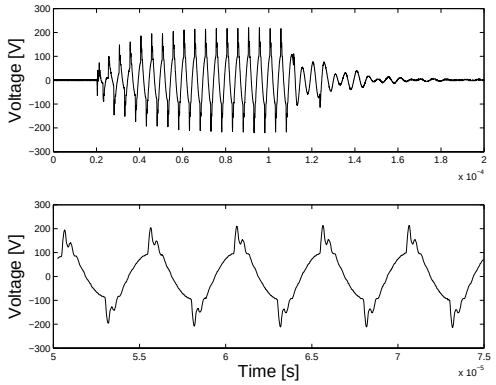

Figure 5.3: Time domain representations of the 200 kHz pulse.

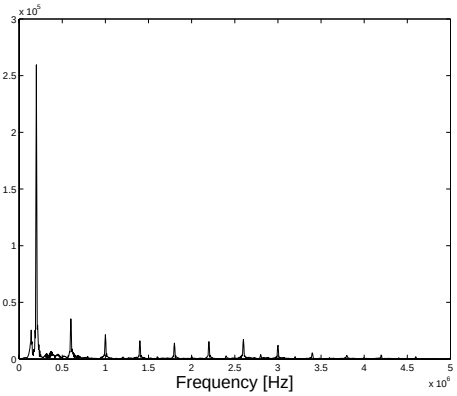

Figure 5.4: Frequency domain representation of the 200 kHz pulse.

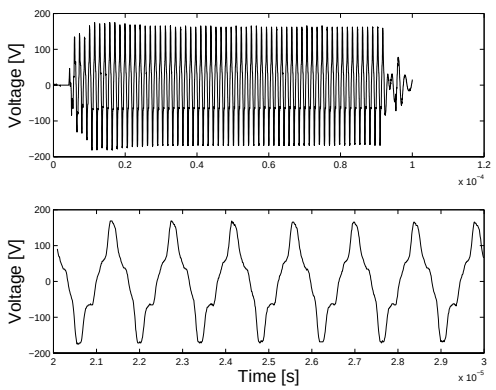

Figure 5.5: Time domain representations of the 710 kHz pulse.

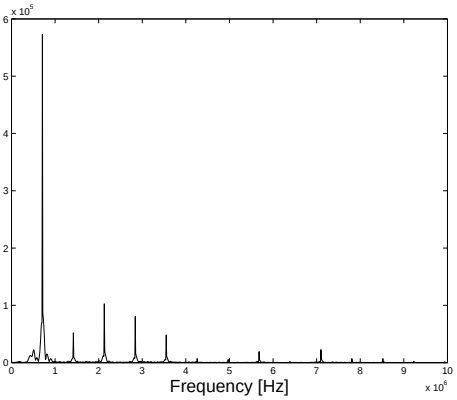

Figure 5.6: Frequency domain representation of the 710 kHz pulse.

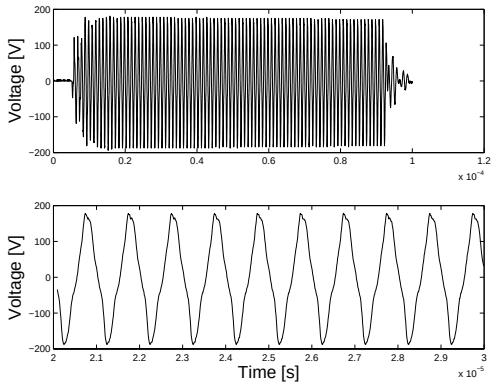

Figure 5.7: Time domain representations of the 1 MHz pulse.

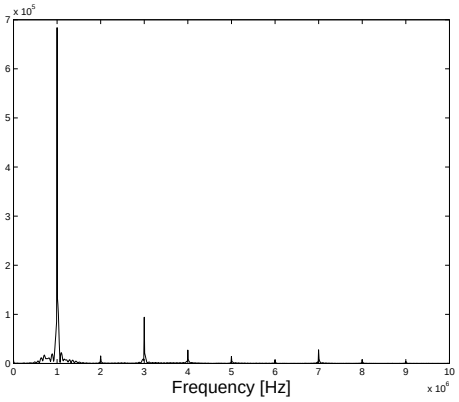

Figure 5.8: Frequency domain representation of the 1 MHz pulse.

another transient period. The minimum duration of the transmitted pulse is given by the decay time constant of the electronics and the transducer and the requested bandwidth of the pulse. A pulse length of 0.09 ms is considered the minimum duration of a pulse. The duration of the steady state phase for the shortest pulse length is about 13 cycles for the 200 kHz frequency, see Figure 5.3. For a shorter pulse than this the bandwidth of the pulse would exceed the bandwidth of the electronics. Discharging of the capacitor of the transmitter electronics for long pulse lengths cause the power in the pulse to decrease throughout the pulse. A pulse length of 0.5 ms is thought to be a maximum length of the system, but any pulse length can be specified by the operator in the acquisition system.

The pulses are filtered as they pass through the transducers. This filtration, the fact that the pulses from the electronics are not pure sinuses, and the drop in power from the batteries after some time, complicate the estimation of the exact power that reaches the transducers.

5.2.2 Voltage and power to the transducers

The output signals were measured at the output of the transmitter electronics. This means that the measurements were performed before the cable that connects the electronics to the transducers. The measured output voltage level is given in Table 5.1.

A number of measurements have been conducted on the output signals. There

Table 5.1: The output voltage for the three frequencies.

Frequency	Output voltage
200 kHz	570 V_{p-p}
710 kHz	420 V_{p-p}
1 MHz	470 V_{p-p}

are some variation in the measured output voltage. This is caused by the variation of the power of the batteries. This variation may cause errors of about $\pm 1dB$ in the measurement within a time period of some days with the continuous running of the acoustical recorder.

The output power to the transducers is higher than the limit specified for those transducers. The short pulses and slow repetition rate prevent destruction of the piezo-electrical elements of the transducers. The output power into the water is so high that nonlinear effects cannot be excluded. Because of the limited size of the water tank, the effects of nonlinearity in the sound level on the acoustic axis are hard to measure. Non-linear effects in the 200 kHz beams have been reported in Tichy et al. [2003]. In the case of non-linear effects, calibration on the basis of measurements conducted at a distance of 2 meters would cause an overestimate of target strength at distances less than 2 meters and an underestimate above 2 meters.

5.2.3 Source level

Measurements of the source level, SL, corrected for fresh water, are given in Table 5.2. As defined in Chapter 2, the source level is the sound pressure on the beam axis in dB relative to 1 μPa at a reference distance of 1 meter. Correction factors used for fresh water compared to sea water are taken from Medvin and Clay [1998].

Table 5.2: The source level, SL, calculated from measured hydrophone signal at distances of 1 and 2 meters from the transducers.

Frequency	Distance 1 meter	Distance 2 meters
200 kHz	220.5 dB re 1 μPa	221.4 dB re 1 μPa
710 kHz	217.7 dB re 1 μPa	217.0 dB re 1 μPa
1 MHz	209.9 dB re 1 μPa	210.0 dB re 1 μPa

The source levels determined on the basis of measurements at 1 and 2 meters vary within 1 dB. The 200 kHz channel has the highest source level, and the 1 MHz the lowest.

The difference in source level of about 1 dB for the 200 kHz signal can be caused by the hydrophone not being far enough away from the transducer. The far field condition might not be entirely met at this distance at this frequency. Nonlinearities in the beam can also explain the difference in source level at the two distances. The correction of the absorption from fresh water to sea water is less than 0.1 dB per meter for the three frequencies at the water temperatures in the laboratory. Inaccuracies in this correction have limited effect on the calculated source level.

5.2.4 The transmit voltage response

The transmit voltage response, TVR, is calculated according to

$$TVR = SL - 20 \log \frac{U_{out}}{U_{ref}} \tag{5.2}$$

where U_{ref} is 1 V. The results of these calculations are given in Table 5.3. The transmit voltage response is quite similar for the two lower frequencies and almost 10 dB less for the highest frequency.

Table 5.3: Calculated transmit voltage response for the three frequencies.

Frequency	Calculated transmit voltage response
200 kHz	174.9 dB re 1 μPa/V
710 kHz	173.9 dB re 1 μPa/V
1 MHz	165.6 dB re 1 μPa/V

The calculated TVR for the 200 kHz transducer is lower than the value given by the manufacturer. According to Simrad AS the TVR for 200 kHz is specified to be 180.1 rel 1 μPa/V. The influence of the cable and the specific waveform makes a direct comparison to the specification from the manufacturer difficult. For more information on the waveform of output signal, see Section 4.2.2.

5.2.5 Beam pattern

The beam patterns measured for the three frequencies are shown in Figures 5.9, 5.10, and 5.11. The data are corrected for the transmission loss and normalized

to the maximum signal strength measured at 1 meter.

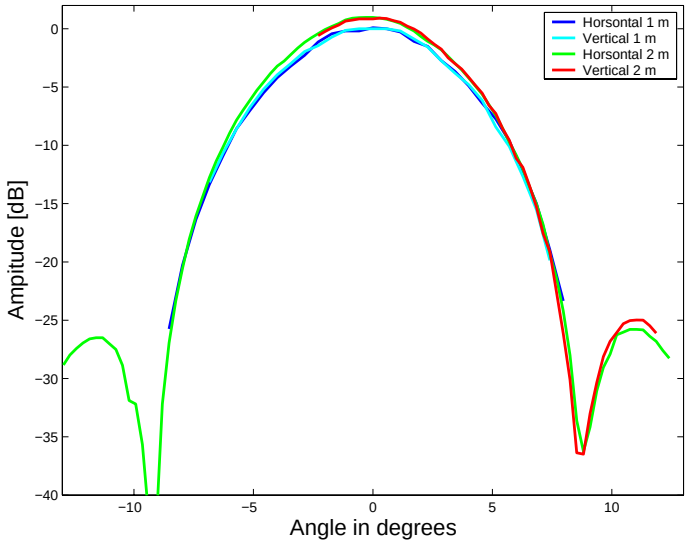

Figure 5.9: The beam pattern for 200 kHz transducer.

Measurements were conducted in both the vertical and horizontal directions and at distances 1 and 2 meters from the transducer. The figures can be compared with the plot of the directivity function of a circular plane disk in Figure 2.4.

Figures 5.9 through 5.11 show that all beams are nearly symmetric, meaning that the beam pattern is the same in the horizontal and vertical directions, which were to be expected as the transducers were circular. The level of the first side lobe of the 200 kHz transducer is approximately -25 dB. The beamwidth of the 200 kHz and 710 kHz transducers are both nearly 5.5 degrees following the definition in Chapter 2, but the beam patterns of the transducers are different. The main lobe of the 710 kHz transducer is quite narrow and the level of the first side lobe is -15 dB. The 1 MHz transducer has a much wider beamwidth of 7.5 degrees. Measurements in the horizontal direction indicate side lobes of -20 dB.

The directions of the three beams are shown in Figure 5.12. The measured beamwidth of the three transducers and the position of maximum beams strength are the bases for calculations.

The beamwidths are the same for the 200 kHz and the 710 kHz transducer, so the dimensions of the beams of these frequencies are the same as can be seen

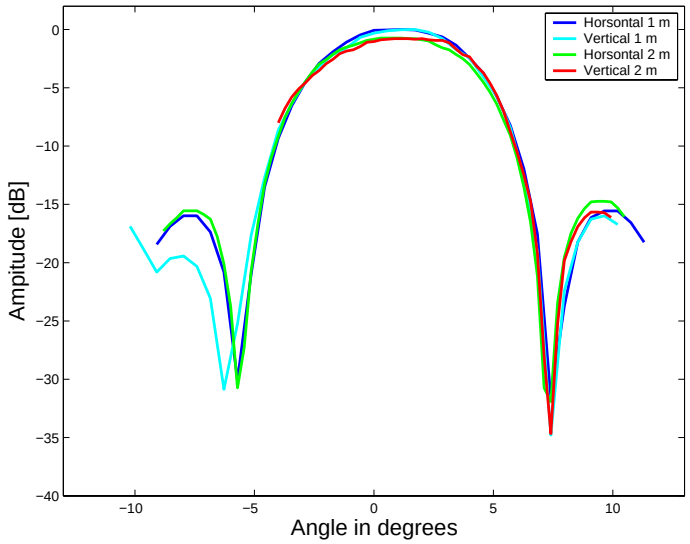

Figure 5.10: The beam pattern for 710 kHz transducer.

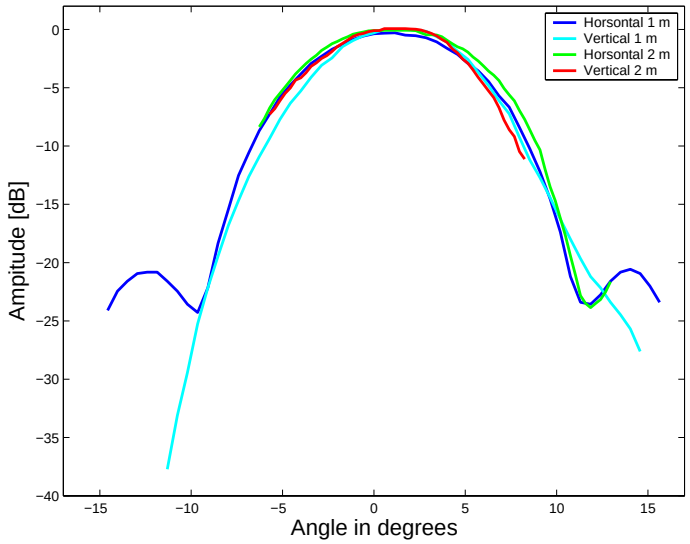

Figure 5.11: The beam pattern for 1 MHz transducer.

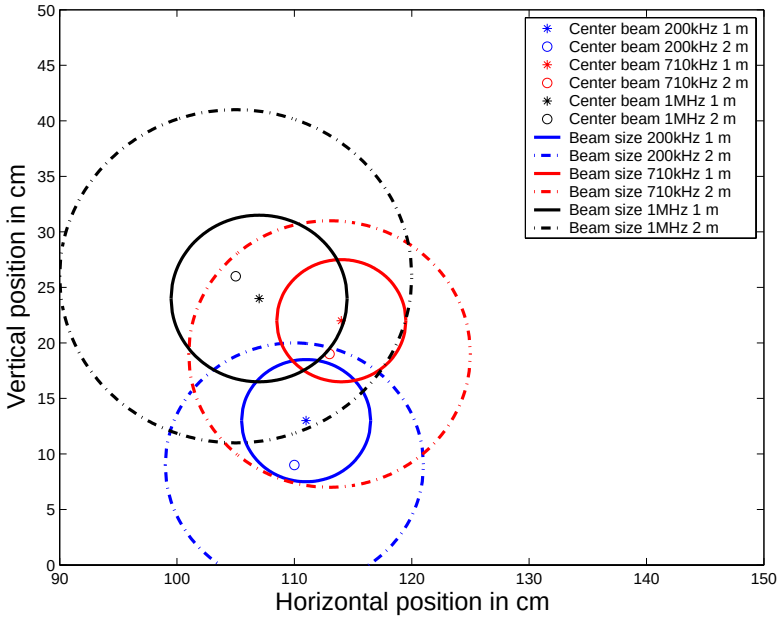

Figure 5.12: The position and size of the beams from the three transducers.

from the figure. The beams of the three transducers overlap, but they do not cover exactly the same volume. Another aspect to be aware of with the APR is the size of the beam. The diameters of the beams at a distance of 2 meters are only 20 to 30 cm.

The direction of the beams could be altered by adjusting the angles of the transducers mounted on the plate. An adjustment of the transducers by 3 degrees could change the position of the acoustical axis with about 5 cm at 1 meter distance. An adjustment in angle in a controlled environment, such as in a water tank, is quite manageable. However, this instrument is used under rough conditions during transport and at sea and the angles of the transducers can easily be altered by a couple degrees due to rough handling.

5.2.6 Pulses on the hydrophone

The signals received on the hydrophone at the three frequencies are shown in Figures 5.13, 5.14, and 5.15. The shape of the signals received at the hydrophone can be compared with the shape of the pulses from the electronics to the transducers.

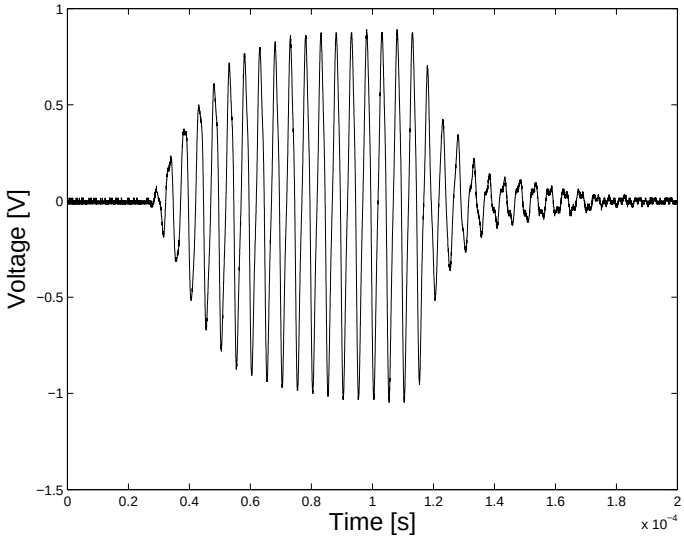

Figure 5.13: The transmitted pulse from the APR measured at the hydrophone for the 200 kHz channel.

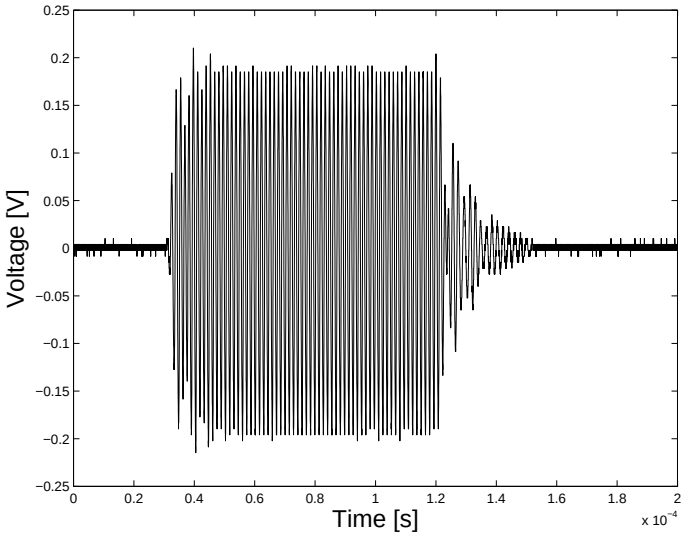

Figure 5.14: The transmitted pulse from the APR measured at the hydrophone for the 710 kHz channel.

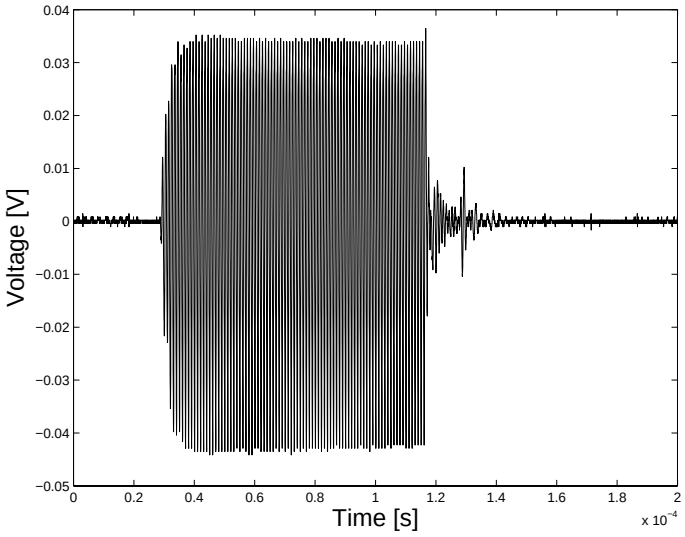

Figure 5.15: The transmitted pulse from the APR for the 1 MHz channel.

5.3 The receiving system

Measurements on the properties of the receiver system of the APR, including the transducers, cables, receiver circuits of the electronics, and sampling and recording system, have been conducted. All the properties of the receiver electronics have been measured separately, and the properties of the complete receiving system can be resolved from the data on the individual parts of the electronics. Receiver sensitivity of the complete system was also measured. The source level of the system was known from the calibration of the transmitting system, a calibration sphere with known target strength was used, and the received voltage into the computer was measured.

It is problematic to use standard spheres in the calibration in the small water tank. The sensitivity of the system is so high that the received signal from the calibration spheres on the acoustical axis of the system is saturated and the signals are clipped in the electronics. To avoid this problem and to be able to measure the receiver sensitivity of the whole system, changes had to be made to the gain setting of the electronics during calibration. The reductions in gain were estimated both from theoretical calculations and from direct measurements in the water tank. For measurements of the backscattered signal for the small sphere, see Table 5.4, the theoretical reduction in gain was 28.45 dB. Measurements on this reduction were done by measuring on the first

reflection in the water tank that was not clipped. The backscattered signal of this reflection was measured with and without the gain correction and the two were compared. For the measurements on the large sphere additional reduction in gain was needed to avoid the backscattered signals from being clipped. These modifications have been corrected for in the presented results.

The echo level, EL, and receiver sensitivity, RS, were computed. These calculations are based on the calculated source level, SL, and known target strength of the different spheres. Calculations are done according to equations

$$\begin{aligned} EL &= SL - 2TL + TS \\ RS &= 20 \log \frac{U_{res}}{U_{ref}} - EL \end{aligned} \tag{5.3}$$

where SL is the source level of the transmitter, $2TL$ is the two-way transmission loss, TS the target strength, and U_{res} the measured signal.

5.3.1 Calibration spheres

Two different tungsten carbide spheres were used in the calibration measurements. The sphere diameter, d, and corresponding target strength, TS, are given in Table 5.4.

Table 5.4: The diameter and target strength of the calibration spheres.

	Small sphere, d=10.3 cm		Large sphere, d=38.1 cm	
Frequency	ka	TS	ka	TS
200 kHz	4.31	-52.6[b]	15.96	-39.4[a]
710 kHz	15.17	-50.5[a]	56.0	-40.8[b]
1 MHz	21.57	-51.6[b]	79.8	-40.3[b]

[a] Calculated by the method in Foote [1982]
[b] Modal solution for a sphere with density 14900 kg/m^3 and sound speed 6853 m/s

The product of the wave number and the radius of the sphere, ka, is above 1 for all combinations of frequencies and spheres. For ka higher than about 1 the target strength, as a first approximation, oscillates around an asymptotic value. The exact target strength of the spheres as a function of ka is complex, especially for the high values of ka where there are many resonance frequencies.

The target strength of the spheres is a critical factor for the calculations. The values for the spheres, see Table 5.4, are found in two different ways. The target strength for the large sphere at 200 kHz and the small sphere at 710 kHz are calculated by the method described by Foote [1982]. The method includes incoming sound pulse on a sphere with a specified density and longitudinal and transversal sound speed in water with a given sound speed. These values are used in the calibration calculations since the accuracy of these values is considered better than those of the modal solution of a dense spheres. The target strength of the dense sphere is calculated with density and wave velocity of the tungsten carbide spheres, but does not include the shear wave or that the sound is pulsed. For the 1 MHz channel the calibration calculations are based on measurements conducted on both the spheres.

The fish line, on which the calibration spheres are mounted, gives a small additional contribution to the target strength. This contribution is assumed to be quite small, but could have some influence at the highest frequencies. Given the magnitude and uncertainties of the measurement system, this method is considered adequate for the purpose.

5.3.2 Amplification and receiver sensitivity

The total amplification of the system is given in Table 5.5. The amplifications of the individual parts of the electronics were measured. This was done with the backscattered signals from both spheres and corrected for the changes made in the electronics. For more information on the electronics, see Section 4.2.2.

Table 5.5: The measured total amplification in the electronics.

Frequency	Total amplification
200 kHz	77.3 dB
710 kHz	89.9 dB
1 MHz	95.8 dB

The amplifications of the three channels are quite different, with greatest amplification at the 1 MHz channel. The reason for this is that the received signal on the 1 MHz channel is considerably lower than the received signal on the 200 kHz channel. To exploit the entire range from 0 to 10 Volt of the AD converter, the received signals must undergo different amplification before being sampled.

The measured total receiver sensitivity of the system and the receiver sensitivity of the transducers are given in Table 5.6. The measured sensitivity of the entire receiving system is the sensitivity of the transducers plus the amplification in the electronics.

Table 5.6: The measured sensitivity of the transducers and the entire receiving system.

Frequency	Sensitivity transducer	Sensitivity system
200 kHz	-192.8 dB re 1V per μPa	-115.5 dB re 1V per μPa
710 kHz	-202.5 dB re 1V per μPa	-112.6 dB re 1V per μPa
1 MHz	-209.8 dB re 1V per μPa	-114.0 dB re 1V per μPa

The measured transducer sensitivity was different from the sensitivity given by the manufacturer. The receiver sensitivity given by the manufacturer was -185.5 dB re 1V per μPa for the 200 kHz transducer and -195.5 dB re 1V per μPa for the 710 kHz transducer. The calculated sensitivity of the transducer is based on the measured signal at the end of the cable from the transducers connected to the electronics. For this reason the measured value and the value given by the manufacturer cannot be directly compared, but the difference in the values between the given and measured sensitivity is approximately the same for the two channels.

For the sensitivity measurement on the 1 MHz channel, the calibration sphere had to be placed at a distance of 1 meter for the received signal after the transducer to be measured directly on the oscilloscope.

Figures 5.16 through 5.21 show the echo from the spheres. The first two figures are for the 200 kHz channel, the next two for the 710 kHz channel, and the last two for the 1 MHz channel. The figures to the left show the echo signal measured after being received by the transducers before being transmitted to the electronics. The right figures display the echo from the spheres after the signal has passed through the entire receiving system and the signal has been recorded in the computer. The absolute value of the signals in the right figures should not be compared since the signals have been damped differently in the various channels to avoid saturation in the electronics, but the shape of the signals has not been modified. The small sphere is used at the 710 kHz and 1 MHz channels while the large sphere was used at the 200 kHz channel.

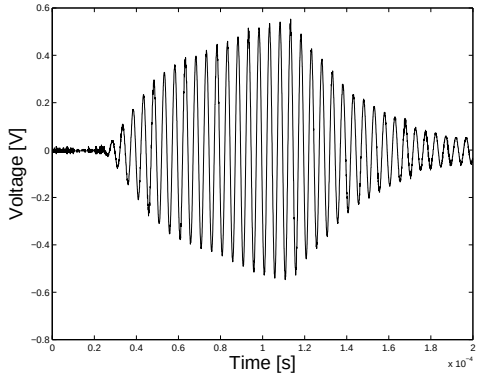

Figure 5.16: The echo of the sphere measured at the end of the cable from the 200 kHz transducer before transmission to the electronics.

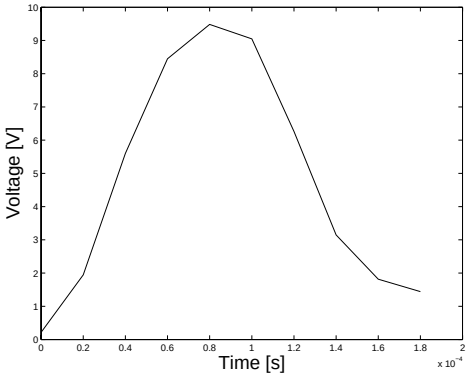

Figure 5.17: The recorded sphere signal on the PC in the 200 kHz channel.

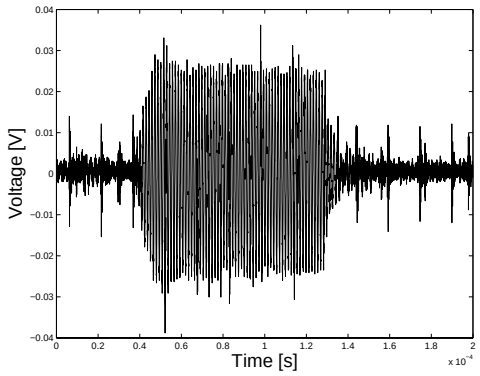

Figure 5.18: The echo of the sphere measured at the end of the cable from the 710 kHz transducer before transmission to the electronics.

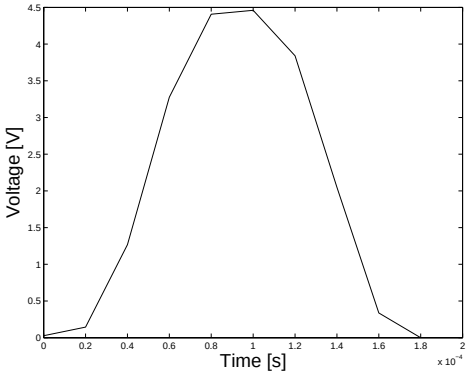

Figure 5.19: The recorded sphere signal on the PC in the 710 kHz channel.

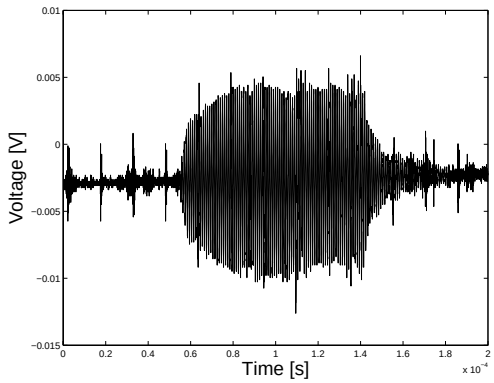

Figure 5.20: The echo of the sphere measured at the end of the cable from the 1 MHz transducer before transmission to the electronics.

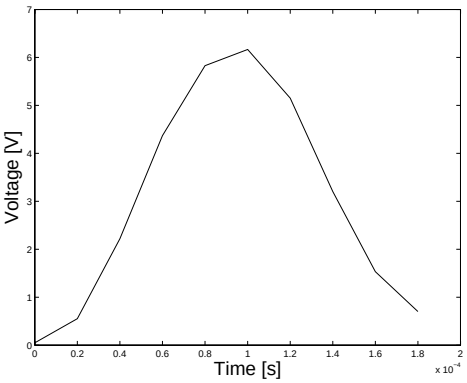

Figure 5.21: The recorded sphere signal on the PC in the 1 MHz channel.

5.3.3 Noise

The noise level was influenced by the condition in the laboratory and the instrument had to be properly grounded during the laboratory measurements. The grounding of the water tank itself was crucial for the noise level in the laboratory.

After the signal has passed through the envelope detector the signal consists of only positive values. The received signal before the pulse transmission has started and after all echoes in the received signal have vanished, is regarded as noise. The mean value of the noise signal has a DC offset from zero. The electronics is adjusted to make this DC offset as small as possible without the noise being clipped. The noise in the received signal is described in connection with noise removal in Chapter 6.

5.3.4 Comments to the measurements

A few comments could be made to the calibration measurements. The hydrophone was positioned manually. In the horizontal direction this was done by moving the assembly with the hydrophone by a mechanical device on the side on the tank and this could be done quite precisely. In the horizontal direction the rod with the hydrophone had to be loosened from the rack and put in

the desired height. The angle of the hydrophone could have changed between each measurement and there is an uncertainty in the height measurement of a couple of millimeters.

The measurements on the sphere turned out to be very dependent on the movement of the sphere. Every measurement had to be conducted after the sphere had come to rest. These measurements therefore became quite time consuming. The same difficulties as for the hydrophone positioning were experienced in the positioning of the spheres. An error in the positioning of the spheres on the acoustical axis would cause an underestimate in the sensitivity.

Chapter 6

Software

Software enhancement is applied to the signals to calculate the volume backscattering strength and to estimate the concentration of scatterers. An important requirement of the software design is to ensure control of the data flow. In addition it is required that the operator has flexibility in the parameters for data analysis.

There exist commercially available dedicated post-processing systems for acoustical recordings of fish and plankton. Despite the advantages in work effort and reliability of using an existing post-processing system, the requirement for control of the signals and the need for system flexibility have triggered the design of new processing software.

The software is intended for evaluation of the performance of the APR and for data analyzes of the measured data. It allows estimates of the concentration of objects in optional size groups. This flexibility is needed as the APR is built for a specific purpose, namely the detection of the plankton species *Calanus finmarchicus*. As flexibility and control have been the main goals in the software design, the processing speed has not been optimized at this stage.

6.1 Post-processing software for the APR

An overview over the processing software is shown in Figure 6.1. The first part contains the real time actions conducted in the electronics and the data acquisition software. The analog signal processing and the description of the data storage are discussed in Chapter 4.

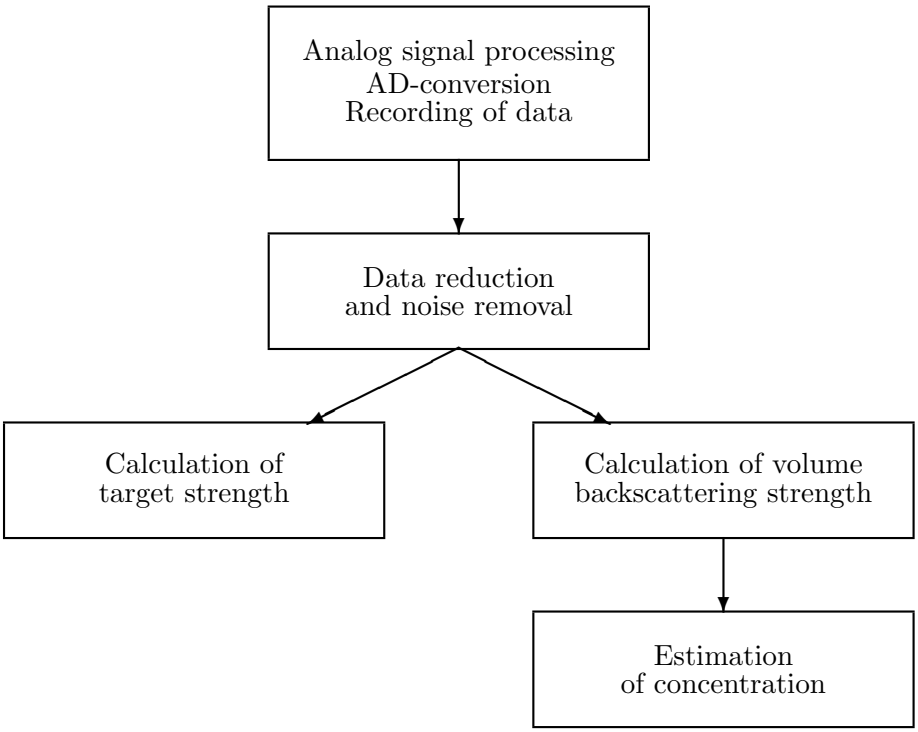

Figure 6.1: A flow chart of the signal flow in the hardware and software.

The data from the acquisition system are saved as ASCII files; refer to the upper block in the flow chart in Figure 6.1. Each of the data files has a name consisting of the date and time it was recorded. The post-processing system, which refers to the designed software for the APR and includes all the rest of the blocks in the flow chart, consists of software developed in Matlab^{TM}. The ASCII files are imported into this software. In the post-processing software, the start time and the end time of the measurement to be analyzed have to be specified. The program then scans for and imports all files with file names between the start and end times. For example, for a difference in start and end time of one minute the software searches for 60 filenames, one for every second. The step of importing ASCII files into Matlab^{TM} is time consuming and limits the speed of the processing.

The first step in the post-processing is conducted to reduce the amount of data to be handled later in the software. Each data file consists of two seconds of raw data when the default values of the acquisition system are used, see Figure 6.2.

With the default settings, each raw file is the return echo from 16 pings. These echoes can be identified in the figure as 16 repeating peaks followed by decreasing signal strength. The peak value is not the echo received from the objects in the water but rather the electrical crosstalk between the transmitter and receiver.

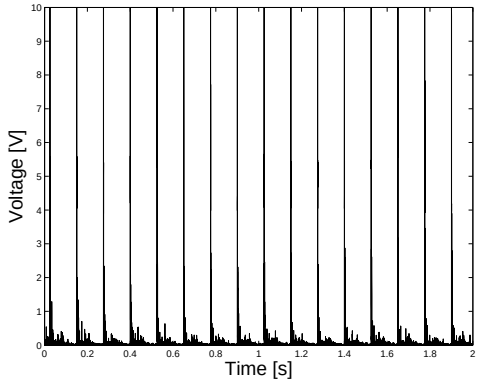

Figure 6.2: A data file with one measurement series; example for the 200 kHz channel. Default settings with repetition rate 0.125 ms and 2 seconds sampling.

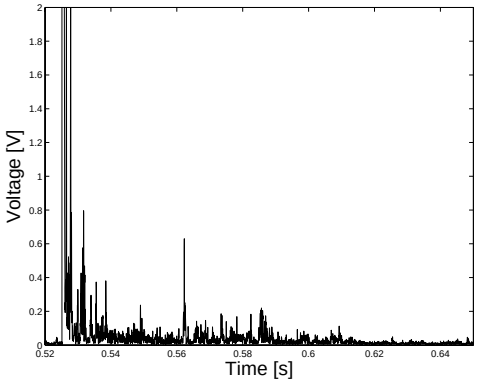

Figure 6.3: Segment of the raw data from one ping; example for the 200 kHz channel. Only the received signal between 0 to 2 V is presented in this figure.

An enlarged segment of the data from in Figure 6.2 is presented in Figure 6.3. The data shows the returned signal of one pulse transmitted into the water. Only the signal values between 0 and 2 V are presented in the figure for better resolution of this part of the signal.

As the timing of the pulse transmittance and the start of the file writing are performed on the same hardware trigger, the time elapsed from the beginning of the file to the first transmitted pulse is the same in all files. Every file is divided into the same number of data sequences as the number of pings transmitted. The range of the data of interest is set and all parts of the data outside this range are removed. A choice has to be made whether to calculate the mean value of the dataset or continue with the separate data from every ping. The operator can choose to analyze every ping separately in case of special features in the data that one wants to investigate more closely. The default value is to calculate mean data since the scattering from multiple targets is a stochastic process, see Chapter 2.

6.1.1 Noise reduction

A noise reduction algorithm can be activated in the software. A decision to use this function depends on the purpose of the measurement. A short explanation of the algorithm follows.

The noise removal algorithm follows the principles of Korneliussen [2000]. The received signal is the sum of the wanted signal and the noise signal. These two signals are assumed to be uncorrelated. The noise reduction function is based on subtracting the mean value of the power in the signal from distances outside the expected range of the system.

The volume backscattering strength, Sv, in Equation 2.12 can be expressed as a volume backscattering coefficient, s_v, that is proportional with the square of the measured signal times the time varied gain

$$s_v \propto g(t)U_{res}^2 \tag{6.1}$$

where U_{res} is the measured signal and $g(t)$ is the time varied gain. The time varied gain compensation of the transmission loss and the increase in volume as a function of distance from the transducers, and the proportionality in Equation 6.1 is caused by the system parameters of the APR.

Assuming that the received signal consists of the wanted signal plus the noise, this can be expressed as

$$U_{res} = U_s + U_n \tag{6.2}$$

where U_s is the wanted signal and U_n is the noise signal.

Assuming that the noise and wanted signals are uncorrelated, the volume scattering coefficient can be expressed by

$$s_v \propto g(t)(U_s + U_n)^2 \approx g(t)(U_s^2 + U_n^2) \propto s_{v,s} + s_{v,n} \tag{6.3}$$

The cross term with U_s times U_n is zero in the case of uncorrelated signals.

The volume scattering coefficient corrected for the noise reduction, $s_{v,s}$, will be

$$s_{v,s} = \begin{cases} s_{v,s} - s_{v,n} & : \quad s_{v,s} \geq s_{v,n} \\ 0 & : \quad s_{v,s} < s_{v,n} \end{cases} \tag{6.4}$$

To use this method to reduce the noise in the measured signal, the noise signal, U_n, has to be known or estimated.

Noise reduction is conducted on the return signals from each measurement series. With the default settings the mean value is calculated from the recorded signal from distances which corresponds to 80 to 90 meters. The number of data series used in the noise calculation is the number of pings minus one because of the way the data is organized. (The signal after the channel is turned on, but before a ping is transmitted, is not used).

The noise signal is calculated for every measurement series and the advantage of doing this is that the noise level in the data is adjusted as the instrument noise changes during long measurements.

6.1.2 Calculations of backscattering strength

Data on the system parameters of the APR including source level, sensitivity, equivalent two-way beam angle, and beam volume, are used in the processing algorithm. Table values for the sound absorption in water are also included. A choice has to be made in the software whether to calculate the target strength or the volume backscattering strength, see Equation 2.12. Even though the system is designed to conduct measurements of volume backscattering strength the calculation of the target strength of one object can be useful in some applications. An example of this can be an experimental situation during measurements with standard spheres.

6.1.3 Concentration in size groups

The volume backscattering strength is used in the calculation of the concentration of the objects in the chosen size groups. The method of concentration estimates is described in Chapter 3 and implemented in the software. The number of size groups can be chosen and the size and properties of the model spheres have to be specified.

Chapter 7

Measurements with the APR

The Acoustical Plankton Recorder (APR) has been tested in different experimental settings and under various environmental conditions. Several measurements have been conducted to gain experience with the performance of the APR and the properties of the recorded backscattered signals. This chapter describes some of these test measurements. Results from measurements on plankton are discussed in Chapter 8 and the overall discussion of the APR is left to Chapter 9.

This chapter is divided into three sections. The first section describes an experiment conducted in an outdoor seawater tank where *Artemia* zooplankton were added into the water. The second section tells about an experiment with the APR attached to a pier measuring horizontally into the fjord. In that experiment different targets were deployed in the acoustic beam. Section 7.3 contains the results from all measurements conducted from a boat during the spring and summer of 2004. These results are characterized by the very low plankton concentrations that was encounted during the entire season.

The results are plotted as a function of the distance from the transducers to the scattering objects. The measured signals are recorded as a function of time after pulse transmission, and the times are transformed to a function of distances by assuming a constant sound speed in the water of 1500 m/s.

7.1 Experiment with *Artemia*

This experiment was conducted at Trondheim Biological Station on 11 March 2004 in an outdoor seawater basin. The main goal was to verify the function of the APR. A brief description of this experiment is included to give an understanding of the function of the APR in a partly controlled environment.

The transducers were mounted on a cement pillar in the sea water basin. The sound was transmitted in the horizontal direction towards another cement pillar at the other end of the basin. The distance between the two pillars was about 8 meters. The population of *Artemia*, a small copepod, was grown for 24 hours from the egg stage and released into the water as shown in the photograph in Figure 7.1. The size of the *Artemia* was below 0.5 mm. Water containing the plankton was added in three parts. The position of the transducers was altered between the releases of plankton. There was no control over the absolute concentration of the *Artemia* population in each release and the size of the released volume varied.

Figure 7.1: A picture of the small zooplankton *Artemia* being added into the water.

Examples of the raw data signals for the three frequencies are shown in Figure 7.2, where the upper figure contains the 200 kHz signal, the middle part the 710 kHz signal, and the bottom part the 1 MHz signal.

The raw data are the signals after sampling and averaged over of 16 pings.

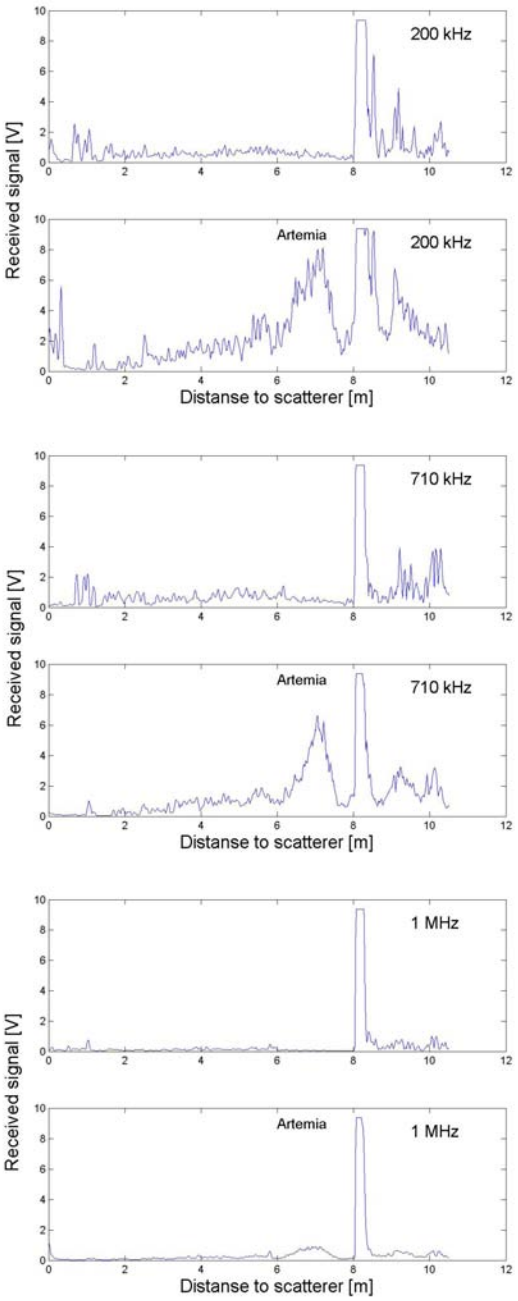

Figure 7.2: The measured signal for the 200 kHz channel (first part of the figure), 710 kHz channel (middle part), and 1 MHz channel (last part), before (upper) and after the *Artemia* was released.

No corrections for the transmission loss or any of the system parameters have been done at this stage. In this figure the raw signals from measurements just before the releases of *Artemia* are compared to the results just after the plankton have been added.

Some comments can be made in connection to the figure. First, the reflection from the cement pillar can be identified at 8 meters (which is the distance between the pillars). The reflection from the pillar is so strong that the received echo signal has been clipped in the electronics for all channels. This can be identified in the figure as the peak at 8 meters that is close to 10 Volt and flat at the top. The signals at greater distances contain backscatter from equipment used in this experiment and the edge of the basin. Increasing the range in the figures even further would display multiple backscatters between the edges of the basin and the cement pillars. The peak in signal amplitude between 6 and 8 meters in the lower figures is caused by the backscattering from *Artemia*. Comparing the upper signals from before the plankton release with the ones after, these peaks in signal amplitude can be identified for all frequency channels. The signal amplitude after the plankton release in the range up to 6 meters is higher than the signal amplitude in the same region before plankton was released. One possible reason could be that; the presented signals in Figure 7.2 are recorded directly after the first volume of plankton was released. The method of plankton releases could have introduced air bubbles and particles from the surface into the water. Another feature in the figure is that the sampled signal of the 1 MHz channel is much lower than the other channels even though this signal has undergone a much greater amplification in the analog signal processing in the electronics than the other signals.

In this experiment the APR was not run continuously; rather it ran separate measurement cycles, one cycle consisting of a 16 ping measurement on each of the three frequencies. The time between each cycle was not constant. The raw data from two such cycles was presented in Figure 7.2. The data was then processed by the software described in Chapter 6 and corrected for transmission loss and system parameters. The volume backscattering strength, SV, of the *Artemia* experiment is shown in Figure 7.3. The upper part of the figure is for the 200 kHz channel, the middle part is for the 710 kHz channel, and the bottom part is for the 1 MHz channel. The vertical axis in the figure gives the distance to the scatterers while the number of the measurement cycle is plotted on the horizontal axis. Measurement number 1 corresponds to the first measurement after the release of the first patch of *Artemia*, number 16 corresponds to the first measurement after the second release, and measurement number 26 corresponds to the first measurement after the third plankton

release.

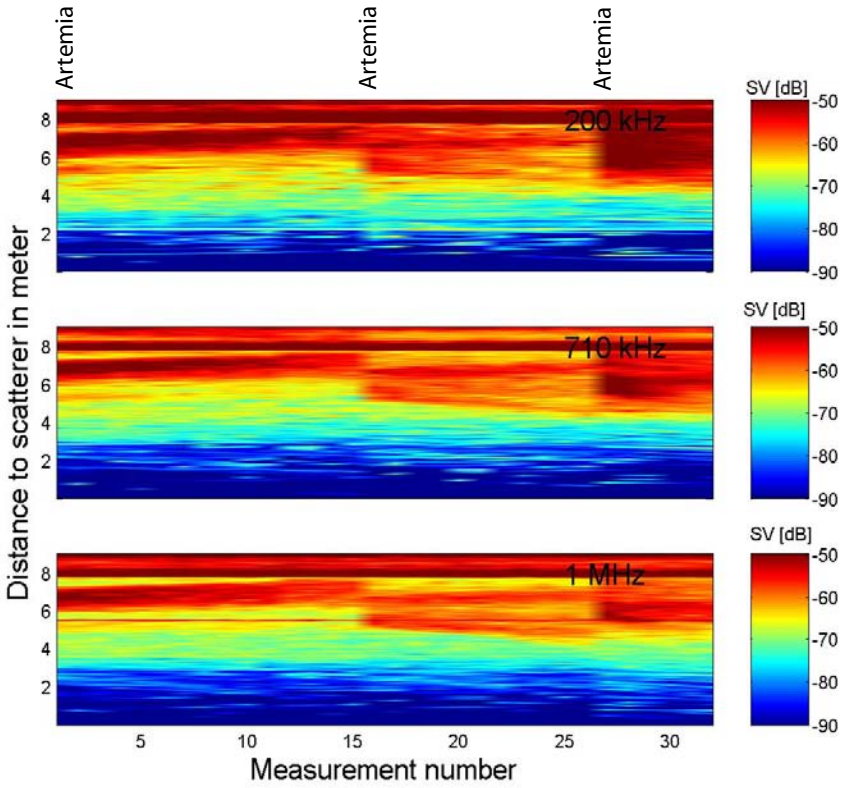

Figure 7.3: Measured volume backscattering strength, SV, in dB re 1 m^{-1} in the *Artemia* experiment for the 200 kHz (upper) channel, 710 kHz channel (middle), and 1 MHz channel (lower) plotted as a function of measurement number and the distance from the transducers.

It can be seen from Figure 7.3 that at a distance of 8 meters the backscatter from the cement pillar makes the received signal very strong. The received signal is so strong at 8 meters that it is clipped in the receiver electronics, as was also seen in the presented raw data. The features in the range from 6 to 8 meters resemble in all the three channels. The maximum value of the volume backscattering strength in the range of the plankton release exceeded -50 dB for all frequencies. The strongest level can be seen in the volume backscattering of the 200 kHz channel. The cloud of *Artemia*, released at measurement number 1, 16, and 26, drifted and diffused after some time. This was also observed visually during the measurements. It can also be seen that

the concentration of plankton in each released patch differed, with a smaller amount of plankton in the second release, and a large amount in the last one.

The estimated concentration of scatterers in number per cubic meter is shown in Figure 7.4. The concentration estimation algorithm used two size groups and the scatterers were modeled as truncated spheres with density ratio, g, equal to 1.025, and sound speed ratio, h, equal to 1.02. The sphere radii were 0.1 and 11.4 mm, which correspond to modeled *Calanus finmarchicus* with body lengths 0.5 and 50 mm. The signals from the first meter closest to the transducers are removed due to cross talk in the electronics and nonlinearties of the beam.

Even though there is only one plankton species present, with all plankton of the same generation, the results show some interesting features. High concentrations, above 100 individuals per cubic meter, of large scatterers are seen just after the first and third plankton releases at measurement number 1 and 26 in Figure 7.4. These high concentrations decrease as time passes after the plankton releases. After the second plankton release only a small increase in the concentration of large scatterers can be identified. The estimated concentration in the smallest size group in Figure 7.4 shows concentrations up to above 10^6 individuals per cubic meter. These high concentrations are found at a range between 5 to 8 meters and seem to cover a larger range interval than those with high concentration in the large size group. The number of scatterers per cubic meter in the small size group is largest after the second plankton release at measurement number 16. The concentrations in this size group are very low, except at distances less than 4 meters, after the third plankton release.

There could be several explanations of the differences in features seen in the concentrations of scatterers in the two size groups in Figure 7.4. It could be that some air bubbles were added into the water together with the plankton. Air bubbles, being strong scatterers, injected in the water at the time and range of the plankton injection could explain the high concentration in the largest size group. The position and direction of the beam could also explain the features in Figure 7.4. Different directions of the beams lead to different measured volumes for the three frequencies. Since the distribution of the plankton in the basin is far from homogeneous this may be a big source of error. Another source of error might be that the assumption for the estimation algorithm fails because the concentration of plankton is so high that the assumption of linearity between the total intensity and the sum of the intensity contribution from the individual plankton are not valid and multiple scattering effects are substantial.

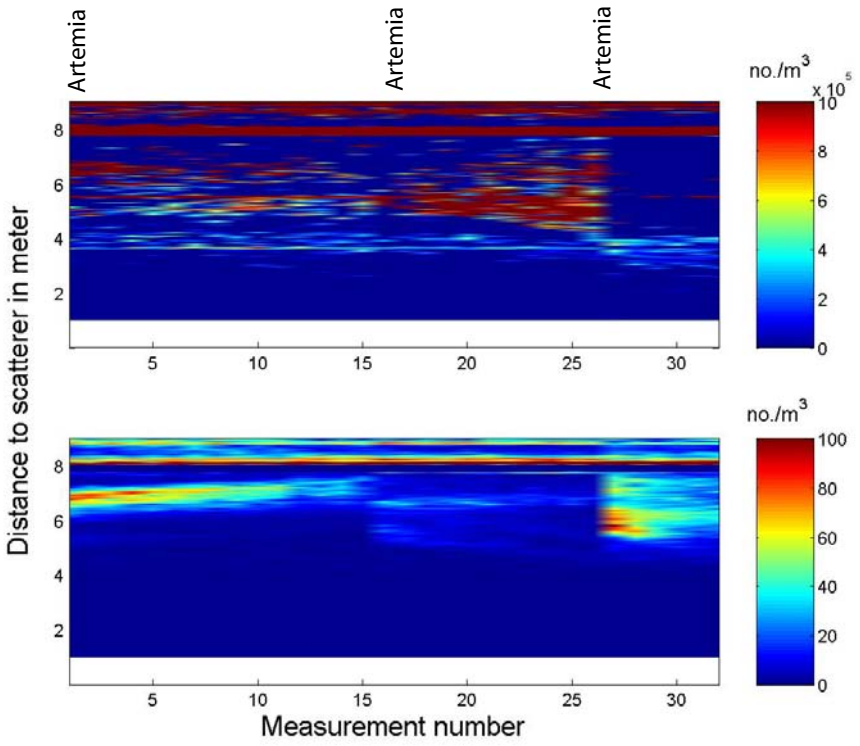

Figure 7.4: Estimated numbers of scatterers per cubic meter for the *Artemia* experiment. The scatterers are modeled as truncated spheres with density ratio, g, 1.025, sound speed ratio, h, 1.02 and sphere radii 0.1 mm (upper) and 11.4 mm (lower). The parameters of the modeled sphere correspond to modeled *Calanus finmarchicus* with body lengths 0.5 mm (upper) and 50 mm(lower).

7.2 Measurements from the pier

These measurements took place 1 and 2 November 2004. The experiment was conducted from the pier outside the Trondheim Biological Station. The APR was mounted on the pier and it was pointing horizontally into the sea. Different particles, materials, and plankton were tossed or injected into the beam. The aim of the experiment was to test the APR and to collect the backscattered signal from different scatterers to gain experience on how signals from different scatterers appear in the recorded data.

The particles were far from homogeneously distributed in the beam and therefore no concentration estimates will be presented from this experiment.

7.2.1 Procedure

The transducers were attached on a rack, and mounted to the lowest step of the ladder of the pier. At the maximum tide the depth of the transducers below the water surface became up to about 2 meters. A sketch of the measurement situation is shown in Figure 7.5.

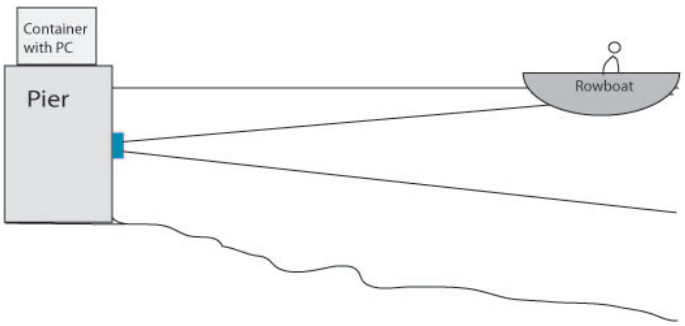

Figure 7.5: A sketch of the measurement situation for the pier experiment.

The measurements were conducted around high tide to achieve maximum water depth and because the water current is weakest at the time of maximum and minimum tide. The weather was nice and stable both days, except for a rain shower on the afternoon on 1 November. During the first measurement day the waves on the water had peak to peak height of about 20 to 30 cm, while on the second day the surface was dead calm.

Tests were made with metallic spheres to get information on the direction of the beam from the transducers. The spheres were lowered into the water to

find the center of the beam both with respect to depth and horizontal position. Two long measurement series were conducted on 1 November. The first series lasted for almost 45 minutes with continuous sampling and the second for 20 minutes. Different particles and materials were injected at different ranges in front of the instrument. The particles and materials that were used in this experiment included shingle, sand, rice, popcorn, couscous, and 4.5 mm steel spheres (steel air gun shot). Most of the substances were thrown from a boat. The boat was also used to tow a metallic sphere through the beam.

On 2 November the APR ran for 1,5 hours. During this time measurements were performed on metallic spheres to investigate the direction of the beam. Plankton was added into the beam, and materials and particles were added as the day before. The plankton used in this experiment was collected with net trawl from between 200 and 300 meters depth.

The handling of plankton without adding any air was challenging. At the pier, water containing the plankton was put into plastic bags. The bags was placed in the boat and brought in front of the instrument. The bags were tied to a long stick together with a heavy metallic sphere. On another long stick a knife was fastened that punctured the plastic bag with plankton. The sticks and metallic sphere were removed and the boat disappeared from the beam.

7.2.2 Measurement results

Overview of the measurements

An overview of the volume backscattering strength for the two measurements on 1 November is presented in Figures 7.6 and 7.7. The continuous measurement on the 2 November is illustrated in Figure 7.8.

The upper part of the figures shows the results for the 200 kHz channel, the middle for the 710 kHz channel, and the lower for the 1 MHz channel. The maximum range in the figures is 30 meters. The maximum volume backscattering strength is -50 dB and red while the dark blue color corresponds to a volume backscattering strength of -90 dB or less. The added substances can be seen in the figures as areas with high SV. A note of the time each substance was added is marked at the top of the figures. The substances were added at different distances from the transducers, and the same features can be identified for all three frequencies. The noise removal algorithm has been applied to these data. The measured noise and the effect of the noise removal algorithm will be discussed later in this section.

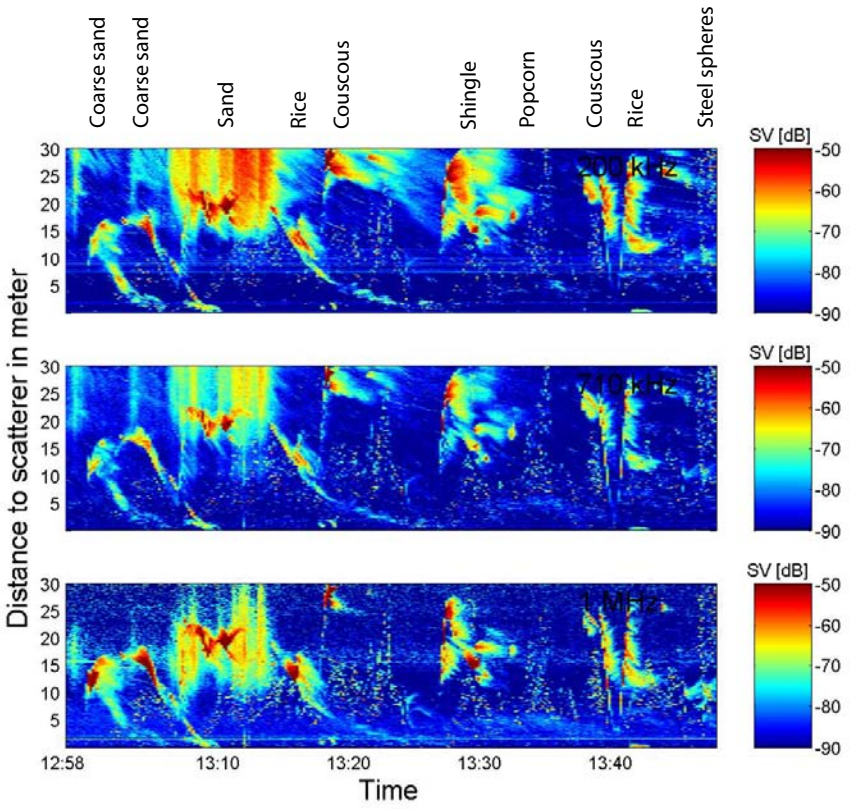

Figure 7.6: Overview of the volume backscattering strength, SV, in dB re 1 m^{-1} for 200 kHz (upper), 710 kHz (middle), and 1 MHz (lower) from the first measurement on 1 of November.

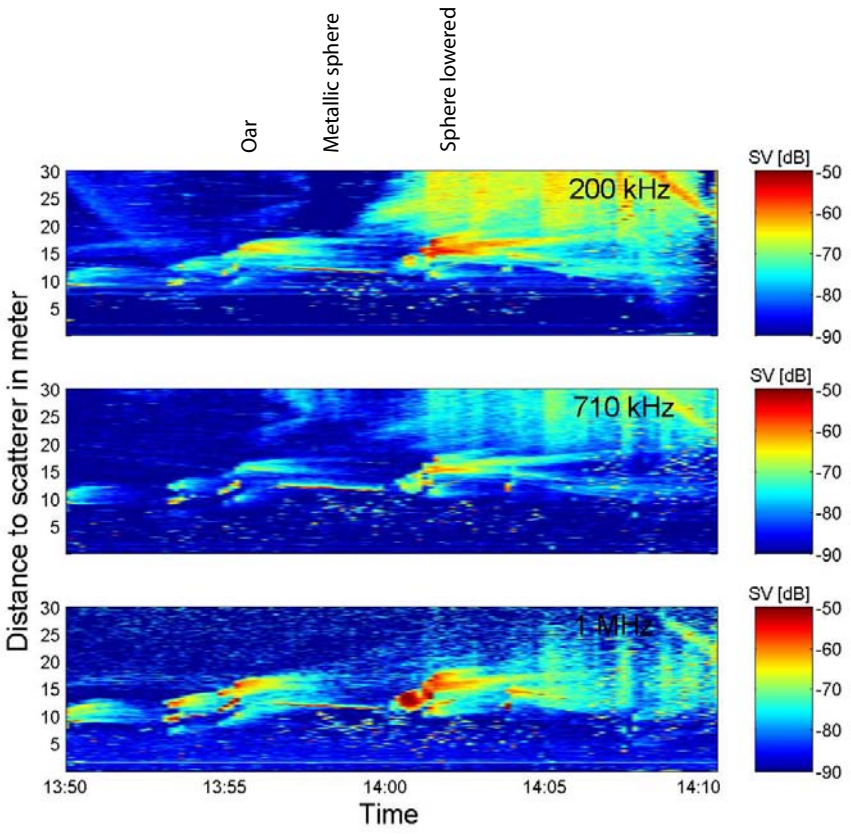

Figure 7.7: An overview of the volume backscattering strength, SV, in dB re 1 m^{-1} for 200 kHz (upper), 710 kHz (middle), and 1 MHz (lower) from the second measurement on 1 of November.

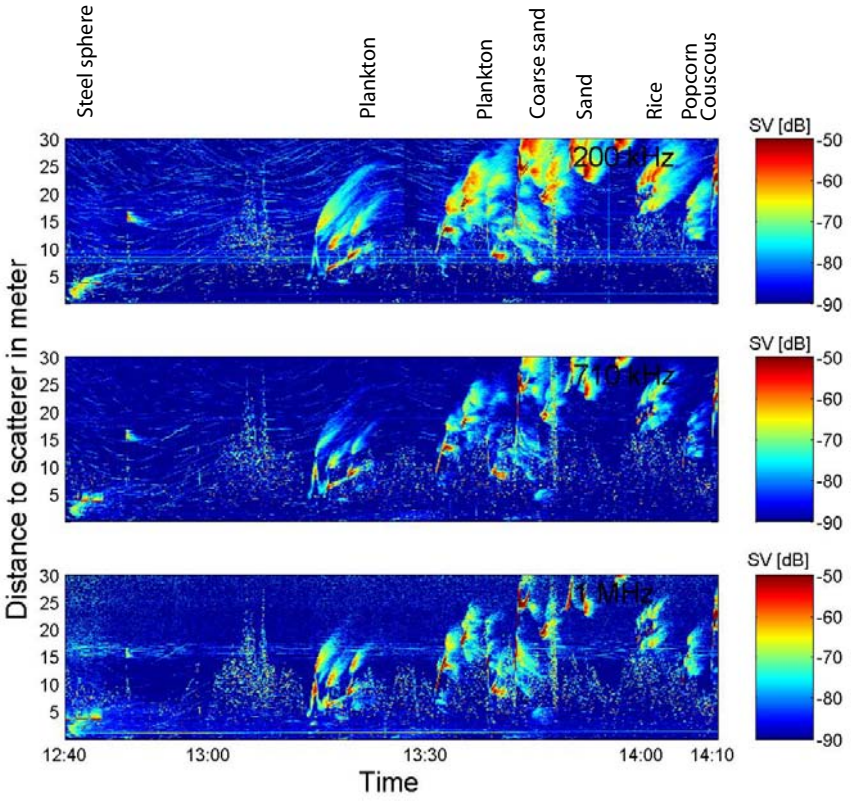

Figure 7.8: An overview of the volume backscattering strength, SV, in dB re 1 m^{-1} for 200 kHz (upper), 710 kHz (middle), and 1 MHz (lower) from the measurement on 2 of November.

With this measurement setup, pointing the instrument horizontally close to the surface, there is a concern that the side lobes of the beam hit the water surface. At large distances parts of the main lobe of the beam could strike the surface. This might cause strong scatterers like near-surface air bobbles and ocean waves to contribute to the received signals.

Some of the features in the figures will be commented on more thoroughly in the following. Various substances were thrown into the beam during the first measurement series on 1 November, Figure 7.6. At 13:10 sand was added. Multiple scattering within the area with sand causes ringing, which can be seen in the data as strong signals from distances behind the sand deployment site. None of the other substances showed the same degree of ringing.

As shown in Figure 7.7, a metallic sphere was lowered from a buoy and towed across the beam. In the left half of the figure the depth of the sphere was 2 meters, and from 14:02 the depth was 4 meters. Features caused by the oars of the boat are visible from 13:50 to 13:57. From that time the signature of the sphere can be seen as a thin line at a distance of 10 meters. At 14:02 the sphere was taken into the boat and the line that the sphere was attached to was adjusted before the sphere was lowered to 4 meters. At this depth it is much harder to identify the signature for all frequency channels than when towing at 2 meters. This shows that the center of the beam must be closer to 2 meters than 4 meters during this measurement series. In the middle of this series it started to rain, and the backscattering from micro bubbles caused by the rain can be seen in the increase in volume backscattering strength above 20 meters in the right half of the figure.

On 2 November several tests were conducted with plankton releases from 13:10 to 13:45. They are presented later in this text. Small "dots" in the measured SV are identified at times where no substances were added. An example of this can be seen in Figure 7.8 at about 13:10, distance between 5 to 15 meters. These "dots" occur at the time and range where small fish were observed and that will also be discussed later in this section.

The "background" SV, see Figures 7.6 to 7.8, was below -90 dB for all frequency channels. This is a low level. The cause for this may be that the water is typically very clear with very little algae and plankton in November.

The change in direction of the current can be identified as the direction of the tail after substances change. The "background" signals show some weak patterns that stand out in the noise. A close-up of the figures would make this more visible. The pattern consists of bent lines. The cause of this is not known, but it seems to follow the water current.

There are some peculiarities in the received signals. One can see a line in the 1 MHz signals at distances corresponding to 1.5 meters; and for 200 kHz around 10 meter. The source of these lines is not known, but they are not present in later measurement series where the cylinder was lowered into the water.

Plankton experiment

Figure 7.9 shows the volume backscattering strength as plankton are being released.

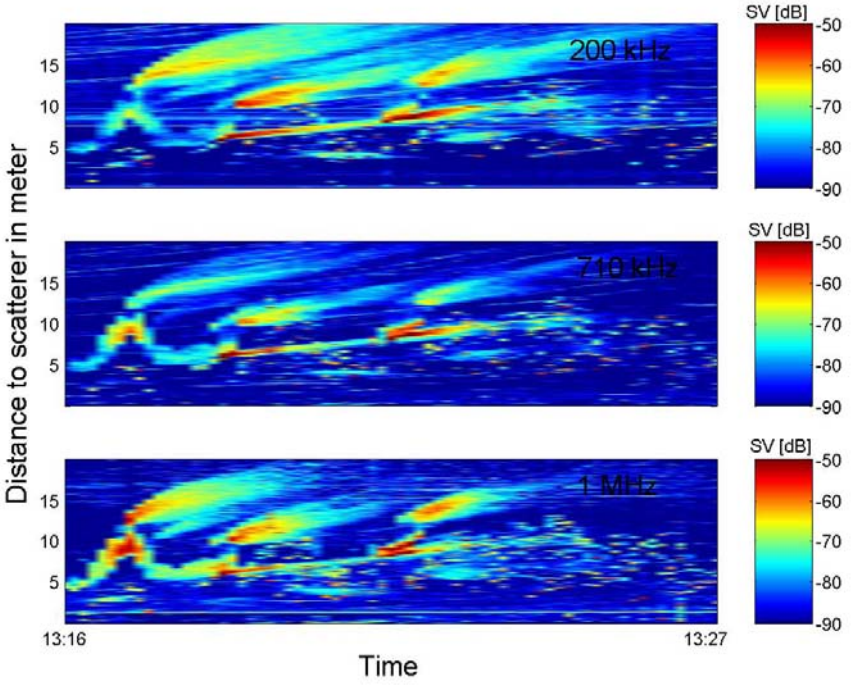

Figure 7.9: Measurements of the volume backscattering strength, SV, in dB re 1 m^{-1} for 200 kHz (upper), 710 kHz (middle), and 1 MHz (lower) from a test where plankton was released on 2 of November.

The results from the experiment with plankton are difficult to interpret. It is clear that not all features that can be seen in the data can be attributed to the plankton itself. These data correspond to two separate plankton release events, although in the figure it could seem as if there were three. The plankton was

released at about 13:20 at a distance of 6 meters and at 13:23 at a distance of 8 meters. The backscattered signal is very weak compared to other features in the figure. There is a red line just before the plankton are being released. This is the signature of the sphere that was lowered into the water with the plastic bags containing plankton. When the red line disappeared the plankton was released. There are a couple of strong backscattered signals before the first plankton event and some strong signals at the time of plankton release a couple of meters further away than the release itself. A probable cause of this is bubbles from the oars of the rowboat.

There are several aspects of the experiment with plankton release that caused problems. First, the net trawl did not give the amount and concentration of plankton that was expected. The aim was to gather as much of the plankton *Calanus finmarchicus* as possible but this proved on the other hand difficult. The trawl contained only a small amount of *Calanus*, but did contain different copepods and other species. The pouring of the water containing the plankton from the bucket into the plastic bags did also prove problematic. In this process air bubbles could have been injected into the water. It was also difficult to close the bags without having any air left in them.

The method of releasing the plankton demanded that the boat itself had to be in the center of the beam horizontally. Because of the wish to see the plankton cloud as soon as possible after the release the boat was rowed fast from the site. This caused the oars to inject clouds of air bobbles into the water.

So, even though an increased volume backscattering strength was recorded after the release of the plankton, problems with the handling of the plankton and the setup of the experiment made these results associated with great uncertainty.

Presence of small fish

There were lots of small fish close to the pier during the experiment. They swam in front of the beam and when they were in the beam the backscattered signal was as expected very high. The fish could both be seen directly from the pier and in the measurement results on the screen of the computer. At some moment in time no fish could be seen neither physically nor in the data. But a little later the ocean seemed to be "boiling" with fish. The size of the fish seemed to be between 10 and 20 cm from physical observations.

Figure 7.10 shows a raw data from the 200 kHz channel where the return of 16 succeeding pings are presented beside each other. Only the first 9 meters are

shown in the figure. At this point in time many fish were seen in front of the

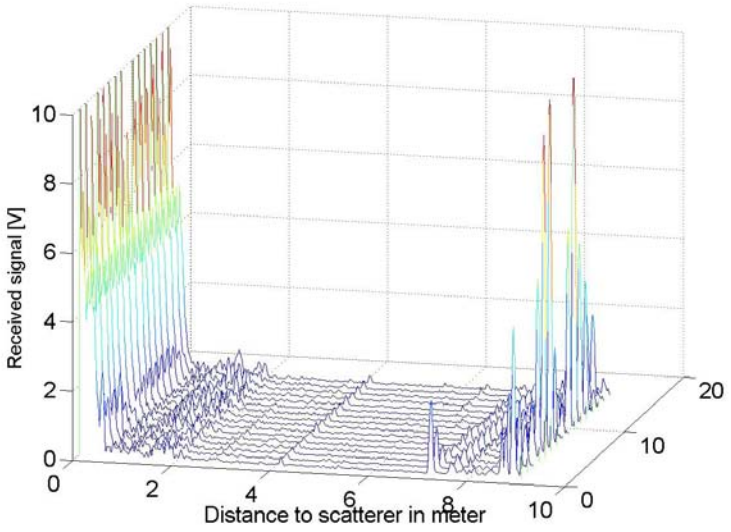

Figure 7.10: The raw data from 16 succeeding pings (on the axis into the plane) from the 200 kHz channel at 13:10:20 on 2 November 2004.

pier. The fish moved very rapidly compared to the time scale of the measurement. From the figure it is clear that the strength of the backscattered signal from about 8 meters varied significantly during the two second measurement period. A fish uses less than 2 seconds to pass through the center of the beam close to the transducers. The echo from fish in the center of the beam will be smoothened and appear much less than the actual value. The amount of fish in the beam was very variable during the time of measurement.

Noise level and noise removal

Figures 7.11 and 7.12 display the first 15 minutes of the of the measurement series from 2 November presented in Figure 7.8. In Figure 7.11 the noise removal algorithm has been employed on the data and in Figure 7.12 the same data has been processed without any noise removal.

Comparing the two figures, the measured volume backscattering strengths for 200 kHz and 710 kHz channels are the same regardless of noise removal. For the 1 MHz channel this is not the case. From Figure 7.12 the effect of the noise in the 1 MHz channel can be identified as an increase in SV as a function of the

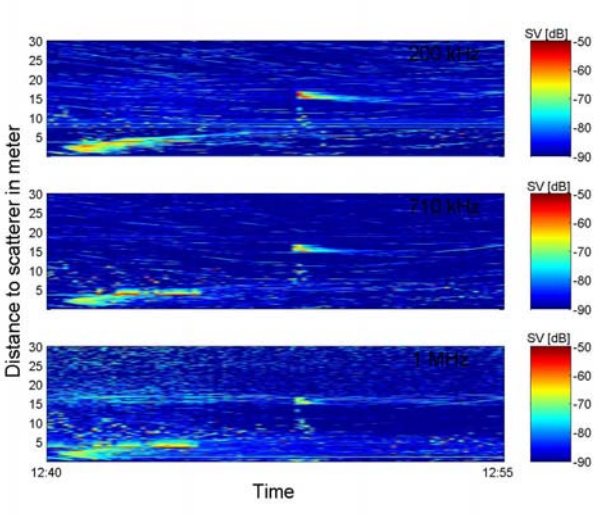

Figure 7.11: Measurements of the volume backscattering strength, SV, in dB re 1 m^{-1} for 200 kHz (upper), 710 kHz (middle), and 1 MHz (lower) on 2 of November. The noise removal algorithm has been applied on the data.

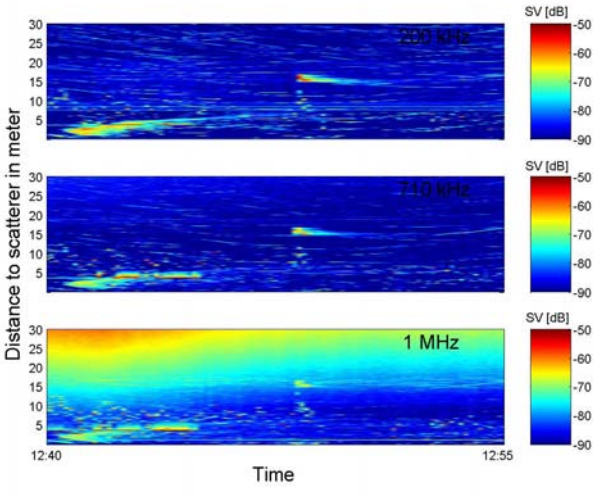

Figure 7.12: Measurements of the volume backscattering strength, SV, in dB re 1 m^{-1} for 200 kHz (upper), 710 kHz (middle), and 1 MHz (lower) on 2 of November. No noise removal has been used.

distance from the transducers. The useful range of this channel is estimated to be 15 to 20 meters but the noise might give a substantial contribution to the measured volume backscattering strength for distances even shorter than that. The noise removal algorithm, applied to the data in Figure 7.11, is able to remove most of the noise from the signals and the background SV is almost constant with distance. For the 1 MHz channel at range above 15 to 20 meters some spots appear with dark blue color. These spots correspond to data points with signal value 0 Volt, where the measured signal is less or equal to the noise signal. So, the range of this channel is limited to about 20 meters regardless of the noise being removed, but the measured volume backscattering strength at the upper limit of this range will be more accurately presented with the noise removed.

Figure 7.13 gives an example of the noise signal on the three frequency channels. The mean value of this signal is used in the noise removal algorithm. This is raw data corresponding to backscattering from 90 meters off the transducers. The voltage on the y-axis is plotted from 0 to 20 mV (10V corresponds to the maximum input signal of the system). This is data taken at 13:00 on the 2 November, which is in the middle of a long measurement series.

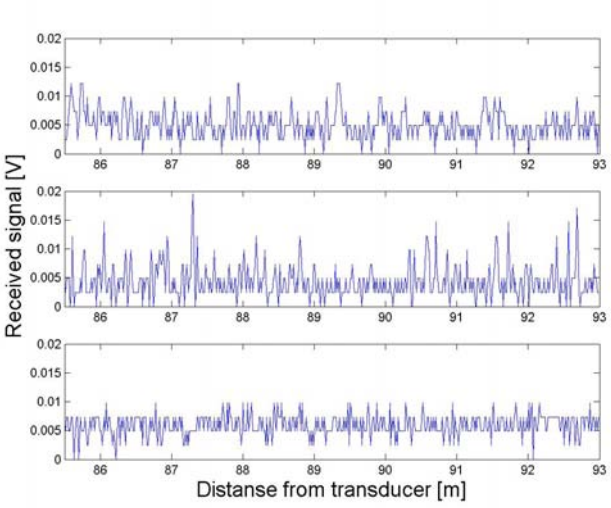

Figure 7.13: The noise level for the 200 kHz channel (top), 710 kHz channel (middle), and 1 MHz channel (bottom). The data are from 13:00 on 2 November 2004.

The noise level decreased during the long measurements from the pier and became stable after about 15 minutes. This was the case for all channels. The

raw data shows that the DC level of the signals decreases and that it was stable above zero for all channels. The mean value of the noise was below 7.5 mV for all frequency channels.

The effect of the change in noise throughout a measurement series will be compensated for with the noise removal algorithm for each measurement cycle. Since the noise removal algorithm seems to improve the accuracy of the calculated volume backscattering strength at distances up to the maximum range of the 1 MHz channel, these results argue that noise reduction should be used in the data processing.

7.3 Measurement at sea during 2004

The first measurements with the APR deployed from a boat were conducted during 2004. The measurements reported in the following text were conducted 5 May, 1 June, 8 July, and 3 September. The two first and the last day of measurements were conducted from the boat "Harry Borten" operated by the people at Trondheim Biological Station. The third day a local fishing boat was used.

The APR cylinder was mounted to a winch and lowered into the water. The beam pointed in the vertical direction for the three first measurement days and horizontally for the last day.

The weather conditions were different during the four days of experiment. The first day there were one to two meter waves. Since the boat was moving so did the instrument. The other days measurements were conducted under quiet weather conditions.

At every measurement location horizontal net haul was conducted at different depths. The contents of the nets were examined for volume and species of plankton. The results showed that there were very small amounts of plankton collected by nets all days.

The presented data are example of the measurement results from the cruises. The examples illustrate various aspects with the APR and the way it can be operated.

Measurement on 5 May

Figure 7.14 displays the volume backscattering strength recorded on 5 May 2004. This was the first time the APR was tested in the sea. The presented

data is the result of two short continuous measurements, where the first consists of 12 measurement cycles and the second of 16 cycles. Each cycle is composed of a two-second registration on each frequency during which 16 pings are transmitted. The noise removal algorithm has not been used in the processing of these data, for reasons that will be explained later in this section.

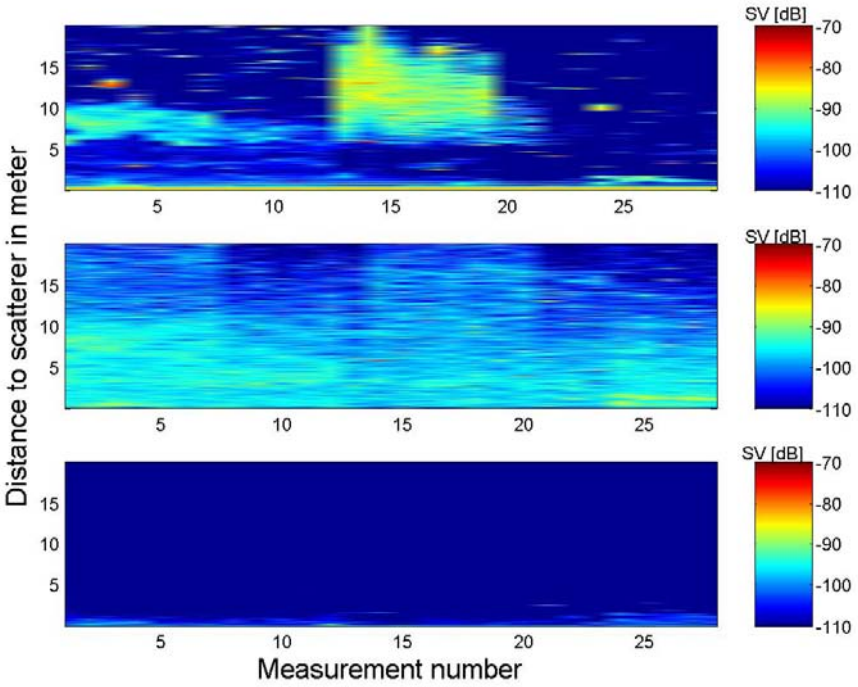

Figure 7.14: Measured volume backscattering strength, SV, in dB re 1 m^{-1} for 200 kHz (upper), 710 kHz (middle), and 1 MHz (lower) are plotted as a function of the measurement number and the distance from the transducers. The measurement was conducted on 5 May 2004.

The measured volume backscattering strength was very low during this measurement for all frequencies, the maximal strength being -85 dB for the 200 kHz channel. The area of maximal strength in the 200 kHz channel can be seen as the second measurement series starts at measurement number 13. This area disappears at measurement number 20. No features can be seen in the 1 MHz channel at longer distances than a few meters from the transducers.

Because of 1 to 2 meters waves the APR moved in the water during the mea-

surement. This can explain that the area of high echo in the 200 kHz channel varies from one cycle to the next.

Measurement on 1 June

Measurements were conducted at several locations in the Trondheimsfjorden. The instrument was operated near the sea surface and at depths 5, 10, and 20 meters. The volume backscattering strengths from those measurements are shown in Figure 7.15. The cylinder depth was 0 meters for the first 5 measurements, 5 meters for measurement number 6 to 12, 10 meters for measurement number 13 through 16, and 20 meters for measurement number 17 through 21. For measurement number 22 through 30 the depth was 0 meter, for measurement number 31 through 36 the depth was 10 meters, and it was 20 meters for the last measurements. No noise reduction was performed.

When the instrument was operated close to the surface, in measurement number 1 through 5 and 22 through 30, increased volume backscattering strength was measured in the first couple of meters for all three channels. When the instrument was lowered the volume backscattering level decreased except for some scattering events in the 200 kHz channel. The results indicate some scattering objects in the surface waters and very few scatterers below 5 to 10 meters.

The biological net samples this day had only a few crustacean and some destroyed jellyfish with attached mud.

Measurement on 8 July

All measurements this day were done vertically with a transducer depth of about three meters. Figure 7.16 shows the volume backscattering strength from a two minutes measurement period, processed without noise reduction.

The figure displays the volume backscattering strength in a range of 50 meters from the transducers. However, the range of the 1 MHz channel is only 20 meters so the features outside this range are due to noise. For the 200 kHz the strong layer appearing at 40 meter is caused by reflection from the bottom for the previous ping. The effect can be clearly seen in the raw data, see Figure 7.17. The water depth was between 130 and 140 meters at this specific location.

Figure 7.17 shows one measurement series with 16 pings. At the time the ping is transmitted the received signal is saturated so that 16 pings can be

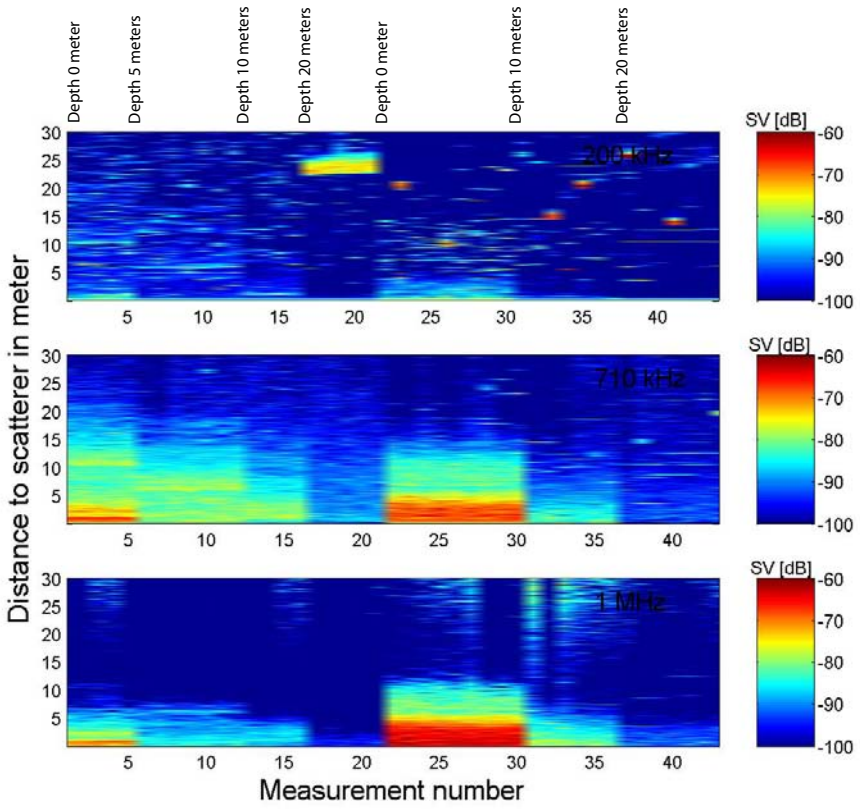

Figure 7.15: Measured volume backscattering strength, SV, in dB re 1 m^{-1} for 200 kHz (upper), 710 kHz (middle), and 1 MHz (lower) is plotted as a function of the measurement number and the distance from the transducers. The measurement was conducted on 1 June 2004.

identified in the figure. The backscattered signal from the sea bottom is about 3 to 4 V. Notice that the first signal from the bottom comes after the second ping has been transmitted.

These results demonstrate the long range of the 200 kHz channel compared to the other frequency channels. This is an important factor for the choice of the APR parameters like repetition rate, beam direction, and the noise reduction algorithm. In the noise removal it is assumed that the signal at a specific distance from the transducers consists only of noise. For the 200 kHz channel this distance could be considerable.

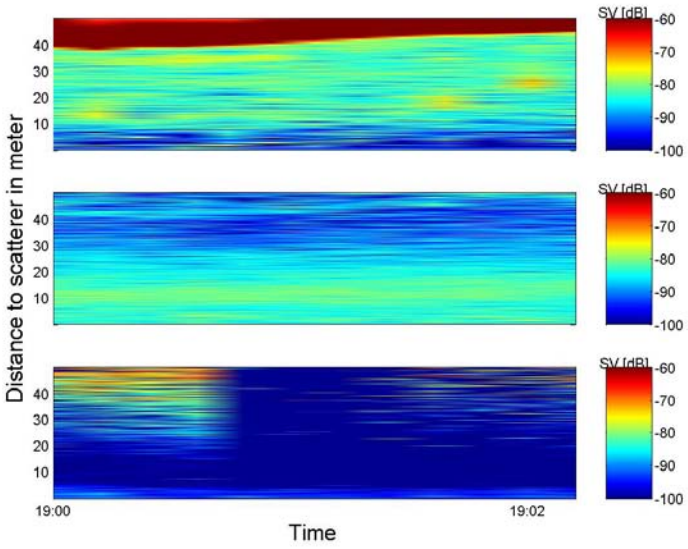

Figure 7.16: Measured volume backscattering strength, SV, in dB re 1 m^{-1} for 200 kHz (upper), 710 kHz (middle), and 1 MHz (lower) is plotted as a function of time and the distance from the transducers. The measurement was conducted on 8 July 2004.

Measurement on 3 September

Measurements were carried out on 3 September with the APR pointing horizontally. Figure 7.18 shows the volume backscattering strength from this measurement. The noise reduction algorithm has been used on the data.

The cylinder was at a depth of 5 meters in the beginning of the measurement and raised to 2 meters after 4 minutes. The measured volume backscattering strength was about -75 dB for both the 710 kHz and 1 MHz channel at 5 meters depth but decreased to below -80 dB at 2 meter depth. For the 200 kHz channel the SV was about -90 dB for both depths. The strong echo close to the transducers at the end of this measurement series is caused by the contents of the biological net samples, mostly plankton, being thrown from the boat.

The estimated numbers of scatterers in three size groups per cubic meter are presented in Figure 7.19. The scattering objects are modeled with the truncated sphere model, with density ratio equal to 1.025, sound speed ratio equal to 1.02, and sphere radii 0.43, 1.1, and 4.5 mm. The parameters of the modeled sphere correspond the parameters found for *Calanus finmarchicus* in

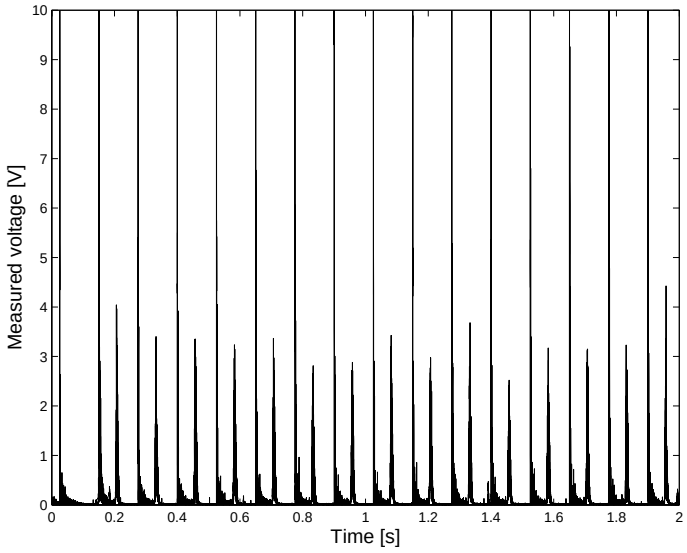

Figure 7.17: Raw data from a measurement at the 1 MHz channel on 8 July.

Chapter 3 with 2, 5, and 20 mm body length.

The scale is different for the three size groups. In smallest size group the red color corresponds to 250 objects per cubic meter, while this color corresponds to 20 and 10 for the middle and large object size. The results shows concentrations of scatterers in the smallest group up to 200 per cubic meter for the first 10 meters closest to the transducers as the APR was situated at 5 meter depth. As the cylinder was raised to two meters the concentration estimates fell to below 75 objects per cubic meter. The concentration in the two larger size groups was below 10 objects per cubic meter for the middle, less at 2 meters, and even lower for the largest size group. This indicates a layer of small plankton at depth 5 meters. The signature of the biological sample being thrown into the beam can be seen in the two smallest size groups.

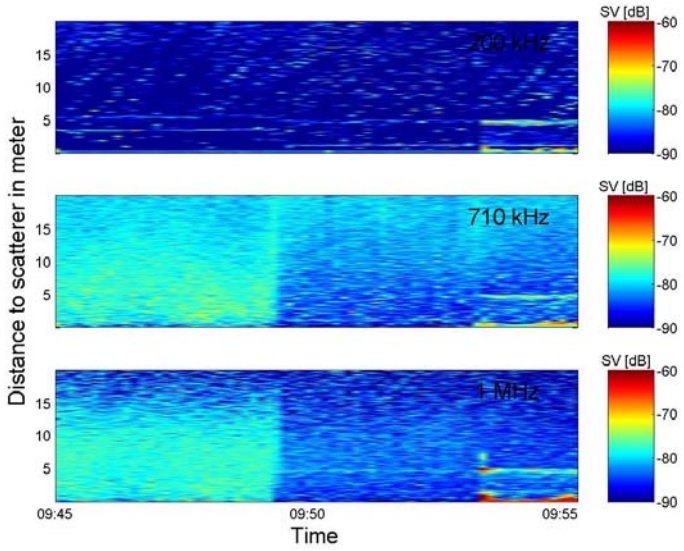

Figure 7.18: The measured volume backscattering strength, SV, in dB re 1 m^{-1} for 200 kHz (upper), 710 kHz (middle), and 1 MHz (lower) are plotted as a function of time and the distance from the transducers. The measurement was conducted on 3 September 2004.

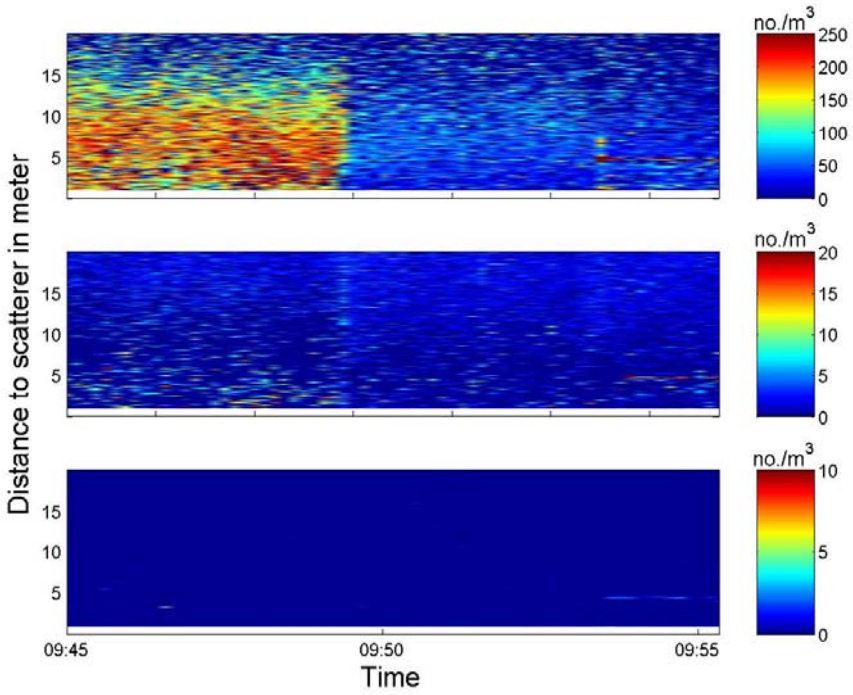

Figure 7.19: Estimated numbers of scatterers per cubic meter from the first measurement on 3 September 2004. The scatterers are modeled as truncated spheres with density ratio, g, 1.025, sound speed ratio, h, 1.02 and sphere radii 0.43 mm (upper), 1.1 mm (middle) and 4.5 mm (lower). The parameters of the modeled sphere correspond to modeled *Calanus finmarchicus* with body length 2 mm (upper), 5 mm (middle) and 20 mm.

Chapter 8

Measurements of plankton

The objective of the APR is to conduct multi-frequency measurements of the volume backscattering strength from a water volume and to use these measurements for estimation of plankton concentrations. Experiments and test measurements with the APR were conducted during 2004. These test measurements included; an experiment in an outdoor seawater tank where the small zooplankton *Artemia* were added into the water, experiment conducted from the pier where different targets were deployed into the beam, and several measurements at sea where different settings of the APR were tested, but were low concentrations of plankton were measured. All these measurements have been described in detail in Chapter 7.

In 2005 field studies were conducted with measurements of high concentrations of plankton. The results of such measurements, which demonstrate the performance of the APR, are presented in this chapter.

The presented results are calculated with the method and the software described in the previous chapters. The noise removal algorithm was used. The default settings of the APR have been used during the measurements and each file of the presented data consists of the mean value from 16 pings. The data have not been subject to any smoothening in order to achieve high resolution data.

The results are presented in several figures. The recording time is given on the x-axis of all figures and the distance to the scatterer is on the y-axis. In the convention of time to range the constant sound speed of $c = 1500$ m/s was used. The maximum range of all figures presented in this chapter is 20 meters.

Three size groups are used in the estimation algorithm applied. The same size

groups are chosen for all the presented measurements so that the results can easily be compared. A body length of 2 mm was chosen to represent *Calanus finmarcicius* since the life stage of the present *Calanus* was not known. The typical body length of a stage CIV individual is 1.7 mm and the typical body length at stage CV and CVI is 2.2 mm as shown in Section 3.2.

8.1 Results from cruises during 2005

Two cruises were conducted at sea during May 2005. The boat started from Frøya outside the coast of Mid-Norway. The first cruise was conducted on 11 May with calm weather and light rain. The second cruise took place on the 19 May 2005. Then the weather conditions were variable, with a hail shower before the measurement started and with a dry spell during the measurements.

Biological net samples were taken for every 5 meter depth in the same area as the acoustical measurements were conducted. The content of the nets was analyzed visually by a biologist. The net samples were collected with small nets at the selected depths, and the boat ran at a known speed for 10 minutes. By measuring the volume of *Calanus* and jellyfish present in the nets, which had run through a known volume of water, estimates of concentrations were achieved. After the biological sampling the boat stopped and the acoustical measurement was conducted. The location of the biological and acoustical measurements was not exactly the same, as the biological measurement covered a larger area and measured the mean concentration while the acoustical measurement can be seen as a point measurement.

The different measurement series are presented according to the date of the cruise and comments to the joint results are made at the end of this section.

8.1.1 Results from 11 May 2005

Two measurements were conducted on 11 May. According to the echo sounder on the boat the depth at the first measurement site was about 40 meters, and it was approximately 150 meters to the shore. The second location was at deeper water further from the shore. The APR was pointing in a 10 degree angle below the horizontal in both two measurements. In the beginning of the first measurement the depth of the cylinder of the APR was about 2 meters. Since high concentrations of *Calanus finmarchicus* could be observed visually in the surface water the cylinder was raised to just 0.5 meter below

the surface a couple of minutes before the measurement ended. At the second measurement series the depth of the cylinder was 1 meter.

The measured volume backscattering strength is presented in Figures 8.1 and 8.2. The upper part of the figures is the result for the 200 kHz channel, the middle part is for the 710 kHz channel, and the lower for the 1 MHz channel. The scale of the volume backscatter strength is the same for all frequencies and is between -60 dB (red color) to -90 dB (dark blue color).

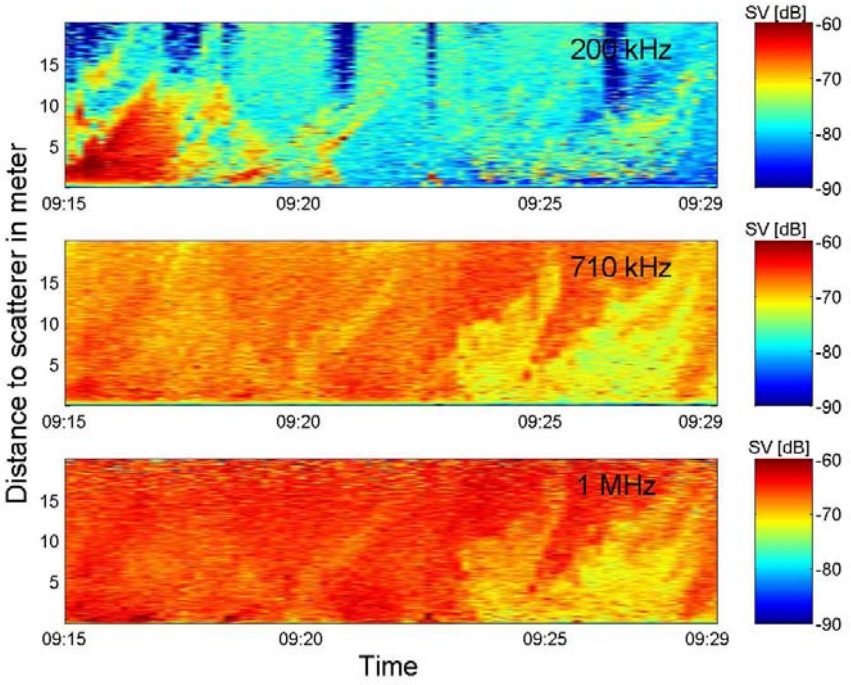

Figure 8.1: Measured volume backscattering strength, SV, in dB re 1 m^{-1} for 200 kHz (upper), 710 kHz (middle), and 1 MHz (lower) is plotted as a function of time and the distance from the transducers. The measurement was conducted on 11 May 2005, first series.

In the first measurement series the volume backscattering strength was -60 dB for large parts of the measured volume for the 1 MHz channel. For the second series it was about -65 dB for this frequency. For the 710 kHz channel large parts of the measured volume backscattering strength in the first series was -65 dB, while it was -70 dB in the second. Large parts of the measured volume were below -80 dB for the 200 kHz channel for both measurements. However,

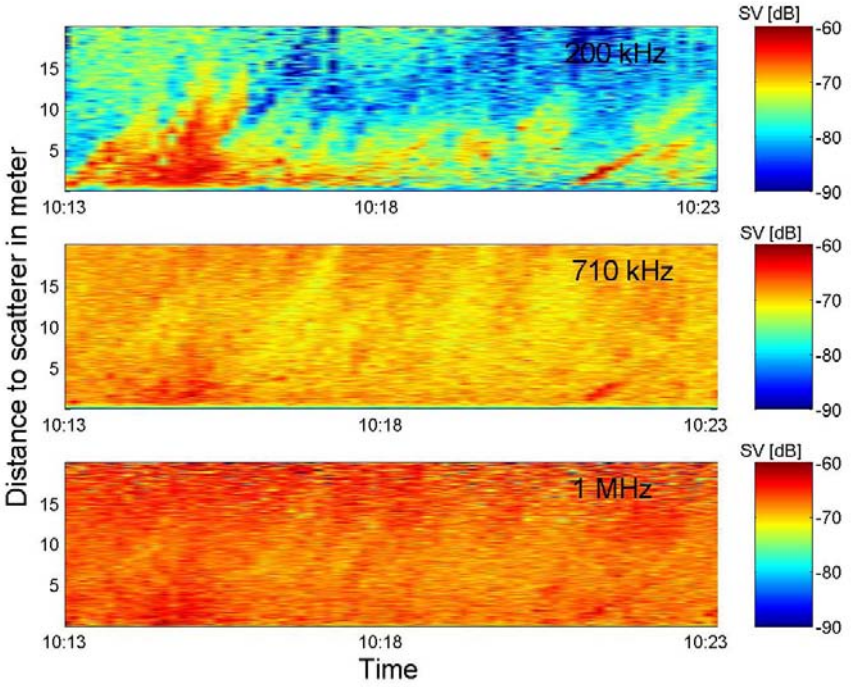

Figure 8.2: Measured volume backscattering strength, SV, in dB re 1 m^{-1} for 200 kHz (upper), 710 kHz (middle), and 1 MHz (lower) is plotted as a function of time and the distance from the transducers. Conducted on 11 May 2005, second series.

early in both measurements strong signals up to -60 dB were recorded in the first 10 meters. After a couple of minutes the signal strength decreased. In the first measurements series in Figure 8.1, the cylinder was raised from 2 to 0.5 meter below the sea level at 9:25. The volume backscattered signal became somewhat weaker for the 710 kHz and 1 MHz frequencies after the cylinder was raised. In the second series in Figure 8.2 there are some features with increased scattering that can be identified in the first meters of the 200 kHz channel.

The overall measured volume backscattering strength was much higher for the 710 kHz and 1 MHz channel than for the 200 kHz channel. It is evident that the scatterers present in the beam must have a larger scattering cross section for the two high frequencies than for 200 kHz. Recall that we earlier in Chapter 7 found that with very little plankton present the measured volume

scattering strength was typically -80 dB or less.

Figures 8.3 and 8.4 show the estimated plankton concentrations for the measurements on 11 May 2005. Three size groups are used in the estimation algorithm and all size groups are modeled with the truncated sphere model, with the following parameters; density ratio equal to 1.025, sound speed ratio equal to 1.02, and sphere radii 0.43, 1.1, and 4.5 mm. The parameters of the modeled sphere correspond the parameters found for *Calanus finmarchicus* in Chapter 3 with 2, 5, and 20 mm body length. The first of the used size groups in the estimation algorithm corresponds to the size of *Calanus finmarchicus*, the second size group to larger zooplankton, and the third group to objects typically larger than plankton.

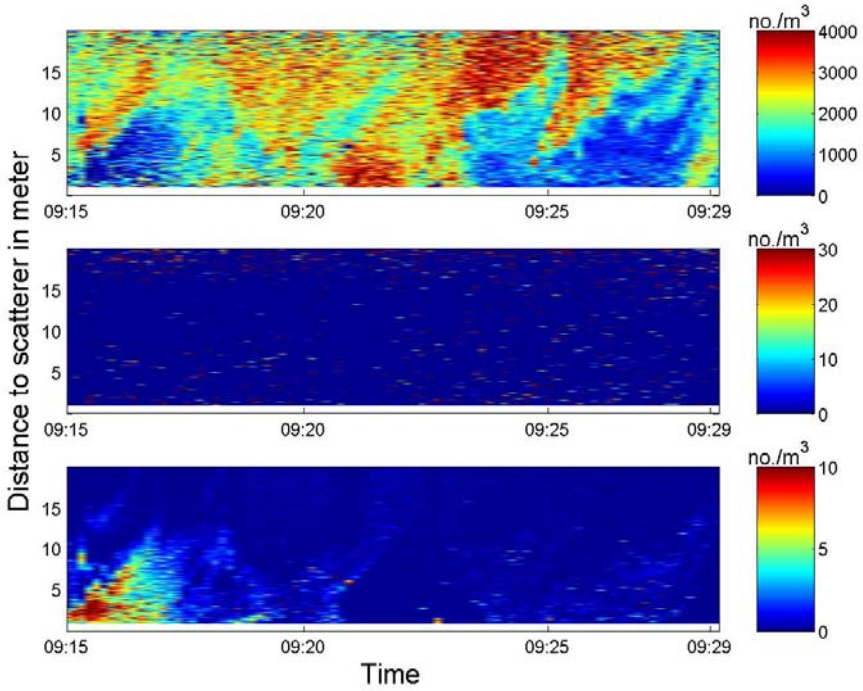

Figure 8.3: Estimated numbers of scatterers per cubic meter. The scatterers are modeled as truncated spheres with density ratio, g, 1.025, sound speed ratio, h, 1.02 and sphere radii 0.43 mm (upper), 1.1 mm (middle) and 4.5 mm (lower). The parameters of the modeled sphere correspond to modeled *Calanus finmarchicus* with body length 2 mm (upper), 5 mm (middle) and 20 mm. This is the result from the first measurement on 11 May 2005.

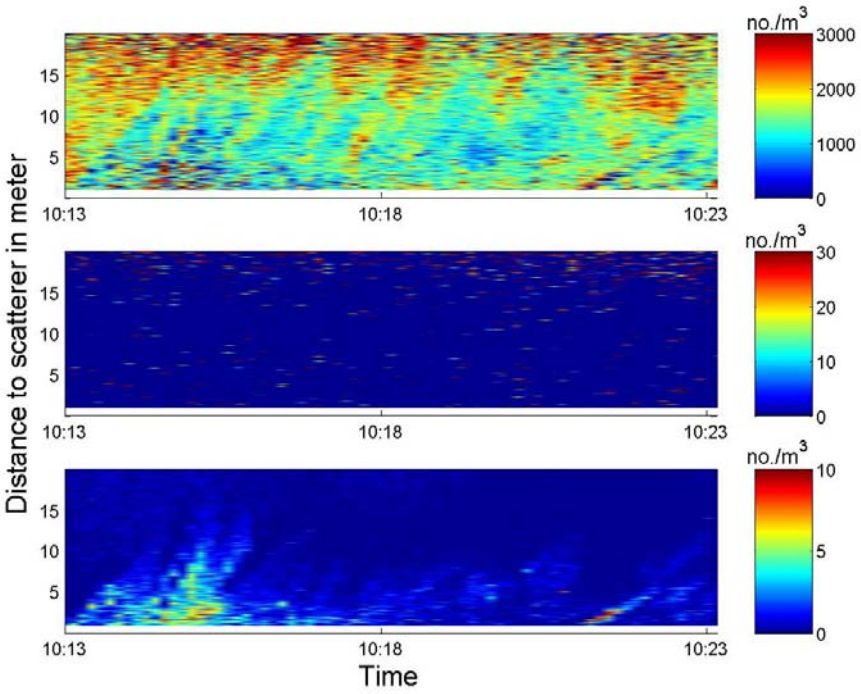

Figure 8.4: Estimated numbers of scatterers per cubic meter. The scatterers are modeled as truncated spheres with density ratio, g, 1.025, sound speed ratio, h, 1.02 and sphere radii 0.43 mm (upper), 1.1 mm (middle) and 4.5 mm (lower). The parameters of the modeled sphere correspond to modeled *Calanus finmarchicus* with body length 2 mm (upper), 5 mm (middle) and 20 mm. This is the result from the second measurement on 11 May 2005.

The upper part of Figures 8.3 and 8.4 shows the concentration of scatterer per cubic meter in the smallest size group, the middle part is for the middle size group, and the lowest part is for the largest size group. Notice that the scales of the concentration axes for the three size groups are different. The data from the first meter closest to the transducer are removed since the measured signal is not reliable in this region due to cross talk in the electronics.

The results show high concentrations of scatterers in the smallest size groups for both measurement series. The concentrations exceeded 2000 individuals per cubic meters in both series, but reached up to 4000 individuals per cubic meter in some parts of the first measurement. The estimated concentration in this group became smaller after the cylinder was raised to just below the

surface, at about 9:25 in Figure 8.3. In the estimated results for the middle size group of scatterers the concentration is less than 10 scatterers per cubic meter except from some dispersed measurement points. The concentration estimates for the largest size group is between 0 and 1 per cubic meters at all times except for the first couple of minutes.

The strong volume backscattering strength in the 200 kHz channel in the beginning of each measurement and the corresponding increase in the estimated numbers of scatterers in the largest size group could be an effect of the way the cylinder was lowered into the water. Air bubbles could have been injected into the water. The track of a larger object passing through the beam can be identified at 10:21 in the second measurement (Figure 8.4) at 2-4 meters.

The net trawl at the first location resulted in concentration estimates of *Calanus finmarchicus* of about 525, 2100, and 525 individuals per cubic meter for depths of 0, 5, and 10 meters. At the second location the biological estimates were 2850, 6600, and 3300 individuals per cubic meter for depths of 0, 5, and 10 meters. Jellyfish (Ctenophora) was also found from 5 to 10 meter and deeper, but was not found in the surface water.

In the first measurement series the APR was tilted with an angle of 10 degrees. The center of the beams in these measurements is at a depth of 5 meter at a distance of 10 to 15 meters from the transducers.

8.1.2 Results from 19 May 2005

The water depth at the measurement site on 19 May was 64 meter in the beginning of the measurement and 50 meters at the end. The boat drifted during the measurement because of wind. The cylinder was pointing almost horizontally in the water. In the initial phases the cylinder was just below the surface. Every second minute it was lowered to resulting water depths of 2, 3, 4, and 7 meters. The measured volume backscattering strength from a 15 minutes measurement series is shown in Figure 8.5.

The measured volume backscattering strength is between -70 and -75 dB for large parts of the measured area for all channels, but somewhat lower for the 200 kHz channel than the others. The results for the 200 kHz channel show high backscattering strengths up to -65 dB early in the measurement. This resembles the feature in the corresponding measurements from 11 May but the echo is weaker. There are also some areas with strong backscattering close to the transducers. The volume backscattering strength of the 710 kHz and 1 MHz channels shows an increase as the cylinder is lowered to 7 meters. The

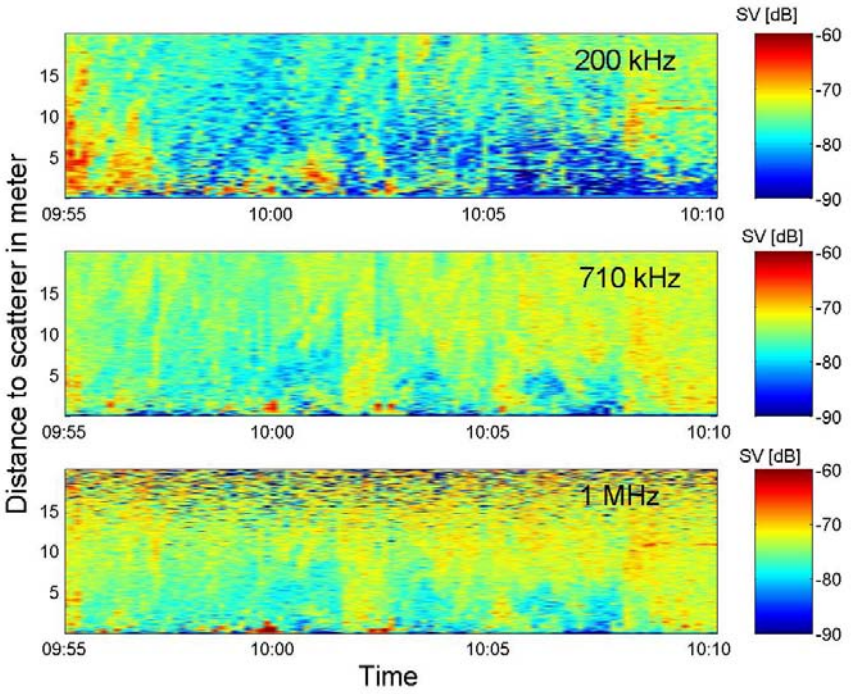

Figure 8.5: Measured volume backscattering strength, SV, in dB re 1 m^{-1} for 200 kHz (upper), 710 kHz (middle), and 1 MHz (lower) is plotted as a function of time and the distance from the transducers. The measurement was conducted on 19 May 2005.

strength of the signals in the two highest frequency channels is considerably lower than that of the measurements the week before.

The concentration estimates of the measurement series from 19 May are shown in Figure 8.6. The same size groups are chosen as earlier with radii 0.43, 1.1, and 4.5 mm of the modeled spheres corresponding to the parameters of *Calanus finmarchicus* with 2, 5, and 20 mm body length.

The estimated concentration in the smallest size group is between 0 and 500 individuals per cubic meter for the first part of the measurement series close to the surface and between 500 and 1000 individuals per cubic meter as the cylinder had been lowered deeper in the water. For the two larger size groups the concentration of scatterers was very low with 0 to 1 scatterers per cubic meters for most of the area in the larges size group. In the middle size group some areas with about 30 scatterers per cubic meter can be identified, partic-

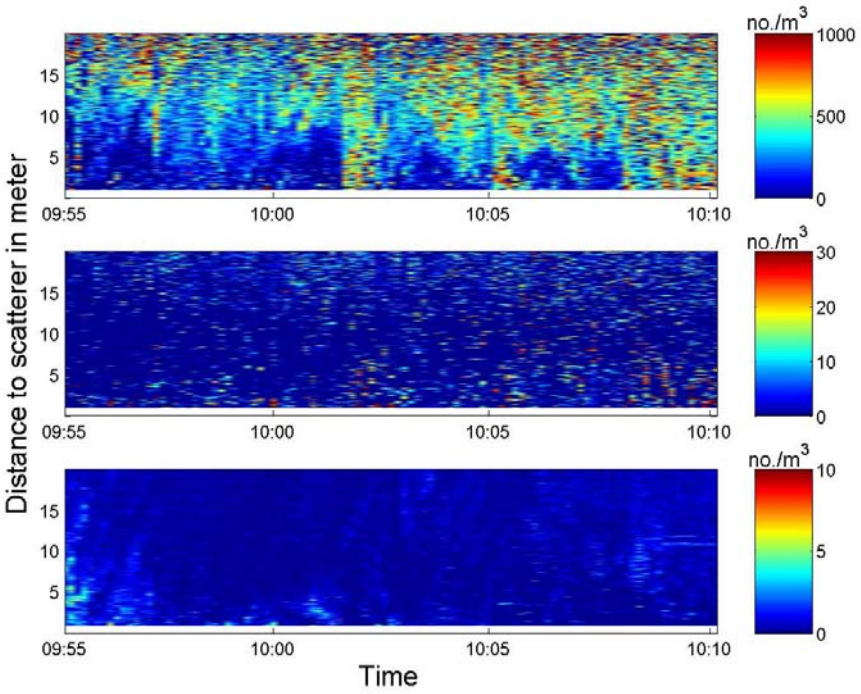

Figure 8.6: Estimated numbers of scatterers per cubic meter. The scatterers are modeled as truncated spheres with density ratio, g, 1.025, sound speed ratio, h, 1.02 and sphere radii 0.43 mm (upper), 1.1 mm (middle) and 4.5 mm (lower). The parameters of the modeled sphere correspond to modeled *Calanus finmarchicus* with body length 2 mm (upper), 5 mm (middle) and 20 mm. This is the result from 19 May 2005.

ularly close to the transducer when the cylinder was situated at a depth of 7 meters, the last minutes of recording in Figure 8.6.

A net trawl was taken of the water column at the site of the acoustical measurement. The nets showed a concentration of *Calanus finmarchicus* between about 450 to 1500 individuals per cubic meter in the upper 10 meters of the water column (450 at 0 meter, 1500 at 5 meters and 600 10 meters). There were also some jellyfish (Ctenophora) from 5 meters and deeper. The jellyfish were destroyed in the nets so it was difficult to determine their exact species and size, but the size was assumed to be on the order of a couple of centimeters.

8.1.3 Comments to the results

All measurements series show frequency dependence of the measured volume backscattering strength. The volume backscattering strength measured during these cruises is generally much higher than what was measured during the testing of the APR during 2004, as can be seen from the measurement on 3 September in Figure 7.18.

The biological recordings demonstrated that there were high concentrations of *Calanus finmarchicus* presented at the time the acoustical measurements were conducted. They also indicated that there was a depth dependence in the concentration with a maximum at 5 meters. Because of the biological recordings it is safe to assume that a significant part of the objects that contribute to the concentration in the smallest size group is *Calanus finmarchicus*. The absolute value of this concentration is more uncertain.

The APR measured the same features as the biological samples. There were high concentrations of small scatterers present at the time of the measurement. The recorded acoustical data showed that there was depth dependence in the concentration of the scatterers. At the same time the acoustical estimates showed very small concentrations of larger scatterers. This agrees with the biological samples that measure almost only *Calanus* and jellyfish, where the jellyfish stayed deeper. The measured concentration of scatterers of the smallest size group was comparable to the biologically recorded concentrations of *Calanus*.

The plankton did not seem to be uniformly distributed in the water and structures could be identified in the concentration estimates. The acoustical recordings showed high resolution data of the distribution of scatterers. A more detailed discussion on the method and performance of the APR will be given in the next chapter.

Chapter 9

Discussion

The method of multi-frequency acoustical detection of plankton and design and construction of the Acoustical Plankton Recorder has been described. The function of such an instrument is the detection of plankton. There are several possible future applications of acoustical plankton instruments both in plankton harvesting and ecosystem monitoring. The design of future instruments has to be adjusted for the specific application. This prototype Acoustical Plankton Recorder has been developed to prove the method, and to gain experience for future instruments. The instrument has proved to be able to measure the backscattering from concentrations of small zooplankton that typically occurs in nature, which was the objective of this work.

This chapter contains comments on both the method and the instrument. The experience from the use of the instrument and the measurements themselves are discussed. The discussion is focused on uncertainties and critical factors since the goal of this prototype is to give experience for future instruments.

9.1 The acoustic method - Plankton measurements

Measurements on plankton are associated with uncertainties. There are at most times a complex assembly of plankton present in a location. Treating the data as if there were only one or a few species that dominates is a simplification of nature. As for plankton, the backscattered signal from a small number containing a gas bubble can easily dominate the backscattered signal from fluid-like plankton such as *Calanus finmarchicus*. The backscattered signal from a larger animal like a fish in the beam may also dominate the

backscattered signals from plankton.

The properties of the plankton, which are the basis for the model treated here, have turned out to be very variable. The size, shape, and chemical composition of the plankton depend on their life stage, the supply of nutrient, and factors such as water temperature and water depth.

The uncertainties associated with the complexity of nature have to be accepted, as it is nature we are interested in. However, it is crucially important to be aware of the uncertainties in such measurements. More accurate measurements on the physical parameters for the plankton at the measurement site and more complicated models for different species might improve the accuracy to some degree. This thesis does not contain any new work on the characterization of the physical parameters of the plankton, and former work on the subject has been used as input to the model of *Calanus finmarchicus*.

It is difficult to identify uniquely the species of the detected objects by using acoustical methods alone. With multiple frequencies it is however possible to distinguish between size groups. Adding knowledge about the properties of the species makes possible concentration estimates of each size group. In the case of concentration estimates of *Calanus*, the way to ensure that *Calanus finmarchicus* is really present is by biological methods like net trawl. From an acoustical point of view it is hard to distinguish between *Calanus finmarchicus* and other species of plankton in the same size group, but biological knowledge on the composition and abundance of various plankton can assist in the understanding of the acoustical results.

When measuring on the plankton, the target strength of individuals is so weak that the system can only detect clouds of plankton. In order to assume linearity of the number of scatterers and the received mean intensity some assumptions have to be valid. The objects must be distributed randomly in the volume and the targets have to move between the pings so that a new random set of phases is generated in the next ping. With these high frequencies, the scale of which the targets have to move is very small. For the accuracy of the received mean intensity to be reasonable, the number of pings that are integrated over should typically be above 20, [Simmonds and MacLennan, 2005]. The linearity between the number of scatterers and the received intensity in not valid if the concentration of scatterers is very high and multiple scattering effects and extinction effects become important. Comparison of the size and target strength of *Calanus finmarchicus* to the plankton in a theoretical study by Gorska and Chu [2001], indicates that multiple scattering effects and extinction effects can be neglected for all *Calanus* concentration likely to be found in

nature.

9.2 The prototype APR and recommendations for future generations of such instruments

The Acoustical Plankton Recorder (APR) is a three frequency acoustical system built for plankton detection. In a system where the backscattered signal from a water volume is compared for several frequency channels, it is desired that the measured water volume is the same for all frequencies. In practice, with several transducers located physically apart this is not possible. The separation of the transducers is one of the reasons that the measured volumes of water differs at each frequency channel. The beam patterns being unlike do also make the measured volume different. The beamwidths and the direction of the axes with maximum beam strength of the various transducers vary. The angle of the transducers can be set so that there is maximum overlap of the three beams at a specific range.

With a beamwidth of 5.5 degrees for the narrowest transducers the width of the beam is only 1 meter at a distance of 10 meters from the transducers. With a pulse length of 0.1 ms the echo from this distance roughly contains the scattering from objects in a volume of 0.06 m^3. This volume is quite small, and the resolution in the recorded data is correspondingly high, but with large variation in the received signal from each measured volume. These variations would decrease by integrating over a larger measurement area. The choice of this area would be determined by the measurement setup and aim of the measurement. With the default settings of the APR the data are integrated over 16 pings. The accuracy of the data would be improved if the number of pings were increased.

The system can measure at one frequency at a time. It is desirable with as little time delay as possible between the measurements on the three frequencies since the presence of the object in the volume changes with time. The time scale of the movement of the scattering objects in the beam is variable. With a measurement cycle of 6 seconds to cover all the three frequencies, rapid moving objects like fish would scarcely stay in the beam during the entire cycle. Plankton is in general taken to be drifting in the water. But even if the plankton were not moving themselves, the current does. The instrument will also be moving, especially when attached to a boat in turbulent weather. Strong scatterers present in the beam of only one frequency channel will have a large effect on the concentration estimates of objects at this range.

While the APR runs continuous measurements, the detected raw data returned from each ping is displayed on the screen of the acquisition software interface. This display gives the operator approximate information on the scattering situation. The processing of the data to achieve volume scattering strength and concentration estimates are time consuming and has to be done after the measurement has ended. The preview of the backscattered signals during a measurements cruise is essential as long as the processing software cannot run in real-time modus for decision making on measurement strategy.

The optimal choice of frequency and the number of frequencies for an acoustical instrument for plankton detection depends on the aim of the measurement. In this work three frequencies were used; 200, 710, and 1000 kHz. The maximum range of these frequency channels is quite different; so are also the backscattering cross sections for plankton at these frequencies. The difference in backscattering cross section is exploited in the estimation algorithm of scatterers in various size groups. But the difference in range introduces challenges to the choice of system parameters. The relative long range of the 200 kHz channel compared to the other frequency channels limits the repetition rate of the system and the rate must be considered in the choice of direction of the beams into the water. This relatively long range most also be accounted for in the possible use of noise reduction algorithms.

The current prototype of the APR can be extended to use more frequencies. This would allow the selection of more size groups in the concentration estimates and could improve the accuracy of those estimates. Whether to use more frequencies or not in future generations of acoustical plankton sensors depends on the task of such investigations. More frequencies complicate the instrument. It has to be considered whether the effort is worthwhile.

The acquisition system is built to be flexible and accurate. It was built on a stationary/table computer because at the time of purchase it was difficult to get laptops with the required bus mastering capacity for the chosen PCI card. Vulnerability of the common laptops under rough conditions was also a concern. A PC intended for rough use was considered too expensive.

The chapter of verification and calibration of the APR in this thesis contains much more than a calibration of the instrument. Rather it is a summary of some of the work done on the APR. Calibration of the APR by finding the backscattered signal from a known target should ideally take place on every measurement cruise, since some of the parameters of the electronics and the charge of the batteries are not constant. So far the instrument has been calibrated under controlled conditions in the laboratory. For the current prototype

it would be difficult to conduct calibration at sea under rough conditions. The uncertainty in the calibration of the instrument does directly influence the accuracy of the measured volume backscattering strength, which again influences the concentration estimates.

Standard targets were used in the calibration measurements in spite of some limitations with the method. According to Holliday and Pieper [1995], standard targets typically used at the lower frequencies in fishery acoustics are not very suitable for the calibration of high frequency transducers because of the complexity of the resonances of the spheres, the effects of attaching a tether to the sphere, and the high levels of scattering anticipated for sizes that can be reliably handled. This is a problem especially for the 1 MHz channel, where the deployed standard spheres are not suitable.

The instrument measures the volume backscattering strength, and the data are used to produce concentration estimates. Potential use of the system as it is today is limited as long as it is in the prototype stage since an operator has to be present and a boat is required with a winch to operate the instrument. In addition, the physical size of the APR makes it difficult to handle. With a weight of about 35 kg the use of winch is preferred when lowering and raising the probe between water and deck.

The absorption of the sound in seawater is highly frequency dependent. The high absorption in the 1 MHz channel limits the range of the system and any acoustical system that uses such high frequencies will have short range. Given the small size of the plankton and that the wavelength of the sound needs to be on the same order of magnitude as the size of the object to be acoustically visible, the frequency of the sound needs to be high.

The absorption in the water depends on different physical properties of the water, particularly temperature. These physical parameters of the water were not properly measured during these cruises. Therefore, typical values are used in the data processing. The APR could in the future be connected to a sensor that measures temperature, salinity, pH, and depth, giving these parameters as input in the data processing of the scattering data. Using only typical values has limited the accuracy of the measured volume backscattering.

Since the range of the system is only 15 to 20 meters it could be advantage for such a system to move in the water column. Alternatively, many small instruments can be placed to cover a larger area of the water column. The prototype of the instrument has to be lowered from a boat and attached to the receiver unit above water with a cable. Depending on the purpose of the measurement, small stationary sensors or sensors scanning the water volume

can be developed in the future.

9.3 Measurement results with the APR

The APR has run without any unexpected failures. The cruises have taken place at different times of the year and under various weather conditions with very dissimilar amounts of plankton present. All these cruises were conduced in cooperation with others working on the Calanus project, mainly biologists and people testing fishing gears for plankton harvesting. The APR has been tested both in the vertical and horizontal direction. In principle it could be pointing in any direction, when taking the direction into consideration in the choice of system parameters for the APR.

The presented results in Chapters 7 and 8 showed the measured volume backscattering strength for the three frequency channels under various conditions. The results from the cruises conducted during May 2006 showed strong backscattering signals for both 710 kHz and 1 MHz channels while measuring on high concentration of plankton.

Chapter 10

Summary and conclusions

The topic of this thesis has been the development and testing of an Acoustical Plankton Recorder (APR).

A prototype instrument has been developed. The design of the instrument is targeted for the zooplankton species *Calanus finmarchicus*, which has a length of 1 to 3 mm. The instrument uses three frequencies, 200 kHz, 710 kHz, and 1 MHz. The system transmits pulses with variable pulse length and repetition rate. The received analog signals are processed electronically and sampled into a computer. Software for digital signal processing is developed in Matlab^{TM}.

The APR has been tested under various experimental settings. Measurements are done at sea in the Trondheim fjord and in the Norwegian sea outside Mid-Norway. The results demonstrate that the APR can be used for plankton estimates.

Suggestions for future work

The exploitation of plankton as a resource will be an issue in the years to come. Acoustical measurements of plankton could be important in different applications like ecosystem modeling, harvesting of plankton, and monitoring of plankton concentrations.

Knowledge and experience from the APR prototype should be incorporated into future generations of acoustical plankton recorders. They could possible be much smaller acoustical plankton sensors. The electronics has to be made much more compact. For many applications like monitoring of plankton stocks and as input to ecosystem models it is desirable with many sensors deployed

over a large area. The sensors should contain data recording units or transmit data automatically so that no operator needs to be present at the measurement site and so that measurements can be done over a large time period.

The acoustical sensor should be connected to temperature, pressure, and salinity sensors. This would improve the accuracy of the estimation of absorption loss in the water.

Additional measurements of the physical parameters of the dominant zooplankton will improve the accuracy of the concentration estimates. These parameters should be tuned according to season.

Appendix A

Electronics circuits

This appendix contains the electric circuits for the transmitter, receiver, and control electronics.

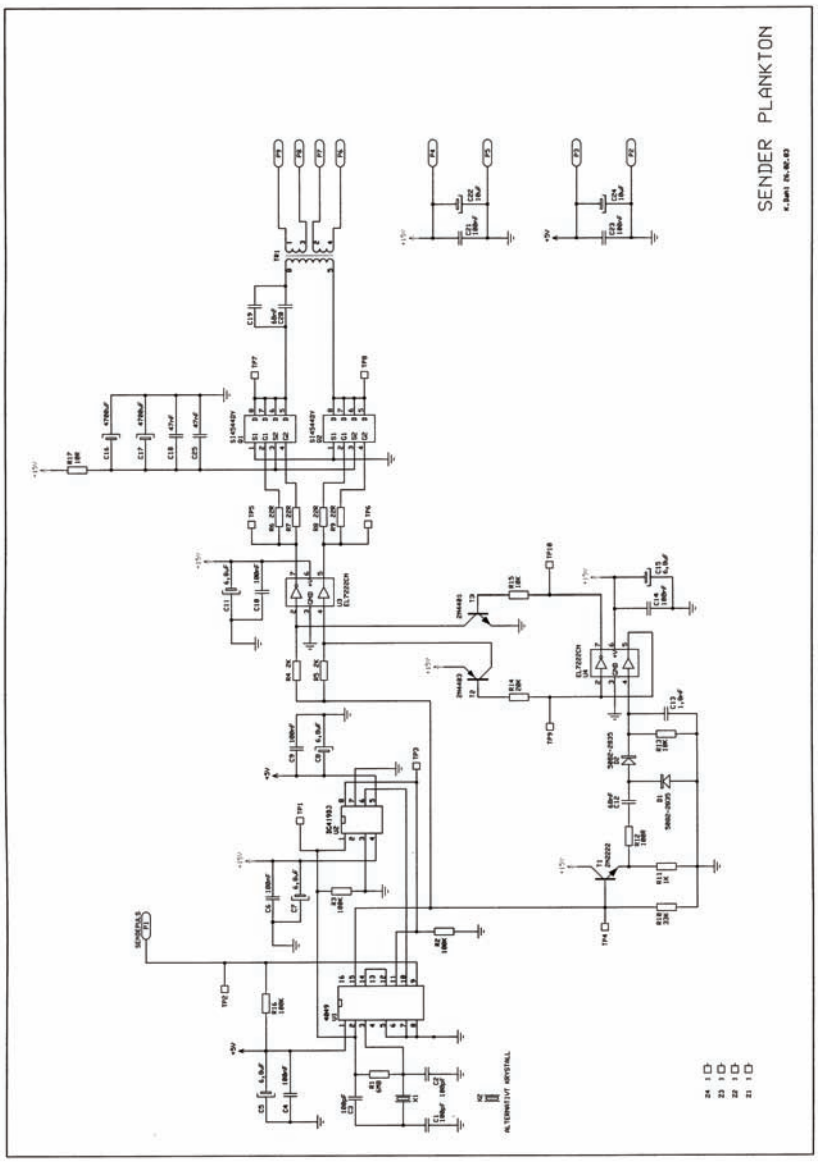

Figure A.1: The transmitter electronics.

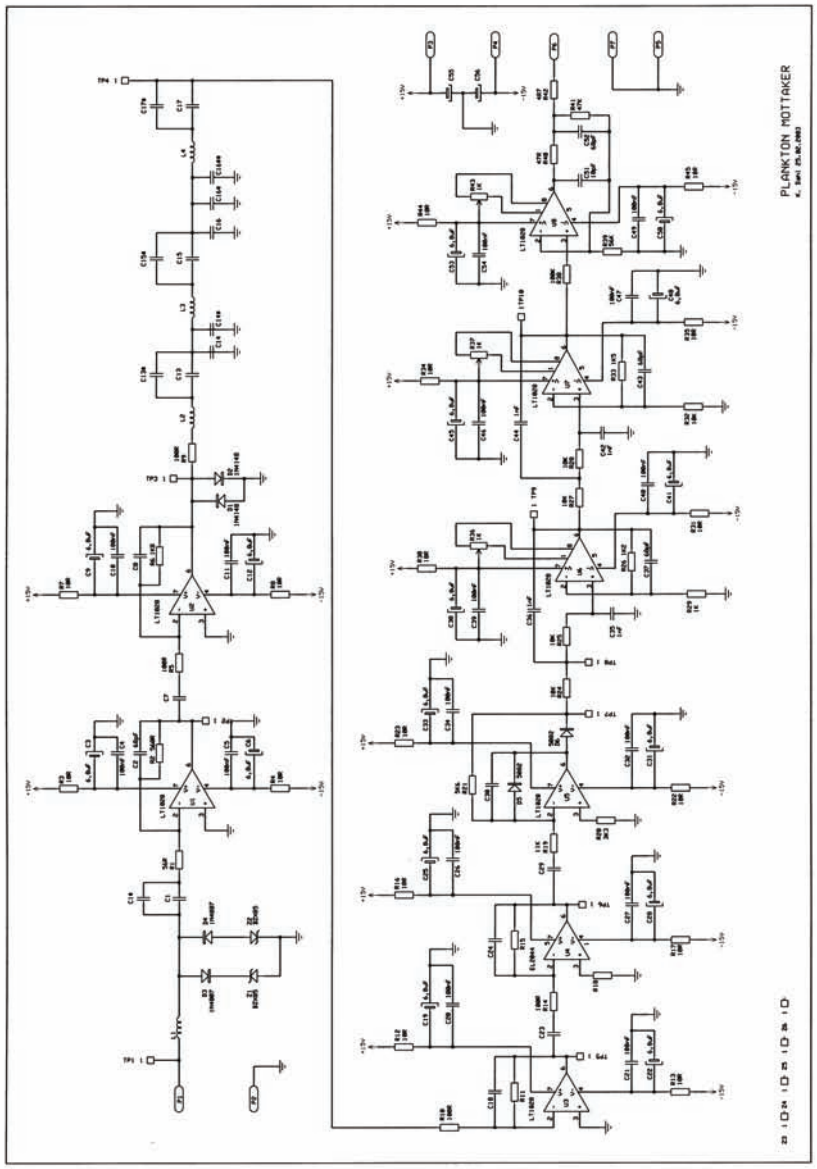

Figure A.2: The receiver electronics.

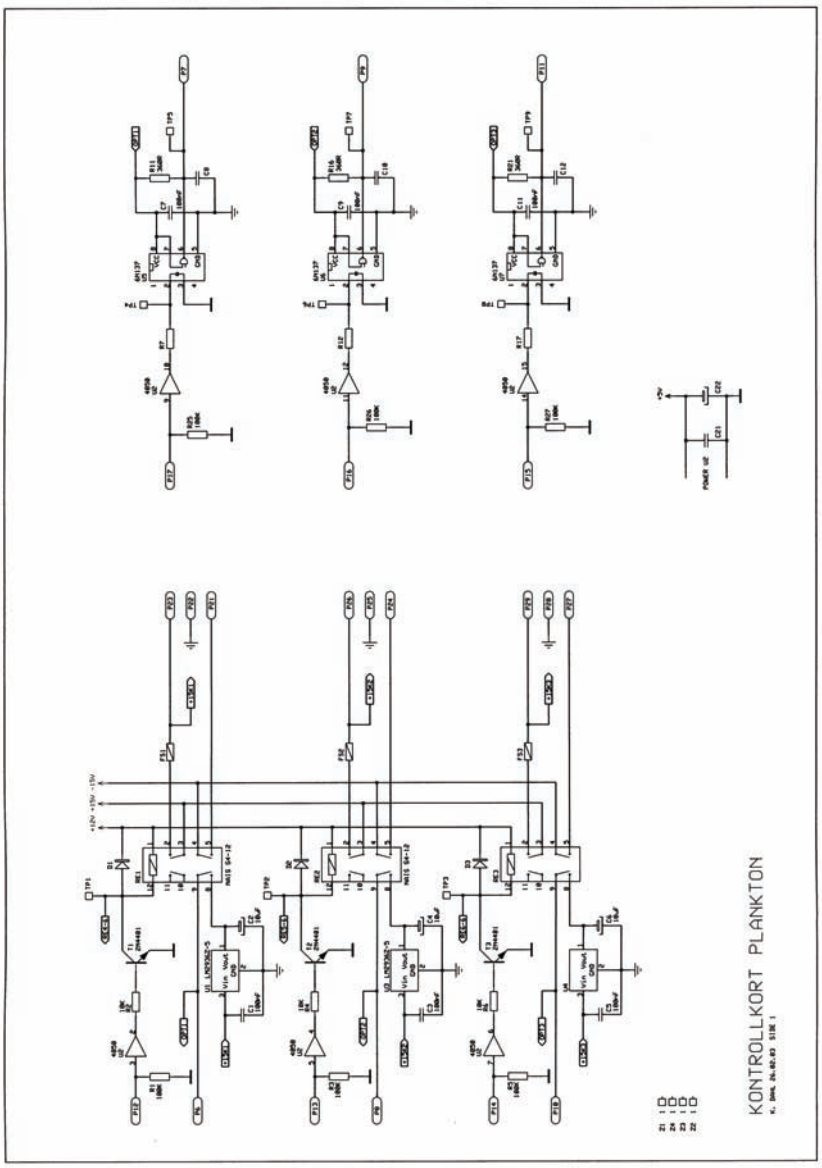

Figure A.3: The electric circuits of the controll unit within the steel cylinder.

Bibliography

J. J. Anderson. Sound scattering from a fluid sphere. *Journal of the Acoustical Society of America*, 22:426–431, 1950.

R. J. Bobber. *Underwater electroacoustic measurements*. Peninsula publishing, 1988.

K. G. Foote. Optimizing copper spheres for precision calibration of hydroacoustic equipment. *Journal of the Acoustical Society of America*, 71:742–747, 1982.

K. G. Foote, T. Knutsen, A. E. Baekkevold, P. Dalpado, and S.E. Johannessen. Initial, collateral measurements of some properties of Calanus finmarchicus. *ICES CM*, 1996.

R.E. Francois and G. R. Garrison. Sound absorption based on ocean measurements. Part I: Pure water and magnesium sulfate contribution. *Journal of the Acoustical Society of America*, 72:896–907, 1982a.

R.E. Francois and G. R. Garrison. Sound absorption based on ocean measurements. Part II: Boric acid contribution and equation for total absorption. *Journal of the Acoustical Society of America*, 72:1879–1890, 1982b.

N. Gorska. Evaluation of sound extinction and echo interference in densely aggregated zooplankton. *Oceanologia*, 42:315–334, 2000.

N. Gorska and D. Chu. Some aspects of sound extinction by zooplankton. *Journal of the Acoustical Society of America*, 110:2315–2325, 2001.

C. F. Greenlaw. Back-scattering spectra of preserved zooplankton. *Journal of the Acoustical Society of America*, 63:44–52, 1977.

C. F. Greenlaw. Acoustical estimation of zooplankton populations. *Limnological Oceanography*, 24:226–242, 1979.

C. F. Greenlaw and R. K. Johnson. Physical and acoustical properties of zooplankton. *Journal of the Acoustical Society of America*, 72:1706–1710, 1982.

C. F. Greenlaw and R. K. Johnson. Multiple-frequency acoustical estimation. *Biological Oceanography*, 2:227–252, 1983.

F. Gross and J. E. G. Raymont. The specific gravity of calanus finmarchicus. *Proc. R. Sos. Edinburgh*, 61:288–296, 1942.

D. V. Holliday. Zooplankton acoustics. *Oceanography of the Indian Ocean*, pages 733–740, 1992.

D. V. Holliday, P.L. Donaghay, C. F. Greenlaw, D. E. McGehee, M. M. McManus, J. M. Sullivan, and J. L. Miksis. Advances in defining fine- and micro-scale pattern in marine plankton. *Aquatic Living Resources*, 16:131–135, 2003.

D. V. Holliday and R. E. Pieper. Bioacoustical oceanography at high frequencies. *ICES J.Mar.Sci.*, 52:279–296, 1995.

D. V. Holliday, R. E. Pieper, and G. S. Kleppel. Determination of zooplankton size and distribution with mulitfrequency acoustic technology. *J. Cons. Int. Explor. Mer.*, 46:52–61, 1989.

J. M. Hovem. *Marine Acoustics. The Physics of sound in Underwater Environments*. Applied Research Laboratories, The University of Texas at Austin, Texas, 2006. In preparation.

J. W. Køgeler, S. Falk-Petersen, Å. Kristensen, F. Pettersen, and J. Dalen. Density- and sound speed contrast in sub-arctic zooplankton. *Polar Biology*, 7:231–235, 1987.

T. Knutsen, W. Melle, and L. Calise. Determining the mass density of marine copepods and their eggs with a critical focus on some of the previously used methods. *Journal of Plankton Research*, 23:859–873, 2001.

R. Korneliussen. Measurement and removal of echo integration noise. *ICES Journal of Marine Science*, 57:1204–1217, 2000.

C. L. Lawson and R.J. Hanson. *Solving Least Squares Problems*. Prentice-Hall, 1974.

H. Medvin and C. S. Clay. *Fundamentals of Acoustical Oceanography*. Academic press limited, 1998.

R. E. Pieper and D. V. Holliday. Acoustic measurements of zooplankton distribution in the sea. *J. Cons. int. Explor. Mer.*, 41:226–238, 1984.

J. Simmonds and D. MacLennan. *Fisheries Acoustics Theory and Practice*. Blackwell Publishing, 2005.

H. R. Skjoldal, editor. *The Norwegian Sea Ecosystem*, chapter Zooplankton: The link to higher trophic levels. Tapir academic press, 2004.

M. L. Smith and J. N. Franklin. Geophysical application on generalized inverse theory. *Journal of Geophysical Research*, 74:2783–2785, 1969.

T. K. Stanton and D. Chu. Sound scattering by several zooplankton groups. II. scattering models. *Journal of the Acoustical Society of America*, 103: 236–253, 1998.

T. K. Stanton, P.H. Wiebe, and D. Chu. Differences between sound scattering by weakly scattering spheres and finite-length cylinders with applications to sound scattering by zooplankton. *Journal of the Acoustical Society of America*, 103:254–264, 1998.

F. E. Tichy, H. Solli, and H. Klaveness. Non-linear effects in a 200-kHz sound beam and the consequences for target-strength measurement. *ICES Journal of Marine Science*, 60:571–574, 2003.

N. E. Tokle. *Are the ubiquitous marine copepods limited by food or predation? Experimental and field-based studies with main focus on Calanus finmarchicus*. PhD thesis, NTNU, 2006a.

N. E. Tokle. Data on the body length of calanus finmarchicus. Unpublished data from measurements on the Trondheims fjord. Norway., 2006b.